UNIVERSITY OF MONTENEGRO

FACULTY OF MATHEMATICS AND
NATURAL SCIENCES

Sonja Ivanovic

IMPROVING QA/QC IN MAMMOGRAPHY SCREENING AND BREAST DIAGNOSIS IN MONTENEGRO

-PHD THESIS-

Podgorica, 2017

UNIVERZITET CRNE GORE

PRIRODNO-MATEMATIČKI FAKULTET

Sonja Ivanović

UNAPREĐENJE KONTROLE KVALITETA I OSIGURANJA KVALITETA (QA I QC) U SKRININGU I DIJAGNOSTIČKOJ MAMOGRAFIJI U CRNOJ GORI

-DOKTORSKA DISERTACIJA-

Podgorica, 2017.

Data and information on the PhD student

Name and surname: Sonja Ivanovic
DOB: 17.07.1972
The name of the completion of the study program and year of completed: Master of science in medical physics, 2009

Data and information on the local mentor

Name and surname: Slavoljub Mijovic
Academic degrees held: PhD in Physics of ionized gases
Position held: Full professor
The name of the University and department: Faculty of Natural Sciences and Mathematics, University of Montenegro, Department of Physics

Data and information on the remote mentor

Name and surname: Hilde Bosmans
Academic degrees held: PhD in medical sciences, Certified as medical physics expert (radiology) in Belgium
Position held: Professor
The name of the University and department: Katholieke Universiteit Leuven, faculty of medicine, Medical Physics and Quality Assessment, Belgium

Commission members:

Olivera Ciraj, PhD, Professor at the Faculty of Electrical Engineering in Belgrade, University of Serbia, chairman

Hilde Bosmans, PhD, Associate Professor at the Katholieke Universiteit Leuven, faculty of medicine, Medical Physics and Quality Assessment, Belgium, remote mentor

Slavoljub Mijovic, PhD, Professor at the Faculty of Natural Sciences and Mathematics, University of Montenegro, Department of Physics, mentor

Mara Scepanovic, PhD, Professor at the Faculty of Natural Sciences and Mathematics, University of Montenegro, Department of Physics

Mira Vuceljic, PhD, Professor at the Faculty of Natural Sciences and Mathematics, University of Montenegro, Department of Physics

Date of defense: 10.June, 2018

Posvećeno mojim roditeljima,
koji više nisu sa nama,
ali čija energija i podrška me i dalje prate

Information on doctoral dissertation

Course of study: Physics, Faculty for mathematics and natural sciences, University of Montenegro

Thesis title: Improving QA/QC In Mammography Screening and Breast Diagnosis in Montenegro

Summary: The leading idea for this PhD project was to contribute, in a scientifically driven way, to Quality Control (QC) of mammography systems. During the project, we obtained however both scientific and practical results. Seen the very poor level in Quality Control of diagnostic radiology in Montenegro at the start of the project, the practical contribution obtained through this PhD on National level is huge. This is of course also thanks to the Technical cooperation project with the International Atomic Energy Agency (IAEA) that provided the Clinical center of Montenegro with a complete kit for mammography QC.
A first task was to perform a QC test on every mammography system in Montenegro, to compare data with European standards and to consequently find out about the situation. Concerning patient doses we were in line with the EU protocol. Concerning image quality we should be on a higher level and aim for the European acceptable level. This situation is mostly due to inadequate image processing devices and absence of any regular maintenance, but there is a factor of lack of staff and proper training, also.
The next phase of the PhD project was performed in the University Hospital of the Catholic University of Leuven, Belgium, with my remote mentor. I learned about the details of QC tests, both for film-screen and full field digital mammography. This center has also 2 breast tomosynthesis systems for which a QC protocol was being developed. More importantly, we made plans for a first scientific paper in which we would test a new feature of the MagicMax multimeter (IBA), the dosimeter that had been provided by the IAEA. This new dosimeter provides an automated estimate of the half value layer (HVL) from just a single exposure. This characteristic was tested for 5 different anode/filter combinations and results were compared to measurements with an ionization chamber, considered gold standard.
First, our scientific contributions will be presented.
In this work a critical analysis of the methodology for evaluating the x-ray half value layer was conducted. Our analysis was performed on mammography units with different anode-filter combinations. Solid state dosimeters can be very energy sensitive and may not be reliable for an automated HVL determination, while ionization chambers are known to be largely energy independent and served as gold standard. A two-phase project was started: to investigate different methods and their associated accuracies to manually calculate the HVL and to subsequently verify the accuracy of the new solid state dosimeter. First, we showed that all manually acquired, experimental data fitted well to an exponential function (correlation coefficients were in most cases more than 99%). Next, the MATLAB curve fitting toolbox was used to assess the errors on the curve fits. The uncertainty of manual HVL determination was less than 10% (usually less than 6%). These results define the errors that can be tolerated with automated equipment. From a series of measurements for analyzing accuracies, repeatability and energy dependencies of the detectors [23], and other factors [24], we realized that they are

not the critical factors in HVL determination. We decided that uncertainties of HVL should not be more than 10%.
A critical factor for the HVL is the number of experimental data. The HVL, determined from the first or last four data points, obtained with successive sheets of Aluminum, was significantly different from HVL values obtained from all eight points. In every experiment three significantly different values of the HVL were obtained: the lowest, obtained from the first four data; an intermediate value, obtained from all experimental data, and the highest value, obtained from the last four points. In some cases these differences were about 25%. We concluded that the X-ray beam is hardening by passing through aluminum sheets. The beam that is being characterized is the beam as measured with the first measurement of the series that is considered in the calculation, and that it defined as the initial measurement.

Next, because new (solid state) dosimeters allow all-in-one shot data acquisition, we used the opportunities of different mammography units in Leuven and Gent to verify whether we can trust kV measurements at all anode/filters and over the complete kV range. In other words, we studied the question: are solid state dosimeters sufficiently energy corrected for (all) beam qualities? Can we trust actual dosimeters which provide 'readymade' data on HVL from a single exposure? Is Robson's approach, a method used for extrapolation of tube output and HVL from a measurement at a single tube voltage, also valid on newly introduced beam qualities?
We showed that differences between the automated, direct HVL measurements of Magic Max and manual measurements did not exceed 0.02 mm Al. Standard deviation was approximately 0.1. We concluded that the direct HVL measurements with the Magic Max are within the confidence interval of manual HVL determinations.
Likewise, we used a linear model and more MATLAB software to show that Robson's model shows a satisfactory agreement between measured and predicted values of air kerma and HVL for the conditions that we have tested.

To derive useful information from a mammogram, image processing plays important role. The x-ray beam that exits the patient contains the 'available information'. However, the imaging system, with its specific image formation part, deteriorates this information to some extent. Part of the information content could be restored or enhanced. The presence of non-avoidable (quantum) noise makes this procedure more complex from a mathematical point of view. We have explored the use of the Wiener filter to restore the information content via 'restoration by deconvolution' [50]. MATLAB software was used to restore image by deconvolution procedures, using the Wiener filter in two ways: 1. with a scalar estimate of the noise/signal power ratio (NSR), 2. with a frequency dependent estimate of the noise/power ratio. In order to proof the concept, the bar-pattern was used, instead of a real breast. It is found that with both approaches, the spatial resolution is improved, although the best result is depicted in methodology 2. where a frequency dependent estimate of the noise/signal power ratio is done via respective autocorrelation functions. The conclusion was that a careful estimation of the quality of the imaging system through PSF (Point Spread Function) or MTF (Modulation Transfer Function), together with an estimation of the sort and magnitude of noise in the image, could be used to improve the spatial resolution.

A first practical contribution in the frame of radiation safety is that for the first time, Average Glandular Doses (AGD) have been measured in Montenegro. Dose reference levels were established and it is in accordance with EU protocols. We performed sensitometry and densitometry measurements at all screen-film mammography systems and they were shown to have low image quality in general. The optimization process is demanding. Optimization of image quality is already done at Podgorica's Health care center. During the QC procedures on

screen-film mammographs, we found discrepancy between the indicated and measured tube voltages, with deviations that are larger than what is allowed following the European protocol (namely ±2 kV) on the Planmed Sophie Classic.

Paper 4., 5. and 6. from the list of published papers reflect that work performed in the frame of present PhD project.

List of published papers:

1. "Dose estimations for persons occupationally exposed to ionizing radiation in Montenegro", published in Arch. of oncology 2008, 16(1-2) 5-6, A.Milatovic, S.Ivanovic, S.Jovanovic

2. Radiation protection of patients in diagnostic radiology: Status of practice in five Eastern-European countries, based on IAEA project; O. Ciraj-Bjelac, A. Beganovic, D. Faj, V. Gershand, S. Ivanovice, 1. R. Videnovicf, M. M. Rehani; European Journal of Radiology 79 (20 II) e70-e73,

3. Status of radiation protection in interventional cardiology in five Eastern -Europian Countries, O. Ciraj-Bjelac, A. Beganovicb, D. Faj , S. Ivanovice,I. R. Videnovicf, M. M. Rehani; Book of abstracts of International Conference on Radiation Protection in Medicine, Varna, Bulgaria, 1-3 September, 2010, Radiologija, Suppl 10, P 22.

4. "Getting started with protocol for Quality Assurance of Digital Mammography in the Clinical centre of Montenegro", published in Radiation Protection Dosimetry 2015, S.Ivanovic, H.Bosmans, S.Mijovic

5. Uncertainties in half value layer determination in mammography, S. Mijovic, S.Ivanovic, F. Bemelmans, H.Bosmans, AIP Conference Proceedings **1722**, 300004 (2016); doi: 10.1063/1.4944308 View online: http://dx.doi.org/10.1063/1.4944308

6. Mammograms restoration by using Wiener filter, M. Dakovic, S. Ivanović, and S. Mijovic, AIP Conference Proceedings **1722**, 300005 (2016); doi: 10.1063/1.4944309 View online: http://dx.doi.org/10.1063/1.4944309

Key words: mammography, breast diagnosis, screening, quality control and quality assurance, X-ray diagnostic, beam quality, screen-film mammography, digital breast tomosynthesis, HVL

Scientific field: Medical physics

Scientific topic: Diagnostic radiology - mammography

Podaci o doktorskoj disertaciji

Naziv doktorskih studija: Fizika, Prirodno matematički fakultet, Univerzitet Crne Gore

Naslov doktorske disertacije: Unapređenje kontrole kvaliteta i osiguranja kvaliteta (QA i QC) u skriningu i dijagnostičkoj mamografiji u Crnoj Gori

Rezime: Osnovna ideja na početku izrade ove doktorske teze bilo je da se kontrola kvaliteta mamografske opreme unaprijedi u naučnom smislu. Međutim, kako su odmicala mjerenja, analize i zaključci, postalo je jasno da će ova teza imati i tehnički, odnosno praktični doprinos. S obzirom da je kontrola kvaliteta u dijagnostičkoj radiologiji u Crnoj Gori na početku ovog projekta bila na nezadovoljavajućem nivou, praktični doprinos ove teze je ogroman i na nacionalnom nivou. Naravno, ovo je omogućeno zahvaljujući pomoći IAEA (Međunarodna Agencija za atomsku energiju) koja je donirala opremu za kontrolu kvaliteta.
Prvi zadatak ove teze bio je odraditi kompletnu kontrolu kvaliteta svih mamografa u zemlji, uporediti rezultate sa evropskim standardima i utvrditi naš kvalitet u odnosu na njih. Pacijentne doze naših mamografa su u okviru dozvoljenih i preporučenih doza po EU standardima. Kada govorimo o kvalitetu dijagnostičke slike, on bi trebao da bude na mnogo većem nivou od trenutnog. Ovakva situacija je najviše zbog neadekvatne opreme za razvijanje filmova, neredovnog održavanja iste, ali i zbog ljudskog faktora.
Sledeća faza je bio boravak u Univerzitetskoj katoličkoj bolnici u Luvenu, Belgija, kod mog vanjskog mentora, gdje sam u detalje naučila izvođenje QC testova za analogne i digitalne mamografe. Ovaj centar ima i 2 mamografska sistema sa tomosintezom za koje je upravo tu razvijen QC protokol. Najvažnije je bilo što je tu razvijen plan za prvi naučni rad u kome je testirana validnost MagicMax multimetra, mjerne opreme koju je Klinički centar dobio od IAEA, a koja je u tom momentu bila nova na tržištu. Ovaj novi dozimetar omogućuje direktnu procjenu podatka o debljini polusloja slabljenja snopa (HVL) iz samo jedne ekspozicije. Ova karakteristika je testirana za pet različitih anoda/filter kombinacija i rezultati su upoređeni sa jonizacionom komorom koja se smatra zlatnim standardom za ova mjerenja.
Prvo će biti objašnjen naučni doprinos ovog rada.
U ovom radu sprovedena je kritička analiza metodologije debljine sloja poluslabljenja snopa X-zraka. Različiti mamografski uređaji sa različitim anoda-filter kombinacijama uz tri različita mjerna uređaja. Čvrsti detektori su energetski veoma zavisni i mogu biti nepouzdani za automasko mjerenje HVL dok je jonizaciona komora veoma energetski nezavisna i zato služi kao zlatni stndard. Prvo smo pokazali da svi eksperimentalni podaci odgovaraju eksponencijalnoj funkciji (koeficijent korelacije je najčešće bio iznad 99%). Kao drugo smo odredili nesigurnost određivanja HVL. Alatom u MATLAB softveru procijenili smo grešku u slaganju krivih. Nesigurnost određivanja HVL je manja od 10% (najčešće manja od 6%) (Slika 3.2). Ovi rezultati su dali grešku koja se može tolerisati u slučaju direktnog mjerenja. Kao sledeće, posle velikog broja mjerenja, analiziranja tačnosti, ponovljivosti i energetske zavisnosti detektora [23], i ostalih faktora [24], zaključeno je da oni nisu kritični faktori u određivanju HVL. S obzirom da se HVL dobija relativnim mjerenjima, on nije funkcija parametra a iz jednačine 3.1. iz čega slijedi da nesigurnost određivanja HVL ne može biti veća od 10%.

Kao treće, dokazano je da je broj eksperimentalnih podataka factor koji najviše utiče na HVL. HVL koji se odredi od prvih četiri mjerenja ili zadnjih četiri, bitno se razlikuje od HVL koji se odredi iz svih osam mjerenja. U svakom obavljenom eksperimentu tri bitno različite vrijednosti HVL se dobiju: najniža vrijednost za prva četiri mjerenja, srednja vrijednost, dobijena od ukupnog broja mjerenja i najveća vrijednost dobijena od zadnja četiri mjerenja. HVL je visoko zavistan od broja izvršenih mjerenja i može se bitno razlikovati u zavisnosti od kojih se podataka računa, prva četiri mjerenja ili zadnja (npr. 0.35mm and 0.42mm). U nekim slučajevima ove razlike su bile oko 25%. Zaključak je da se ove razlike javljaju kao efekat ,,otvrđavanja'' snopa usled prolaska kroz listove aluminijuma.
Sledeće, zbog novih ,,solid state'' dozimetara koji omogućavaju dobijanje svih relevantnih podataka sa jednom ekspozicijom, iskorišćena je mogućnost provjere mjerenja kV za sve anoda-filter kombinacije u čitavom opsegu kV, zatim da li se može vjerovati novim dozimetrima koji određuju vrijednost HVL iz samo jedne ekspozicije, kao i validnost Robsonovog modela koji koristi metodu ektrapolacije mjerenih vrijednosti izlaza cijevi i HVL na samo jednoj vrijednosti napona. Pokazano je da odstupanje direktnog mjerenja HVL sa MagicMax multmetrom od određivanja MATLAB krivom u svakom našem slučaju ne prelazi razliku od 0.02 mm Al. Procjena standardne devijacije daje vrijednost 0.1 tako da se zaključuje da direkno očitavanje HVL sa MagicMax multimetrom unutar opsega greške određivanja HVL.
Takođe, koristeći linearni model i MATLAB softver pokazano je da eksperimentalna verifikacija Robsonovog modela (za ovu studiju odabranih kombinacija parametara) daje zadovoljavajuće slaganje između mjerenih i predviđenih vrijednosti kerme i HVL.

Da bi dobili korisnu informaciju od mamografa , obrada slike ima važnu ulogu. Uticaj sistema za dobijanje slike u toku njenog formiranja obično kvari ,,uhvaćenu'' sliku i potrebna joj je restauracija. Prisustvo neizbežnog šuma čini ovu procedure komplikovanom sa matematičkog stanovišta. Za restauraciju mamografskih slika dekonvolucijom [50] korišćen je Viner filter kao najobjektivniji. U ovu svrhu je korišćen MATLAB softver I to na dva načina: 1. Skalarnom procjenom jačine šum/signal odnosa (NSR), 2. Procjenom zavisnosti frekvencije ovog odnosa. Umjesto pacijentkinje, korišćen je bar-patern. Nađeno je da je spacijalna rezolucija obje slike poboljšana, iako je bolji rezultat dobijen metodom 2. gdje je procjena zavisnosti frekvencije jačine odnosa šum/signal urađena respektivnom autokorelacionom funkcijom. Zaključeno je da se pažljivom procjenom imidžing sistema pomoću PSF (Point Spread Function) ili MTF (Modulation Transfer Function), zajedno sa procjenom vrste i magnitude šuma u slici spacijalna rezolucija značajno poboljšati.

U smislu tehničkog (praktičnog) doprinosa, u Crnoj Gori je u toku ove teze prvi put urađena procjena pacijentne doze (AGD – prosječna glandularna doza). Uspostavljeni su nacionalni nivoi doza koji su u skladu sa preporukama EU. Urađeni su senzitometrijski testovi i denzitometrija za sve mamografe u zemlji i ustanovljen loš kvalitet slike, generalno. Optimizacija je neophodna.
Takođe, tokom sprovođenja QC procedura na analognim mamografima pronađeno je neslaganje oko tačnosti napona cijevi između EU protokola (± 1 kV) i tehničkih uputstava proizvođača najzastupljenijeg mamografa u zemlji - Planmed Sophie Classic (±2 kV).

Radovi sa liste publikovanih radova pod 4, 5 i 6 su publikovani u toku doktorskih studija.

Lista publikovanih radova:

1. "A dose estimation for person occupationally exposed to ionizing radiation in Montenegro", published in Arch. of oncology 2008, 16(1-2)5-6,A.Milatovic, S.Ivanovic, S.Jovanovic

2. Radiation protection of patients in diagnostic radiology: Status of practice in five Eastern-European countries, based on IAEA project; O. Ciraj-Bjelac, A. Beganovic, D. Faj, V. Gershand, S. Ivanovice, 1. R. Videnovicf, M. M. Rehanig; European Journal of Radiology 79 (20 II) e70-e73,

3. Status of radiation protection in interventional cardiology in five Eastern -Europian Countries, O. Ciraj-Bjelac, A. Beganovicb, D. Faj , S. Ivanovice,I. R. Videnovicf, M. M. Rehani; Book of abstracts of International Conference on Radiation Protection in Medicine, Varna, Bulgaria, 1-3 September, 2010, Radiologija, Suppl 10, P 22.

4. "Getting started with protocol for Quality Assurance of Digital Mammography in the Clinical centre of Montenegro", published in Radiation Protection Dosimetry 2015, S.Ivanovic, H.Bosmans, S. Mijovic

5. Uncertainties in half value layer determination in mammography, S. Mijovic, S.Ivanovic, F. Bemelmans, H.Bosmans, AIP Conference Proceedings **1722**, 300004 (2016); doi: 10.1063/1.4944308 View online: http://dx.doi.org/10.1063/1.4944308

6. Mammograms restoration by using Wiener filter, M. Dakovic, S. Ivanović, and S. Mijovic, AIP Conference Proceedings **1722**, 300005 (2016); doi: 10.1063/1.4944309 View online: http://dx.doi.org/10.1063/1.4944309

Ključne riječi: mamografija, dijagnostika dojke, skrining, kontrola kvaliteta i osiguranje kvaliteta, dijagnostička radiologija, kvalitet snopa, analogna mamografija, tomosinteza i digitalna mamografija, poludebljina sloja

Naučna oblast: Medicinska fizika

Uža naučna oblast: Dijagnostička radiologija - mamografija

Content

1. Mammography and mammography systems

1.1. Introduction

Mammography is an X ray examination of the breast. Its principal purpose is to facilitate the detection of breast cancer at a point earlier in its natural history than is possible by clinical examination [44].
Mammography is currently considered to be the best tool for early detection of breast cancer.
Mammography is a particular technique since it must enable soft tissues to be radiographed and this aspect makes it much unlike conventional radiography. In fact, in conventional radiography the difference in density and in effective atomic number among various anatomic structures (bone, muscle, adipose tissue, lung – tissue and so on) sets out high contrast in the subject to be radiographed. On the contrary, in mammography, it is necessary to obtain images of an organ which is substantially composed of soft tissues (glandular and adipose structures) having effective densities and atomic numbers very close to one another. This reflects itself in slight differences of x-ray attenuation coefficient and consequently, in slight contrast differences of the object to be radiographed. Visibility of small high contrast details or small masses could be assessed for a variety of different input situations in order to establish the relationships among them. Such a systematic study has not yet be published in the scientific literature. Specific difficulties in mammograms are due to low contrast between "structures of interests" and "background".
In breast radiography, it is necessary to use an X–ray energy spectrum which allows accentuating differential absorption of tissues very similar to each other.
Mammography was initially performed by means of conventional apparatuses, since 1913 by Albert Salomon (1) in Germany, but had limited diagnostic results.
The lack of adequate devices hampered the development of breast imaging. A renewed interest arose in 1960 when in the USA, R. Egan (2) started the utilization of low energy spectra up to 30 kV.
By using low kV values, high mA values and direct film exposure, it was possible to obtain good diagnostic results. This application cleared the way to mammography development, with a first prototype system completely dedicated to mammography developed in France by Gross (3), and not very different from today's mammography units.
Since then, mammographic units have had an ever increasing industrial development incorporating more and more advanced technologic solutions.
Figure 1.1. displays a screen-film mammography unit considerably spread on international level. This spreading is linked to the awareness that breast cancer is the main cause for woman's death and it is the main reason of death if compared to other risks to women of 40 to 50 years of age.
At international level and in industrialized countries, one women of seven is subject to a breast tumor during life. It affects about 12% of women worldwide [2]. Breast cancer comprises 22.9% of invasive cancers in women [3] and 16% of all female cancers [4]. In 2012, it comprised 25.2% of cancers diagnosed in women, making it the most common female cancer. In 2008, breast cancer caused 458,503 deaths worldwide (13.7% of cancer deaths in women and 6.0% of all cancer deaths for men and women together) [3]. The incidence of breast cancer

varies greatly around the world: it is lowest in less-developed countries and greatest in the more-developed countries. In the twelve world regions, the annual age-standardized incidence rates per 100,000 women are as follows: in Eastern Asia, 18; South Central Asia, 22; sub-Saharan Africa, 22; South-Eastern Asia, 26; North Africa and Western Asia, 28;

(a) (b)

Fig. 1.1 (a) screen-film unit, (b) CR film developer

South and Central America, 42; Eastern Europe, 49; Southern Europe, 56; Northern Europe, 73; Oceania, 74; Western Europe, 78; and in North America, 90 [5]. The number of cases worldwide has significantly increased since the 1970s, a phenomenon partly attributed to the modern lifestyles [6,7]. Breast cancer is strongly related to age with only 5% of all breast cancers occurring in women under 40 years old [8]. There were more than 41,000 newly diagnosed cases of breast cancer registered in England in 2011, around 80% of these cases were in women age 50 or older [9]. Based on U.S. statistics in 2015 there were 2.8 million women affected by breast cancer [2].

According to the Montenegrin registry, the number of newly diagnosed breast cancers is annually of 270 to 300 and there is an annual mortality of 70 to 80 women. This is a significant number compared with the number of population. Therefore, screening as a method for early diagnosis is a requisite.

It is universally acknowledged by experts in breast diseases that at the present, early diagnosis is the only way to have effective treatment and to get breast tumor mortality reduction.

1.2. Breast anatomy

The structure of the female breast Figure 1.2 is complex — including fat and connective tissue, as well as lobes, lobules, ducts and lymph nodes.

Fig. 1.2. Structure of the female breast

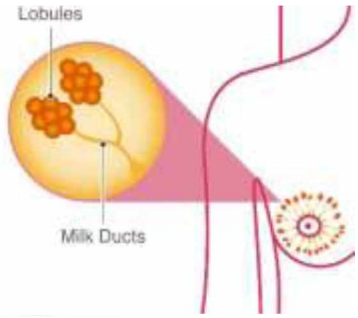

Fig. 1.3. Breast lobules and ducts

The female breast is mostly made up of a collection of fat cells called adipose tissue. This tissue extends from the collarbone down to the underarm and across to the middle of the ribcage. In the adipose tissue there is a network of ligaments, fibrous connective tissue, nerves, lymph vessels, lymph nodes, and blood vessels. Clusters of bean-shaped lymph nodes are fixed in areas throughout the lymph system and act as filters by carrying abnormal cells away from healthy tissue. A healthy female breast is made up of 12–20 sections called lobes. Each of these lobes is made up of many smaller lobules, the gland that produces milk in nursing women. Both the lobes and lobules are connected by milk ducts, which act as stems or tubes to carry the milk to the nipple. These breast structures are generally where the cancer begins to form (Figure 1.4).

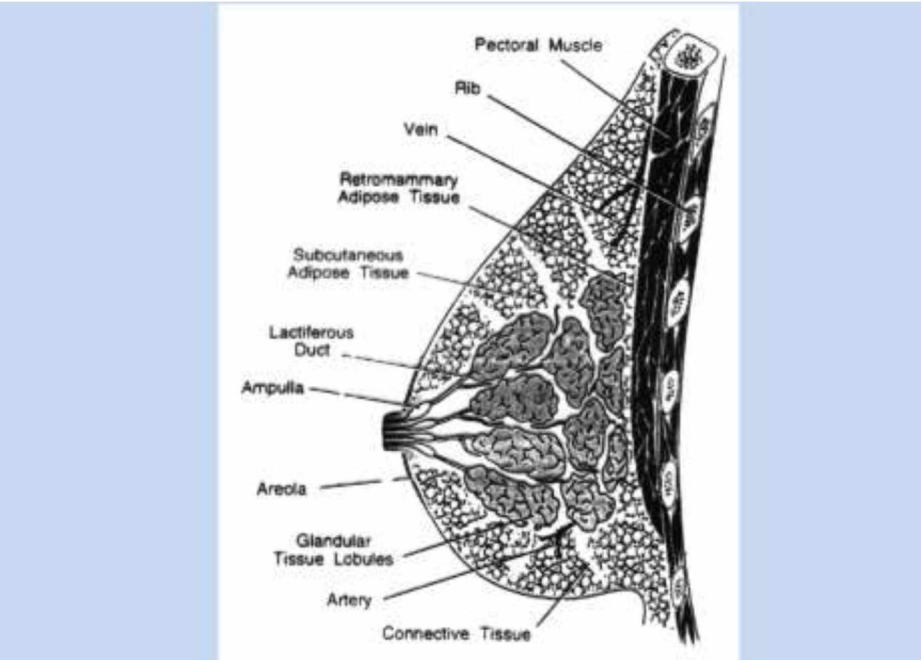

Fig. 1.4 A picture of a lateral image of a breast

The glandular tissue is slightly more dense than the surrounding background of fat. Glandular and adipose tissues have very similar atomic number (Z= 7.4 and 6.5, respectively). The distribution of fat and glandular tissue can be very variable. The internal part of the breast is composed of a mixture of glandular and adipose tissues, while the external part is adipose tissue (fat).

The type of breast cancer is generally determined by the origin of the growth of cancer cells, which is almost always in the lobes, lobules, or ducts.

The spread of the cancer is an important factor in determining the treatment. If the lymph nodes nearest to the cancer contain cancer cells, additional nodes are usually examined for the presence or absence of cancer cells to understand how far the disease has progressed.

Early signs of possible breast cancer visible at the skin are shown on the figure below (Figure 1.5)

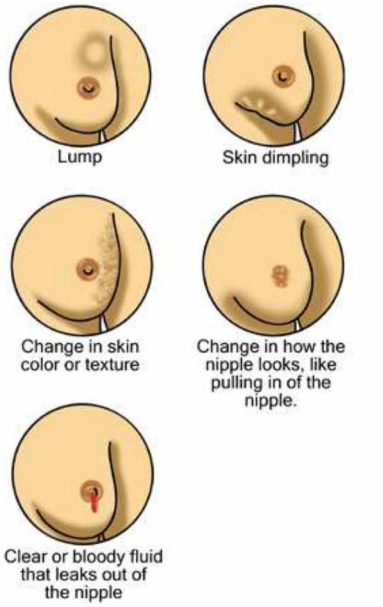

Fig. 1.5 Early signs of possible breast cancer

The difficulty in identifying a small tumor in mammal tissue is due to the fact that it is often contained in the glandular tissue, which has practically the same absorption coefficient as the tumoral tissue.

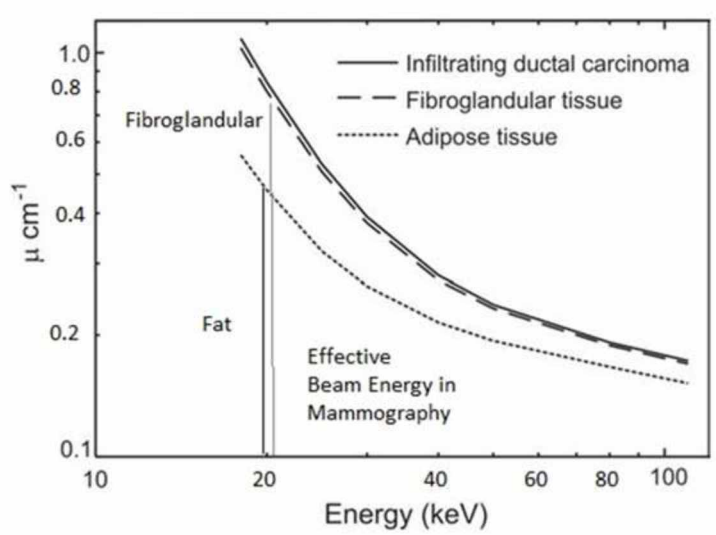

Fig. 1.6 Attenuation properties of breast tissues as a function of the Beam Energy

An important concept is the one of "glandularity", the proportion of glandular tissue to the total amount of tissue. As a general rule, in thin breast the proportion of glandular tissue is of the order of 50%, while the proportion decreases for thicker breasts. This breast composition is known to vary with the woman's age and breast thickness.

A tumor is more easily identified when it is contained in adipose tissue (fat), which, as we know, has an absorption coefficient considerably smaller than the one of the other soft tissues, and is therefore almost "transparent" to X-rays with energy between 15 and 20 keV.

In Figure 1.6, the attenuation properties of a ductal carcinoma can be compared to these of fibroglandular tissue and fat.

It clearly appears that to differentiate the various tissues a low energy beam is required; in the Figure 1.6 the two narrow lines point to the values of the linear attenuation coefficients for the three types of tissues around a beam energy of 20 keV.

Table 1.1 Density and Linear Attenuation Coefficient of the various breast tissues

Breast Tissue Type	Density g/cm^3	Linear Attenuation Coefficient at 20 keV (cm^1)
Mammary tissue		
Fibroglandular tissue	1.035	0.80
Adipose tissue (fatty)	0.93	0.45
Skin	1.09	0.80
Average breast (50% glandular, 50% adipose)	0.98	0.62
Lesion		
Carcinoma	1.045	0.85
Calcification	2.2	12.5

In Table 1.1 we have included the values of the density and the linear attenuation coefficient (at 20 keV) of the various tissues composing the breast.

The purpose of a mammography is to highlight the glandular tissue and two types of anomalies:

a) micro-calcifications, which have, at least for X-rays of about 15-20 keV, an attenuation coefficient that is substantially larger than the one of the healthy glandular tissue, but are very small (hundreds of microns or even smaller); there are often many of them, forming a cluster that can be very irregular. Individual calcifications can be rounded (benign) or more irregular (malignant). Detection of these microcalcifications is greatly interesting for diagnosing breast tumour.

b) nodules, which have greater dimensions (from a few mm to several cm), but possess both an attenuation coefficient and a density close to those of the healthy glandular tissue.

To highlight these two types of anomalies by means of radiography, optimal resolution (microcalcifications) and high contrast (nodules) are necessary.

The detecting system should therefore possess: high spatial resolution, excellent contrast sensitivity, high S/N ratio, freedom from artifacts and all that with a reasonable dose.

1.3. The basis of mammography

Generally there are five types of interactions with matterby photons which are considered in radiological physics:
1. Compton effect
2. Photoelectric effect
3. Rayleigh scattering
4. Pair production
5. Nuclear photoeffect

For the production of an electron/positron pair, a photon energy of at least 1.02 MeV is needed and photonuclear interactions are only significant for photon energies above a few million electron volts. Therefore, only the first three processes are relevant for X-ray diagnostic radiology. From these the first two are the most important, as they result in the transfer of energy to electrons, which then impart that energy to material in many (mostly small) coulomb-force interactions along their tracks [22]. Moreover the Compton effect results in the emission of scattered radiation, which gives rise to a lot of problems in medical imaging with X-rays, creating in this way blurring effect, while photo-electric effect gives higher contrast on the film. The photoelectric effect is the dominant process at the lower end of the diagnostic range of X-ray photon energies. In this energy range, it predominates over the Compton effect, particularly with respect to the energy transferred to the secondary electrons.
Since the tissues in the breast have a very similar densities and atomic numbers, it is not possible to apply conventional radiological techniques. In fact, if voltages between 70 and 100 kV would be used for X-ray imaging of the breast, Compton effect would prevail and there would be a minimal interaction difference between the various soft tissues of the breast. This is the reason why lower voltages are applied: this makes photo-electric interactions more abundant and allows tiny differences of absorption to be highlighted.
Differences in density can be visualized with both Compton effect and photo-electric effects. Density and absorption are proportional. On the contrary, absorption caused by differences in effective atomic number is still directly proportional to the effective atomic number, owing to Compton effect, whereas it depends on the cube of the atomic number for the photoelectric effect. It is furthermore possible to prove that photoelectric absorption prevails, in comparison with Compton diffusion, when low energy is applied.
This is why in mammography, in order to obtain X-ray low energies, tube supplying voltages between 20 and 35 kV are used. However, it is necessary to take into consideration that a voltage decrease also reduces the X-ray capability to transmit the tissue. Because of this lower energy, a higher photon number should be used, namely a rise in current (mA or mAs value). This causes an increasing dose to the breast.

Three types of mammography systems with different kind of detectors are generally employed: Screen-Film Mammography, Ful Field Digital Mammography and Digital Breast Tomosynthesis.

1.3.1. Screen – Film Mammography

The X ray unit must be specifically designed for mammography and include the following key features [44]:
—X ray tube with a nominal focal spot of 0.3 mm;
—If magnification mammography is performed (this capability should be present on systems that are used for diagnostic mammography and not exclusively for screening), a magnification stand and a second, smaller focal spot of nominal size ≤ 0.15 mm;
—Molybdenum target. Supplementary targets composed of materials such as tungsten or rhodium may also be available;
—Tube current $\geq$80 mA for a Mo target for contact mammography and $\geq$20 mA for magnification mammography;
—Beryllium exit window;
—Beam filter of molybdenum. An additional filter composed of rhodium is highly desirable;
—Motorized compression device;

—Readout of compression thickness and force is highly desirable;

—Automatic exposure control (AEC) with a sensor whose position is adjustable;
—Fine control of optical density on AEC;
—Moving grid designed for mammography;
—Focus–film distance ≥60 cm;
—Buckys that can accommodate film of sizes 18 cm × 24 cm and 24 cm × 30 cm are desirable.

1.3.1.1. X-ray tube and X-ray spectrum

The X-Ray tube is generally constructed with a metal envelope (instead of the more usual glass envelope) and with a thin Beryllium exit window. This design has the advantage of reducing or even suppressing extra-focal radiation.

The generator must have a very small focal point, e.g. 0.3 mm (less than half the size used in general radiography). More precisely, dual focus tubes are being used, with a focal point of 0.4 mm for general mammography and 0.1-0.15 mm for magnification mammography (that we will not discuss). The resulting heating of the anode will limit the tube current to a maximum of no more than 100 mA at 25 kV (to avoid melting the anode), so that long exposure times, up to 3 seconds or more, are needed. This implies that patient movement must be suppressed during this time interval.

Figure 1.7 shows a sketch of a mammography system.

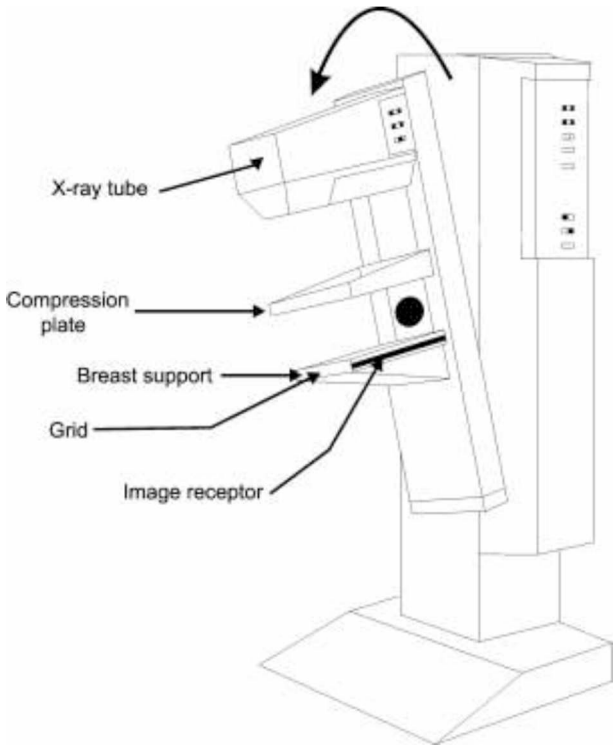

Fig.1.7. Sketch of a mammography system, showing the X-ray tube, the compression plate, the breast support and the detector (Image receptor)

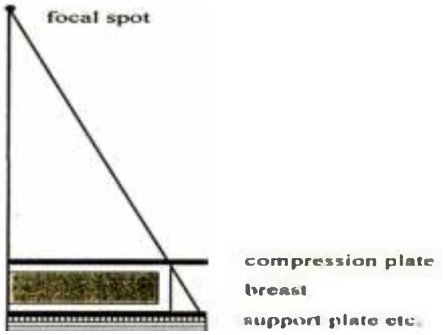

Fig.1.8 Geometry of mammographic exposures

Figure 1.8 shows the geometry of mammographic exposures. The region of the figure labelled "support plate etc." contains the breast support, anti-scatter grid and image receptor.

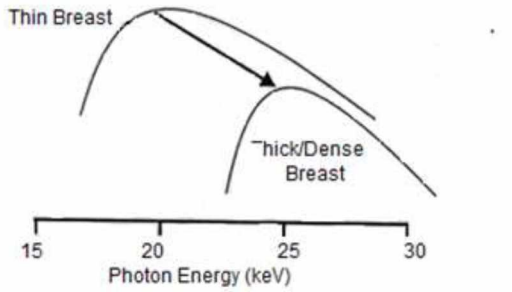

Fig. 1.9 X-ray energy spectra to examine thin or thick breast

The X-ray beam (as well as the applied tube voltage) must be optimized to the type of breast; thin and thick/dense breast should be imaged with different X-ray beams.
Figure 1.9 shows how the X-ray spectra can be chosen to optimize the absorption in a thin or in a thick/dense breast (in this picture, a Tungsten target is presumed and the X axis shows the different tube voltages).
The argument to use different X-ray energies to explore different thicknesses is obvious: the figure of merit of the lower energies is too low for the thicker breasts.

1.3.1.2. Filters

The beam produced by the anode, with the characteristic lines superposed, is still too broad. It can be made much narrower, with an appropriate choice of a filter.

It is well known that additional filters (in addition to the minimum filtration required by law) increase the X-ray beam half-value layer (HVL) and lead to decreases in patients' surface entrance dose (skin dose), when both the X-ray tube peak voltage Up and the system dose at the image receptor input are held constant [22].
The HVL is that thickness of a specified material (as a rule given in millimetres Al or Cu) which attenuates, under narrow beam conditions, X-radiation with a particular spectrum to such an extent that the air-kerma rate, exposure rate or absorbed dose rate is reduced to one-half of the value that is measured without the material.

The main purpose of a filter is to reduce the less optimal parts of the continuous spectrum, exploiting the effect of the K-edges.
This is done with an appropriate choice of the combination of the anode material with the filter material. Traditionally, mammography relies on the characteristic X-rays and K-edges of target/filter materials to produce a low energy spectrum around the ideal 16-22 KeV.

Additional filtration of the incident X-radiation (without changing the X-ray tube voltage) generally - with the exception of the special situation in mammography –leads to a reduction in image contrast. In mammography the image contrast is improved with increasing thickness of the K -edge filter located at the X-ray tube output, although the HVL of the incident primary radiation is increased. Reason for this effect is that especially the radiation above and below the K-edge is attenuated and therefore the HVL behind an object thickness of about 20 mm PMMA and more is reduced with increasing primary beam filtration [22].
The filter absorbs preferentially the low-energy radiation, that would otherwise be completely absorbed by the tissue increasing the dose and contributing little to image formation, as well as absorbing the higher energy X-rays which would otherwise degrade the subject contrast.

Two of the metals that are often used for the anode are: Molybdenum (Mo, Z = 42) and Rhodium (Rh, Z = 45).
Their relevant properties are shown in the Table 1.2.

Table 1.2 The properties of Molibdenum and Rhodium

	K-edge(keV)	Characteristic X-rays (keV)	
Mo	20	17.6	19.7
Rh	23.22	20.3	22.7

Often the filter material is the same as the anode material. An example is the Molybdenum anode coupled with a Molybdenum filter (Figure 1.10)

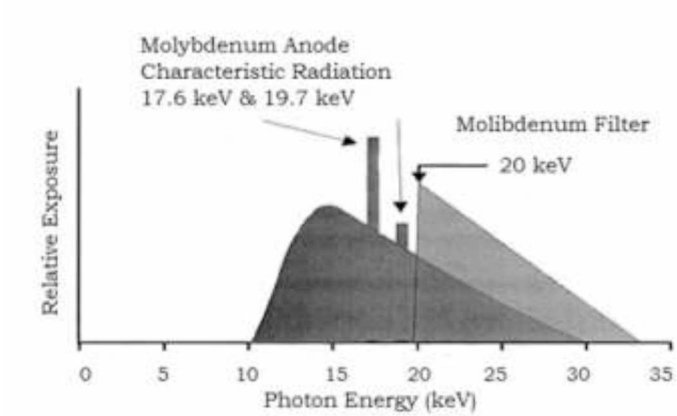

Fig.1.10 Mo anode coupled with a Mo filter

When a Molybdenum anode is used coupled with a Molybdenum filter, the portion of the spectrum above 20 keV is carefully filtered out by the Molybdenum filter (The K-edge is at 20 keV).

1.3.1.3. Screen-film detector

As for the spatial resolution of the detector, screen-film mammography systems are capable of ~15 lp mm^{-1} or better (up to ~20 lp mm^{-1}, compared with about 7 lp mm^{-1} for general radiography).

The two requirements of a high spatial resolution and of a very good contrast are often contradictory.
The shape of the signal is shown in four cases. Starting from the left (Figure 1.11):

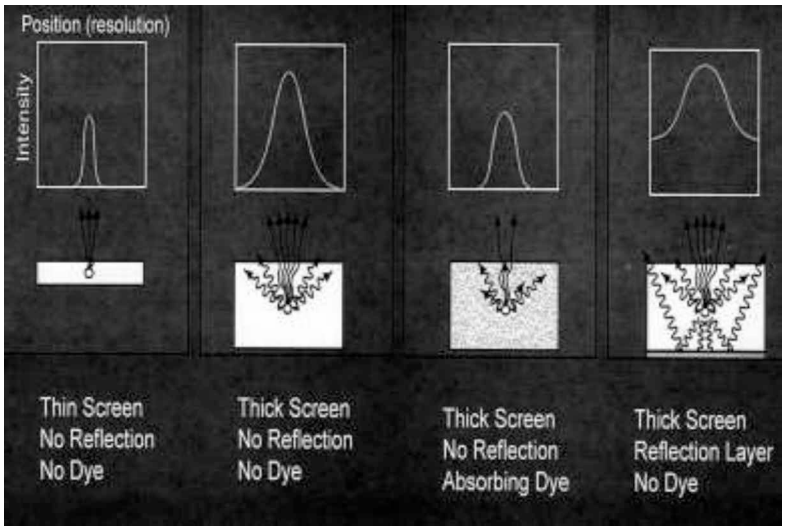

Fig.1.11 Shape of the signal with different choices of the screen

a) a thin screen without a reflection layer and without a dye; the spatial resolution is good, but the sensitivity is low;
b) a thick screen without a reflection layer and without a dye; the sensitivity is good, but the spatial resolution is low;
c) a thick screen, without a reflection layer but with a dye; the sensitivity is good, and the spatial resolution is reasonable;
d) a thick screen, with a reflection layer but without a dye; the sensitivity is very good, but the spatial resolution is very bad.

The choice (c), namely a thick screen with an absorbing dye, appears to be the best compromise between spatial resolution and sensitivity.
Obviously the dye, increasing the spatial resolution, slows the speed of the film.

1.3.1.4. Compression plate

As shown in Figure 1.8, a compression plate opposite to the breast support can be noticed.

The compression plate can be made from a thin plate of a polycarbonate and has the function of compressing the breast.
The main reason to use a compression plate is a consequence of the shape of the breast: the X-ray beams cross sections of the breast that have different thicknesses; this would ideally require beams of different hardness to penetrate these different thicknesses.
To avoid this inconvenience, the breast is compressed, in order to "equalize" and reduce its thickness and therefore to lower the absorbed dose, especially due to the use of lower energy radiation (photo-electric effect).

Moreover, the compression plate holds the breast during the exposure (as it was said, the exposure times can be quite long due to low mA) – and this reduces motion unsharpness. The typical compressed breast thickness is 40-50 mm, and rarely greater than 80 mm. There are other advantages such as inducing a spread of the tissues making lesions better visible and reducing the amount of scatter radiation. Typically, compression reduces the scatter-to-primary ratio from values of the order of 0.8-1 to values of the order 0.4-0.5 (a reduction with a factor 2).

1.3.1.5. System for automatic exposure control

Mammographic images should have the same overall optical density in all patients, regardless of their breast size and glandularity
This can be achieved with an automatic exposure controller (AEC). This is an operational mode of an X-ray machine by which the tube load is automatically controlled and terminated when a preset radiation exposure to a dose detector located under the image receptor is reached. Some more sophisticated equipment also allow the automatic selection of tube voltage (kV), target and filter materials [10].

Obviously, the film development system and the AEC are linked: the AEC has to guarantee the proper exposure of the film.
If exposure is not correct, breast structures will not be detected on the image with the highest possible leading to a loss of important information for tumour diagnosis.

1.3.1.6. Optical density

The optical density is a measure for the degree of film darkening. Technically it should be called "transmitted density" when associated with transparent-base film since it is a measure of the light transmitted through the film. Optical density is the logarithm of two measurements: the intensity of light incident on the film (Io) and the intensity of light transmitted through the film (It).

$$D = log \frac{Io}{It} \tag{1.1}$$

The values of the optical density of the film are in general comprised between 1.5 and 2.5. The contrast improves as OD increases up to 2.0-2.5. High contrast (high gamma) films are used; this is critical to ensure that exposure factors are matched to the film.
In Figure 1.12 the shapes of the optical density for a general radiographic film and for a mammography film are compared.

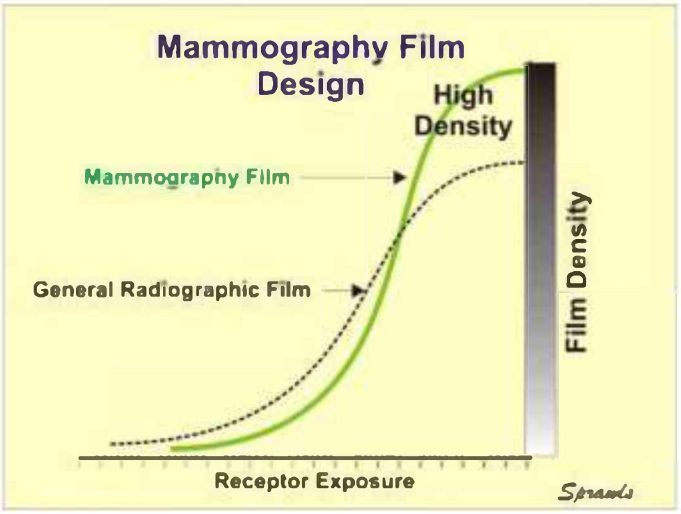

Fig. 1.12. Shape of the optical density for a general radiographic film compared with a shape of the optical density for a mammography film

1.3.1.7. Scattered radiation and grid

In mammography, the scattered radiation degrades the quality of the image. In fact, unless scatter is controlled, only 40-75% of the possible contrast is imaged in mammography. It is therefore necessary to employ special mammography grids.

The moving anti-scatter grids are incorporated in the support platform (Bucky) to improve image contrast. These Mammography grids transmit 60-70% of primary X-rays and absorb 75-85% of the scattered X-rays.
Two kinds of grids are employed: Conventional Linear Grids and High Transmission Cellular Grids (HTC Grids), shown in Figure 1.13.

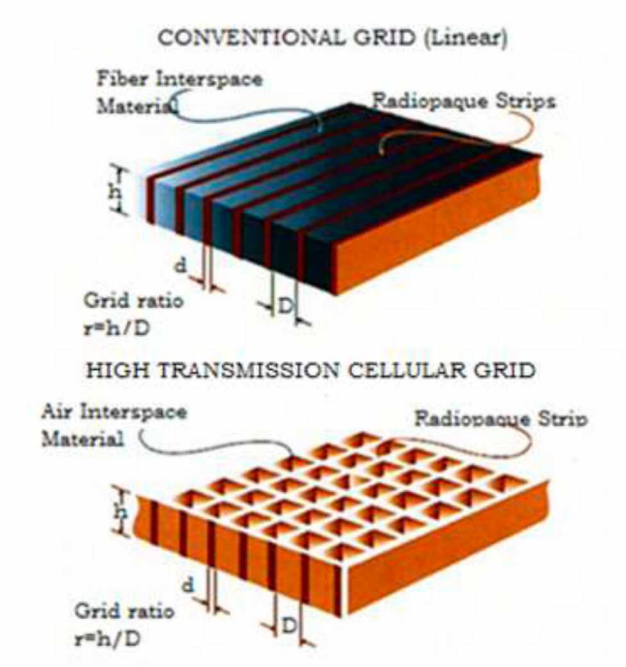

Fig. 1.13 Two types of grids: Conventional Linear Grid and High Transmission Grid

In the conventional Linear grids, narrow linear strips (thickness = d) of radiopaque materials (usualy Copper) are separated by wider linear strips (thickness = D) of Carbon Fiber Interspace Material. The grid has a thickness = h. The grid ratio is defined as r = h/D. The X-rays can go through the interspace material and are absorbed in the radiopaque strips. In the HTC grids, "honeycomb cells" of interspace material (Air) are enclosed by radiopaque material (again Copper). Thickness and grid ratio are defined as before.

1.3.2. Digital Mammography

Screen-film systems are still limited by the fixed dynamic range of the film. In addition to the SF (Screen-Film) technology, digital detectors are also used in mammography. Digital Mammography is often called Full Field Digital Mammography (FFDM).
In digital mammography, the screen-film combination is replaced by a detector that samples a finite number of locations and procedures an electronic signal for each location. The magnitude of each signal is related to the transmission of X rays through the breast, and is digitized and stored in computer memory [1].
Digital detectors offer the following advantages over the screen-film detectors:

- Image acquisition and display are separated,
- Wide dynamic range; a Figure 1.14 compares the dynamical range of a film and a digital detector.

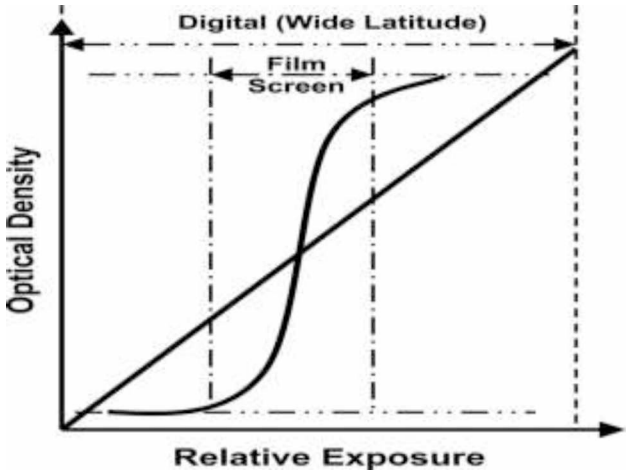

Fig.1.14. Comparison of the dynamical range of a film and a digital detector

- In digital mammography higher values of kVp (+3 kVp as compared to screen-film technology) can be used, since this systems can be operated with more freedom in terms of contrast and dose level. In addition, mage post processing can further increase the apparent image contrast.
- Digital mammography tends to use W/Rh combination that have shown to have a better figure of merit [48].
- Moreover, some digital mammography systems allow lower doses to be used for the same image quality; in practice, contrast resolution in digital is much better than film.

1.3.2.1. Types of digital mammography system

There are two generic types of detector system for digital mammography. One incorporates a photostimulable phosphor plate held in a cassete during exposure. It is frequently referred to as

computed radiography (CR) technology. Systems containing other types of detector, normally integrated into the system rather then enclosed in separate cassetes, are often referred as digital radiografy (DR or DX) systems.

a) Photostimulable phosphor system (CR)

This system employs an X rays photostimulable material, typically BaFBr [11,12]. After exposure, the phosphor plate is placed in a reading device where it is scanned with a fine laser beam (Figure 1.15)

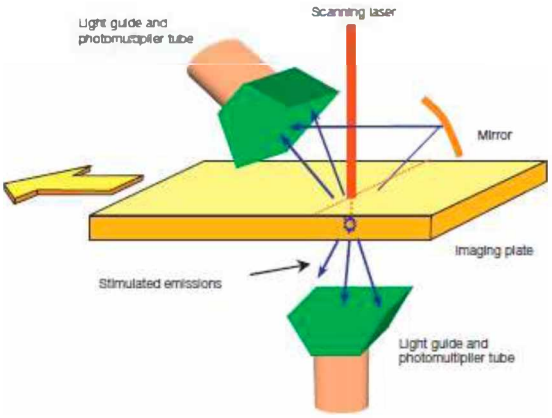

Fig.1.15. Schematic diagram of a dual sided reading CR unit. Some CR units may read the stored signal only from one side of the phosphor plate [1].

b) Flat plate CsI with photodiode array

In these systems, a CsI (Tl) phosphor layer is deposited directly onto a large area matrix of photodiodes formed on a flat plate amorphous silicon (a-Si, or α-Si) substrate (Figure 1.16.)

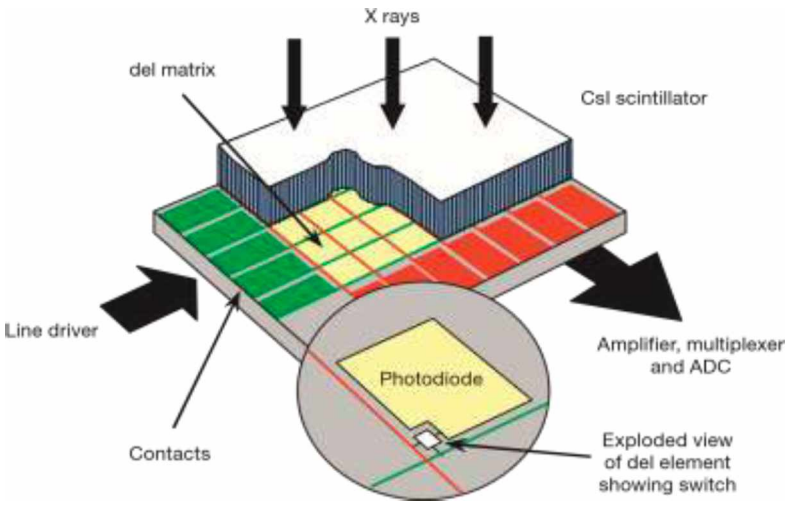

***Fig. 1.16. Indirect flat plate detector based on a CsI scintillator with amorphous silicon (a-Si) switching diodes or thin film transistor readout. The X rays absorbed in the CsI layer are first converted to light, which is then converted to a charge signal by the photodiodes and ultimately digitized. ADC — analogue to digital converter* [1].**

c) Flat plate amorphous selenium with electrode array

This system does not employ a phosphorous material. Instead, X rays are absorbed in a layers of amorphous selenium (a-Se, or α-Se), which is deposited on an array of electrodes formed on a large area a-Si substrate (Figure 1.17.).

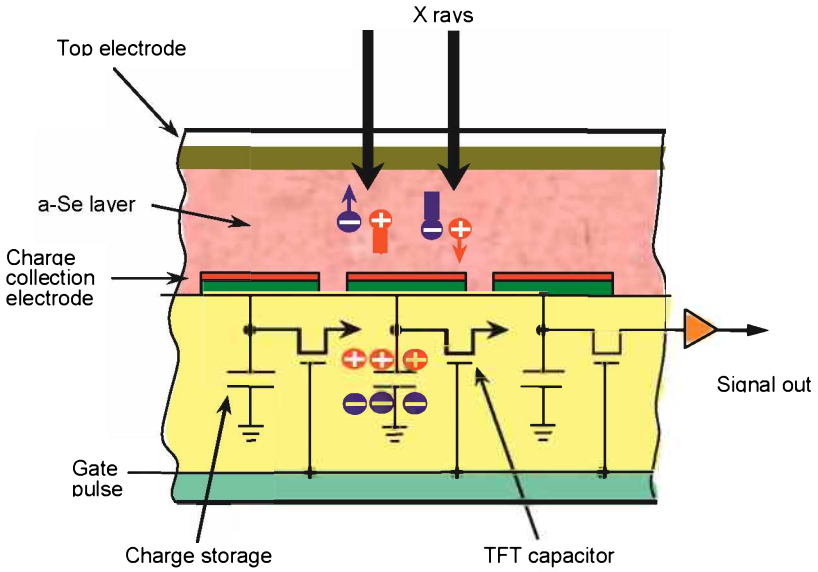

***Fig. 1.17. Direct flat plate detector utilizing amorphous selenium (a-Se) as the X ray absorber. When a voltage is applied across the a-Se layer, the charges produced are collected by the electrodes and digitized* [1].**

d) Slot scanning photon counting detector

In this system the energy of absorbed X rays is converted to charge in a set of many single-line detectors based on depleted crystalline silicon or on high pressure gas ionization strip (Figure 1.18.)

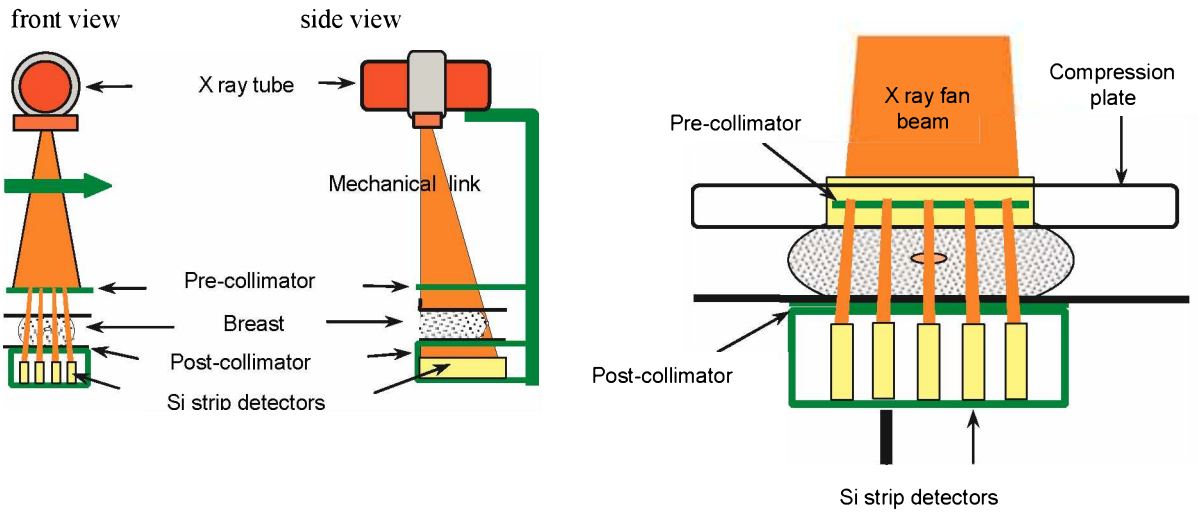

***Fig.1.18. Figure shows multi-slit scanning unit. Narrow slit collimators define fan beams that image part of the breast. Post-collimators further reduce the impact of scatter. The multi-slit device moves across the breast, ensuring that all the breast tissue is imaged. The crystal Si detector elements are also unique in that thay collect and record the energy from individual X ray quanta* [1].**

The detailed information about digital detectors employed in mammography systems are well explained elsewhere [1].

1.3.2.2. Automatic exposure control on digital mammography system

The design of the automatic exposure control (AEC) in digital mammography units differs from that in analogue mammography X ray units. The dose to the detector is no longer constrained to the relatively narrow dynamic range of the screen film combination. This freedom applies also to the choice of technique factors such as kV, and target and filter material. Generally, digital system will select X ray spectra that are more penetrating than would be the case with screen film systems. Moreover, greater detector dose can be used, if desired, leading to better image noise characteristics. Once the dose is increased beyond a noise limited image, the image provides very little subjective indication that the dose is excessive, and 'dose creep' may well result in long term increases beyond optimal levels.

Most DR systems use a measurements of the compressed breast thickness (produced by a sensor in the compression mechanism) to choose some of the technique factors (kV, target, filter) to be employed in the exposure. Some sophisticated AECs identify the area of greatest attenuation within a defined area of the detector during the trial exposure. This is then used to select an appropriate kV and filtration, and sufficient exposure to achieve predetermined pixel value, contrast or detector dose set by the manufacturer. The dose received by inhomogeneous real breast and the image quality may not be easily predicted from measurements of such physical quantities as the SDNR and MGD obtained using uniform blocks of polymethyl methacrylate (PMMA) [1].

1.3.2.3. Standard image formats

The DICOM Committee has created a standard for digital medical images known as DICOM MG for digital mammograms.

Two types of DICOM image format have been defined for digital mammography (Fig. 1.17). The DICOM ‘for processing’ image is the image initially provided by the detector with some basic corrections for detector non-uniformity and sometimes detector blurring. These images can then be processed to create DICOM ‘for presentation’ images, which are suitable for display on a monitor or for printing [1].

1.3.2.4. Image processing

Image processing of all digital mammography systems and processing operations may be applied at several stages of image formation (Figure 1.19).

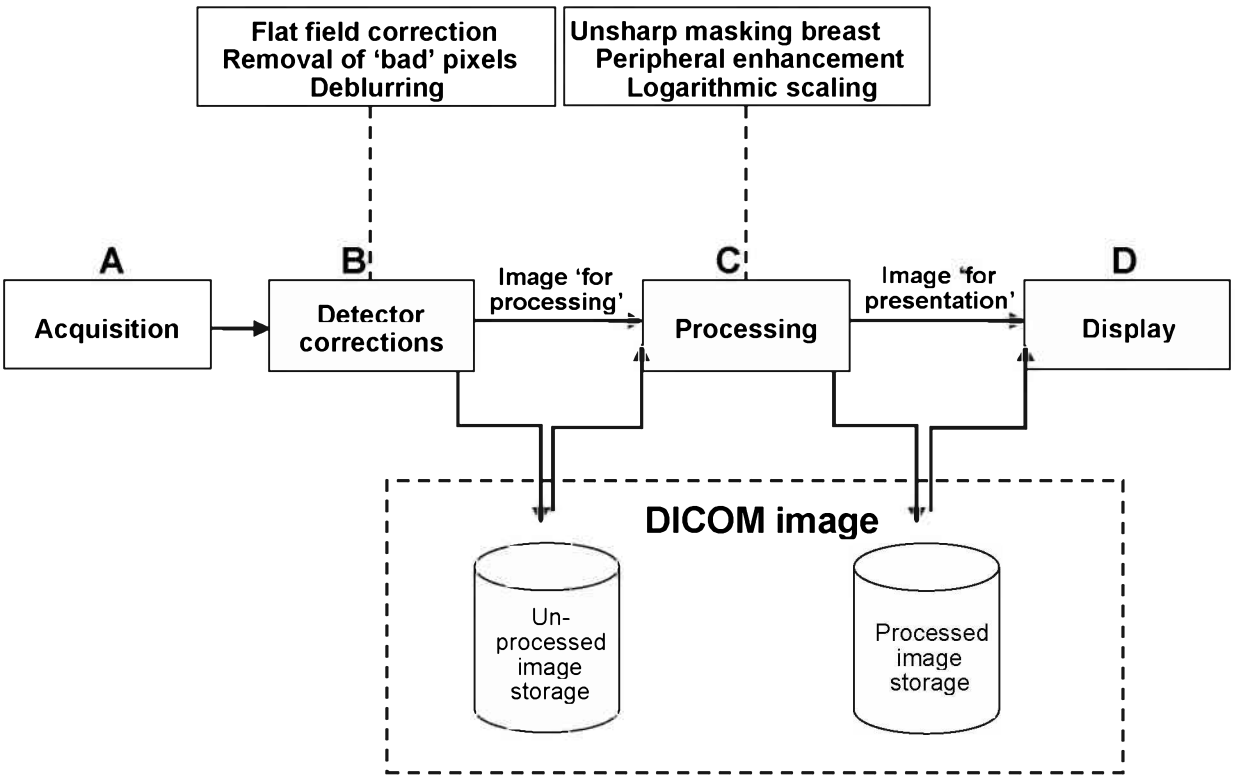

Fig.1.19. Concept of the DICOM 'for processing' and 'for presentation' formats **[1]**

1.4.2.5. Display system

The display must have a suitable number of high quality monitors (normally two 5 megapixels (MP) are recommended) [13] to allow viewing of as much of the mammogram as possible at the required resolution level. A single 3 MP monitor is recommended on the acquisition workstation. The quality must be high enough to allow the radiographer to assess the adequacy of the acquired image without having to walk to the radiologists workstation, which may be located considerably distance away.

1.4.3. Digital Breast Tomosynthesis System

Tomosynthesis system measures X – ray transmission through the breast over a limited range of angles, followed by reconstruction of a series of images of the breast reconstructed for different heights above the detector. These images represent breast tissue of the corresponding focal planes as well as a remaining portion of overlying tissue [14].

There are two types of DBT geometries:

a) Full-field geometry: DBT systems incorporating a detector as used in conventional 2D full field digital mammogrphy (FFDM), and an X-ray tube that rotates above this detector. A series of individual projection images, in which the whole breast is irradiated in each exposure, is acquired over a range of angles, as in Figure 1.20.

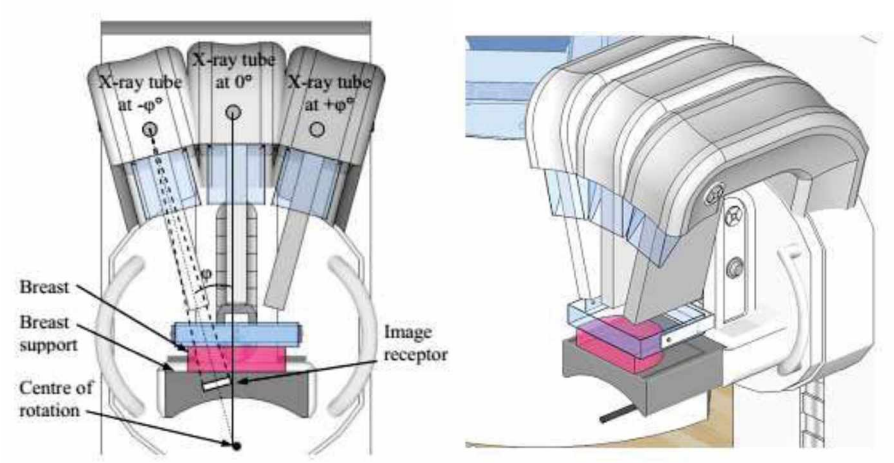

Fig. 1.20. Typical geometry used for a breast tomosynthesis system with a full field detector, showing three positions of the X-ray tube, the tube rotation angle φ and the projection angle Θ for the rotated position **[14].**

b) Scanning geometry: DBT systems utilizing a narrow collimated X-ray beam which scans across the breast as the X-ray tube rotates, and by which the breast is only partially irradiated at each position of the X-ray tube, as in Figure 1.21. Due to the design of the system and continuous readout from the detector, individual projection images might not exist.

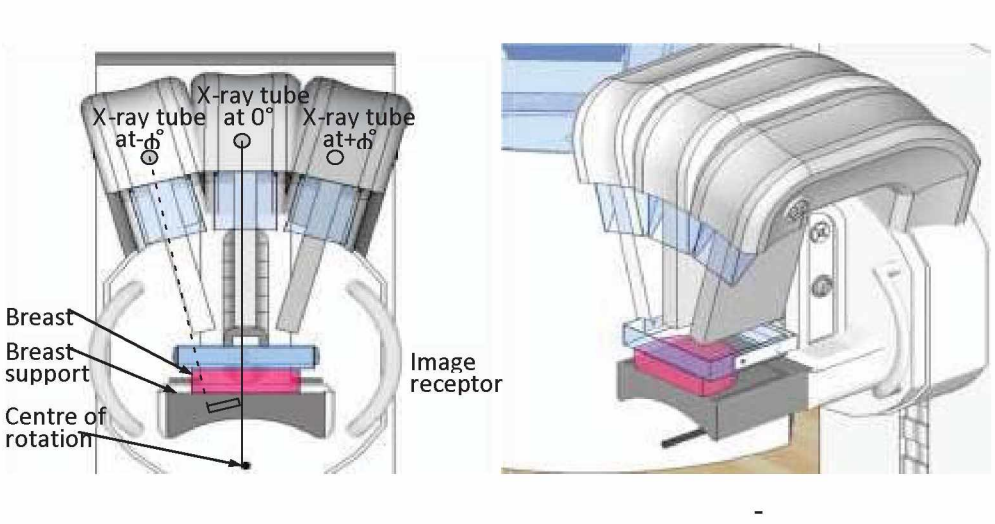

Fig. 1.21 Geometry of the scanning breast system with a narrow X-ray beam (currently under development) showing three positions of the X-ray tube (not to scale). In this system both the X-ray tube and image receptor rotate. The X-ray field is collimated to the image receptor. The limits of the X-ray field and the ray passing through the centre of rotation are shown **[14].**

DBT is an active area of research. Currently available DBT systems have very different characteristics, such as the angular range for projections, step and shoot versus continuous motion of the tube, new target/filter combinations, AEC working principles, different reconstruction algorithms, etc.

1.4. Dose quantities and terms in mammography QC

Absorbed dose (D), a physical non-stochastic quantity, is defined as the ratio:

$$D = \frac{d\varepsilon}{dm} \quad (1.2)$$

where de is the expectation value of the energy imparted by any ionizing radiation to the matter of mass, dm. Absorbed dose is expressed in joules per kilogram (J/kg) or gray (Gy) [15].

Average Glandular Dose - Reference term (ICRP 1987) for radiation dose estimation from X-ray mammography i.e. the average absorbed dose in the glandular tissue in a uniformly compressed breast. The AGD value depends on incident air kerma, X ray beam quality (HVL), breast thickness and composition. If breast thickness and composition are not known, AGD can be referred to a standard breast [10].

Contrast to Noise Ratio - The CNR is calculated as follows for a specific test object (e.g. a squere of 0.2mm Al thickness on 45 mm PMMA) [10] :

$$CNR = \frac{mean\ pixel\ value\ (signal) + mean\ pixel\ value\ (background)}{\sqrt{\frac{standard\ deviation\ (signal)^2 + standard\ deviation\ (background)^2}{2}}} \quad (1.3)$$

Del - Discrete element in a DR detector [10].

Diagnostic Reference Levels (DRLs) - a form of investigation level [16]. Perhaps the most succinct definition comes from the Council of the European Union, which stated that DRLs are dose levels that *"are expected not to be exceeded for standard procedures when good and normal practice regarding diagnostic and technical performance is applied"* [17].
Diagnostic reference levels are not dose limits. Diagnostic reference levels are used as a trigger to identify those facilities using unusually high doses in a specified radiologic procedure, for which optimization actions are needed [18].
Diagnostic reference levels are indicators for the typical practice in a country or in a region.
For diagnostic radiology, national and regional diagnostic reference levels are usually set at the 75% percentile of the distribution of typical doses for the sample.

Exposure time - The time between the first and last moment that primary X-rays reach an individual part of an imaged object [10].

Half Value Layer - Thickness of absorber which attenuates the air kerma of (nonmonochromatic) X ray beams by half. The absorber normally used to evaluate HVL of low energy X-ray beams, such as mammography beams, is high purity aluminium (≥ 99.9%) [10].

Kerma - the physical, non-stochastic quantity kerma (K) is related to the energy transferred from uncharged particles to matter. Kerma is the acronym for kinetic energy released per unit mass. It is defined as:

$$K = \frac{d\varepsilon}{dm} \quad (1.4)$$

where the quantity dε is the expectation value of the energy transferred from indirectly ionizing radiation to charged particles in the elemental volume dV of mass dm. The SI unit of kerma is joules per kilogram (J/kg), which is given the special name gray (Gy) [15].

Air Kerma - Quotient of dEtr by dm where dEtr is the sum of initial kinetic energies of all the charged ionising particles liberated by uncharged ionising particles in a mass of air dm (adapted from ICRU 1980). The common unit for air kerma is milliGray (mGy) [10].

Modulation Transfer Function (MTF) - Function, which describes how the contrast of image components is transmitted as a function of their spatial frequency content [10].

Noise - Fluctuations in pixel values which are unrelated to the imaged object. The standard deviation in a ROI in the output image is taken as a measure of noise [10].

Noice Power Spectrum (NPS) - Function which describes image noise as a function of spatial frequency [10].

Optical Density - Logarithm (base 10) of the ratio between light intensity produced by a visible light source and perpendicularly incident on a film (Io), and light intensity transmitted by the film (I) [10]:

$$OD = \log_{10} (Io/I) \quad (1.5)$$

Pixel - Picture element, the smallest unit in the image [10].

Pixel value - Discrete value assigned to a pixel, in mammography systems the number of pixel values range from 1024 (10-bits) to 16384 (14 bits), depending on the detector [10].

Pixel value offset – Constant value that is added to the values of all pixels [10].

PMMA - The synthetic material polymethylmethacrylate. Trade names include Lucite, Perspex and Plexiglas [10].

Signal to Noice Ratio (SNR) - The SNR is calculated as follows for a specific ROI[10] :

$$SNR = \frac{mean\ pixel\ value - pixel\ value\ offset}{standard\ deviation\ in\ pixel\ value} \quad (1.6)$$

Spacial Resolution - Describes the smallest detectable detail at a defined contrast level to a given background [10].

Tube loading - Product of the X-ray tube current (milliampere, mA) and the exposure time (seconds, s). It is quantified in units of mAs [10].

Tube potencial - The potential difference in units of kilovolt (kV) applied across the anode and cathode of an X-ray tube during a radiographic exposure [10].

2. Objectives of the thesis

2.1. Introduction to QC

Mammography is technically very demanding and requires close attention to every step in its performance. Quality control is necessary even if the best equipment is used. As for all X-ray examinations, and of special importance when investigating a large population of women, the relationship between radiation risk and diagnostic accuracy must be optimized.

It has been well established that to achieve high quality mammography, the following elements are essential:

(1) Well trained and experienced personnel (radiologist, radiographer, medical physicist);
(2) Modern, well designed equipment;
(3) Equipment in good working order;
(4) Proper positioning and technical factors for exposure;
(5) Appropriate image viewing conditions [1].

An effective quality assurance (QA) programme is necessary to ensure that all of these elements remain in place over time. The part of this programme that is concerned with the technical aspects is referred to as quality control (QC) [1].

In Montenegro mammography is operational since about fifteen years, thanks to the donation of thirteen analogue mammography devices to public health units. One digital mammographic unit with tomosynthesis and stereotactic biopsy has been donated to the Clinical center of Montenegro.

A regulatory requirement in Montenegro is that QC tests of mammography units should be performed on an annual basis or after significant maintenance services. Basic controls of radiation protection should be performed by independent technical service but don't include the control of film-processing units, image quality and image viewing conditions.

In our country there is no experience with systematic quality testing. There is no baseline for quality and QC concepts are not well developed.

2.2. Purpose and objectives of the thesis

One of the purposes of this work is to analyze current quality assurance and quality control (QA/QC) practices and results in the field of radiation protection and medical imaging optimization in Montenegro and compare it with international standards. The Montenegro regulatory body faced a lot of problems: lack of a national legal system in this field, expertise, appropriate equipment etc. The method of analyzing is a holistic one, starting from the law, regulations and decisions through the protocols of quality control and finishing with the reports and database of important parameters and data.

The overall objective of this thesis is to investigate and improve methods for evaluation of average glandular dose (AGD) and image quality in mammography and to correlate physical

and technical quality to clinical image quality. The practical guidance will help the regulatory agency of Montenegro to certify sites with proper installations, practices and controls. The national dose reference levels had to be determined in accordance with international standards on dose and image quality in mammography.

Specific objectives we aimed for were:
- evaluation of the technical situation of the Montenegrin mammography systems;
- improvement of methods for evaluation of average glandular dose (AGD) and image quality;
- establishment of national dose reference levels from data acquired according international standards;
- verification of reliability of automated filter measurements with the MagicMax multimeter.

Understanding the relationship bewteen image quality and radiation dose is a prerequisite to any optimization in medical diagnostic radiology. Image quality should be linked with specific medical tasks. In mammography, a good visibility of micro-calcifications and small masses in the breast glandular tissue is required. The quality of the various components of the imaging chain has influence on all this.
According to the ALARA concept, the image quality must be sufficient for the medical task while radiation exposure has to be minized. There are a lot of quantities which can describe and quantify the image quality, like contrast, sharpness, noise, signal-to noise ratio, image quality index etc. These quantities depend on the dose, X-ray tube assembly, radiographic unit, image receptor and patient characteristics which further depend on various other parameters. The number of parameters, with an influence on image quality, further increases if digitization or digital mammograms are used with different image processing software etc. We published a paper *Mammogram restoration by using Wiener filter* where we show selected determining parameters among many, in order to obtain a high-quality digital image. It is clear that some statistical approach can be used to discover correlation among this data and parameters. For example knowing MTF (Modulation Transfer Function) of the unit and estimation of sort and magnitude of the noise can significantly improve image quality with the same exposure. Different QA guidance documents contain minimum requirements for image quality, but they don't explain the links among different quantities, and they don't tell how to optimize a complete system.

Breast tomosynthesis is a new breast imaging modality with huge potential but a so far unproven impact. There are different ways to use tomosynthesis: as breast cancer screening technique; as add-on to 2D mammography during screening; to screen specific parts of the population like young women or high risk women; in diagnostic settings only; to replace MRI; etc. An evidence based choice is required to guide future investments and ensure best use of the available technology. In the group of the remote mentor, new test methodologies are being developed to find out the potential role of breast tomosynthesis by a new type of strictly comparative study between different breast imaging modalities. For our DBT mammograph we explored emerging QC methods currently used in the EU. Some of these measurements are presented in this thesis.

2.3. Steps and outputs of this project

Steps taken during the project:
- Collected specifications of all existing screen-film mammographic devices in Montenegro (15 units) and performed a first set of measurements and tests, according to The European

Protocol for the Quality Control of the Physical and Technical Aspects of Mammography Screening;

- Visited the relevant center in EU (in Belgium) to learn how to practically evaluate dose and image quality in mammography (European Protocol on Dosimetry in Mammography-EUR1623); Performed HVL measurements with a number of QC devices on three DBT mammographs in order to estimate whether the MagicMax dosemeter measures the correct HVL value, even when using only a single exposure. The MagicMax is new QC device we got through a Technical cooperation with the IAEA. As far as we know, the use of this new device that can extract several parametrs from just one exposure, had not been validated. We Estimated the method of HVL determination and conducted validation of automated filter measurements
- Started common activities with the remote mentor via the creation of a QC network;
- Conducted all the tests of the QC protocols on existing mammography devices in Montenegro; For the first time in Montenegro HVL was determined for all units and patient dose was estimated. We determined optical density and image quality using an anthropomorphic phantom.
- The restoration of digital mammograms, as a pre-processing tool, using deconvolution procedures, was analyzed. It uses the Modulation Transfer Function (MTF) of the mammography device and the estimation of the mammogram's noise. Wiener filter is used, as the most objective mathematical procedure in mammograms restoration by deconvolution. Using a MATLAB program, the deconvolution procedures were conducted in two ways with different levels of approximation.
- Created quality and dose awareness among all radiologists and radiographers taking part in the screening program;
- Analyzed results of measurements and proposed national dose reference level with a plan for optimization.

The goals we achieved (on the national level) thanks to this project:

- We created a database reflecting the current situation in terms of dose and image quality in mammography in Montenegro;
- We established guidance for dose optimization and image quality improvement in mammography;
- We established the national dose reference level.

3. Validation of new instrumentation for beam quality measurements

3.1 Uncertainties in Half Value Layer Determination in Mammography

One of the most relevant quantities for patient-dose estimation in mammography is the half value layer (HVL), as it has been used to characterize the radiation quality. It is defined as the absorber material thickness necessary to reduce the X-ray beam intensity to half of its incident value. Nowadays different solid state-dosimeters have the ability to obtain the HVL value with a single X-ray exposure; that is distinct advantage over the need to make a series of measurements with thin Al attenuators [19,20]. The vendor of our device did however not explain in detail how they obtain HVL value from one X-ray exposure, and the error on the measurement or the approximations were not documented. The problem arises when significant discrepancies in HVL determination are found, even in the cases where the measurements with Al attenuators were done in accordance to the well prescribed methodologies and procedures [21]. In this work a critical analysis of the methodology for evaluating the x-ray half value layer was conducted.

3.1.1. Method

The traditional method of deriving HVL by using a set of, usually, seven pure aluminum sheets of 0.1mm of thickness was conducted. Air kerma was measured versus the thickness of aluminum barrier, placed between the X-ray source and detector [21]. The measurements were repeated on different mammography units with different anode-filter combinations to get rid of machine specific confounding factors. Three different calibrated solid state detectors and one ionization chamber were used for the same reason.
The experimental data, were then fitted with an exponential function, using the MATLAB curve fitting toolbox:

$$f(x)= a\cdot\exp(-bx)\ (1) \qquad (3.1)$$

Finally, HVL was derived, simple, as

$$HVL= 0.693/b \qquad (3.2)$$

The same procedure of HVL determination was firstly applied to all measured data (eight points), and then, for the first four and finally for the last four points.
The HVL were measured at tube voltages of 24, 26, 28, 30, 32 and 35kV.

3.1.2. Results and analysis

The first task was checking, how well an exponential function fits experimental data. The typical experimental data and fitting curve is shown in Figure 3.1. Although the energy spectrum of the x-ray source is not monochromatic, all experimental data fitted well to an

exponential function (correlation coefficients were in most cases better than 99%). It means that the assumption about applying the exponential attenuation law, also to polychromatic x-radiation, was valid. The similar situation was referenced for the spectrum of other mammographic units [22], where instead of the attenuation coefficient for mono-energetic radiation, the effective attenuation coefficient was used.
The second task was the estimation of the uncertainty for HVL determination. The MATLAB curve fitting toolbox gives the uncertainty for determination of the free parameter b, and the uncertainty of HVL was the easily calculated from equation 3.2. The uncertainty of HVL determination was less than 10% (usually less than 6%) (Figure 3.2). These results are very important information for comparing HVL values, obtained from different detectors and different methodologies. In other words, for the comparison of different values of HVL, one has to know whether these differences are significant or not significant.
Although, a lot of work was done analyzing the accuracies, repeatability and energy dependences of the radiation dose measurements by the different radiation detectors [23], and other factors [24], they are not the critical factors in HVL determination, since the HVL was derived from the relative measurements i.e., it is not a function of parameter a (equation 3.1).

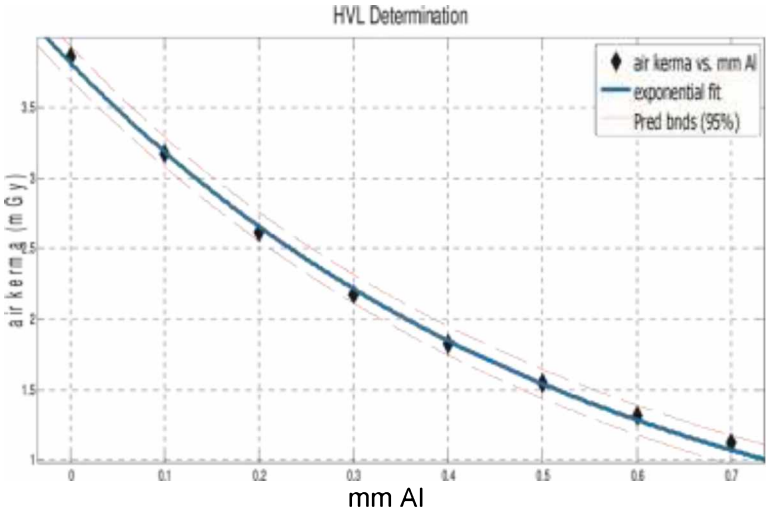

Fig.3. 1. HVL derived from eight measuring data

The third task was simply to repeat the above procedures but now taking into account only the first four experimental data, or only the last fours.
It was found that the most critical factor is the number of experimental data. The HVL, determined from the first four data, was significantly different from HVL values obtained from all eight points. The same situation was observed for the comparison made with HVL, derived from the last four points. In every experiment three significantly different values of the HVL were obtained: the lowest, obtained from the first four data; intermediate value, obtained from all experimental data and the highest value, obtained from the last four points. The HVL is highly dependent of the number of experimental data and can be quite different if it was derived from the first four experimental points or the last four points (e.g. 0.35mm and 0.42mm). In some cases these differences were about 25%. We concluded that the X-ray beam was hardening by passing through aluminum sheets, thus these differences were effect of it.

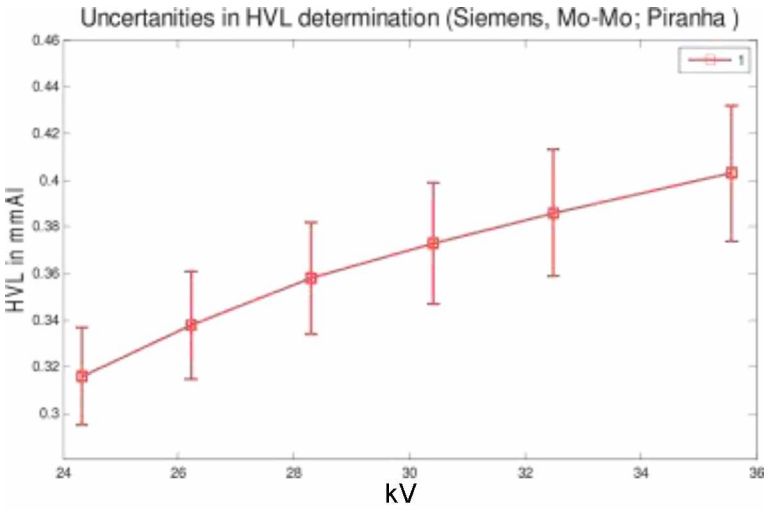

Fig. 3.2. HVL versus kV on a mammo unit and uncertainties

3.1.3. Conclusion

We have observed a strong dependence of HVL determination in mammography from the type and amount of measuring points making up the HVL measurements. It is found that the HVL determination highly depends of the used methodologies, and even within the same methodology, on the number of measurements. The discrepancies in HVL determination were sometimes more than 25%. Measurement procedures for HVL should be better specified, especially given that these days other anode/filters are used with higher HVL than in earlier days with mainly Mo/Mo.

3.2. Validation of automated filter measurements

The X-ray beam is a crucial part of an imaging system, linked with safety, thus beam quality is an important input parameter for patient dose calculations. Different parameters describing the quality of the X-ray beam. Obtain the necessary input parameters in a single exposure was a challenge until recently. New (solid state) dosimeters allow all-in-one shot data acquisition. This gives the opportunity to be verified:

- Can we trust kV measurements at all anode/filters and for the entire kV range?
- Are solid state dosimeters sufficiently corrected for (all) beam qualities?
- Actual dosimeters provide 'ready made' data on HVL from a single exposure… can we trust this?
- Is Robson's approach, a method used for extrapolation of energy response of tube output and HVL, also valuable for current anode/filter combinations?

3.2.1. Material and method

The aims of this work were to compare direct measurements of HVL to calculated values. In order to verify the validity of the new measuring equipment which gives a direct value of HVL from a single measurement, we performed a large set of measurements at different

mammography systems. Our study was part of a larger study that included several other dosimeters, the results of which will not be included in present study.
HVL measurements were made on two full field digital mammography systems with a range of target/filter combinations: Hologic Selenia Dimensions with W/Rh and W/Ag and Siemens with Mo/Mo, Mo/Rh and at different tube voltages (24, 26, 28, 30, 32, 35) kV.
For all exposures, a sheet of lead in rubber was placed on the breast support platform to protect the digital detector. The dosimeter was placed 6 cm back from the chest wall edge in the midline and the compression paddle was always in the beam.
For each target/filter combination, HVL was calculated using high purity aluminum (Al) filters.

In this study we compared data of calculated HVL using the values closest to the half dose point (as in the Euref protocol), next we calculated the HVL using all the points with a proper curve fit and we registered also the indicated auto calculated HVL from Magic Max QC equipment.

First we verified the kV measurements across the anode/filter combinations. Rationale: when using the same nominal kV, the same tube voltage is applied over the tube, irrespective of the anode/filter and therefore the kVp indicated by the device should be the same. This was tested for all devices that have different anode/filter combinations.

3.2.2. Results and analysis

3.2.2.1. Verification of kV measurements

Figure 3.3. shows the measurements for Hologic: measured kV-s for W/Ag versus the measured kV for W/Rh. As the same kV is applied, it was expected that the indicated, measured kV would be the same. The results are re-assuring for the device.

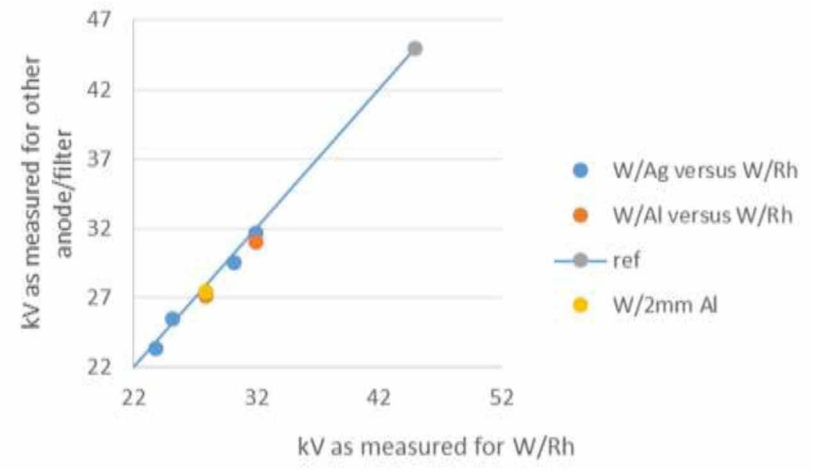

Fig.3.3. Verification of kV measurements across anode/filter combinations

3.2.2.2. Comparison between different HVL determinations

Figure 3.4. compared HVL values obtained with three ways: by curve fitting in MATLAB, by direct reading on Magic Max and calculated by EUREF formula from measurements. The study

was performed for different kVs and for the target/filter combination W/Ag on the Hologic Selenia Dimensions mammography system.

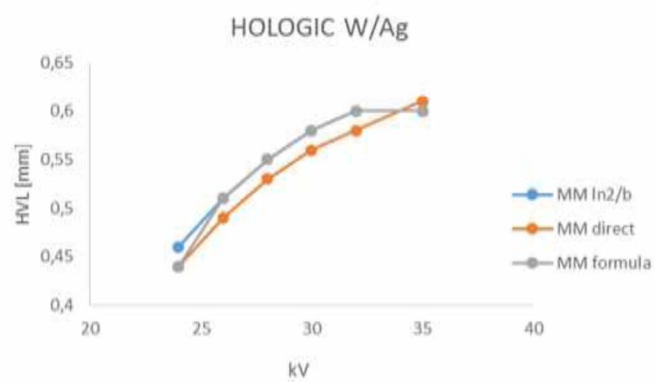

Fig.3.4. HVL versus kV obtained by curve fitting in MATLAB (MMln2/b), direct reading on Magic Max (MM direct) and calculated by EUREF formula (MM formula); all for target/filter combination W/Ag on HOLOGIC mammo system

Figure 3.5. shows as previous, but for target/filter combination W/Rh.

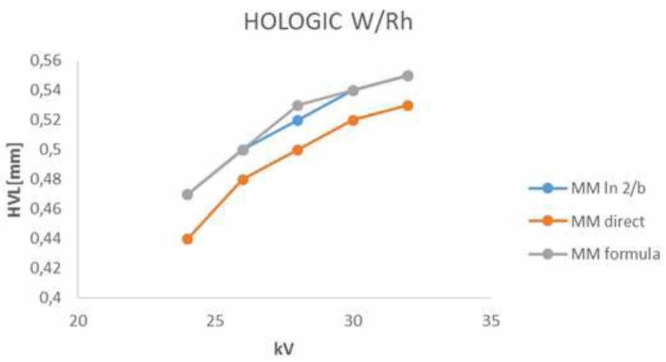

Fig.3.5. HVL versus kV obtained by curve fitting in MATLAB (MMln2/b), direct reading on Magic Max (MM direct) and calculated by EUREF formula (MM formula); all for target/filter combination W/Rh on HOLOGIC mammo system

Figure 3.6. shows comparison of HVL values versus kV for Mo/Rh target/filter combination on the Siemens Inspiration system.

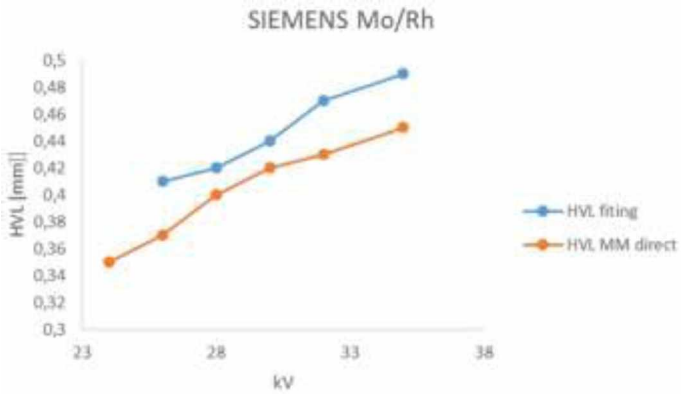

Fig.3.6. HVL versus kV obtained by curve fitting in MATLAB (HVL fitting) and direct reading on Magic Max (HVL MM direct); for target/filter combination Mo/Rh on SIEMENS mammo system

We illustrate the HVL measurements for 32 kV for Siemens with Mo/Rh target/filter combination. First, the calculations by our MATLAB toolbox (see previous chapter):
General model Exp1:

$$f(x) = a^* \exp(b^*x) \quad (3.3)$$

Coefficients (with 95% confidence bounds):

$$a = 3.664\ (3.203, 4.124) \quad (3.4)$$

$$b = -1.488\ (-2.051, -0.9252) \quad (3.5)$$

Goodness of fit or statistical data describes how well it fits a set of observations (calculated by MATLAB): Sum of Squared Errors: SSE=0.001334, Coefficient of Correlation: R^2= 0.9991, Root Mean Square Error: RMSE=0.03652

The difference between the direct HVL measurements of Magic Max from MATLAB curve fitting does not exceed the difference of 0.02 mm Al.
Estimate of standard deviation was approximately 0.1 mm Al thus we can conclude that direct HVL measurements of Magic Max are in the range of the errors of HVL determination.

3.2.3. Validation of Robson's formula

3.2.3.1. Method

In the breast screening program, regular assessment of the average glandular doses is conducted for all different parameters, like tube voltages and anode-filter combinations. It requires a lot of measurements and could be inadequate for a routine quality assurance program.

Robson [25] developed a method which can be stated as follows: A computer simulation of X-ray production and filtration has been used to produce data that allow the user to calculate the air kerma and HVL for any value of tube voltage (in the range 25-32 kV) from a measurement of the tube output and HVL for each target/filter combination made at a single tube voltage. This would be very practical in dose surveys, since many combinations of different factors require tedious, repetitious measurements. Our task is to check accuracy of this method.

Conventionally, the output of an X-ray tube in μGy mAs^{-1} is empirically related to the measured tube voltage by a relationship of the form

$$\text{Output}=A(kV)^n \quad (3.6)$$

where A and n are constants, with n typically taking a value between 2 and 3.
By taking the logarithm of each side, equation 3.6 reduces to the linear form given in equation 3.7 [25].

$$\log_{10}(\text{air kerma}) = n\log_{10}(kV) + \log_{10}(A) \qquad (3.7)$$

The calculated values of HVL were plotted against tube voltage [25] and the MATLAB curve-fitting program was used to fit second order curves of the form

$$HVL = a(kV)^2 + b(kV) + c \qquad (3.8)$$

through the data, where a, b and c are constants.
Robson tabulated the calculated values of constants a, b and n for a range of target/filter combinations.

3.2.3.2. Results

Here were presented experimental verification for selected combination – Siemens Inspiration system, Mo/Rh target/filter combination, Piranha measuring device.

In Figure 3.7. the logarithm of calculated air kerma is plotted against the logarithm of the tube voltage for selected combination.

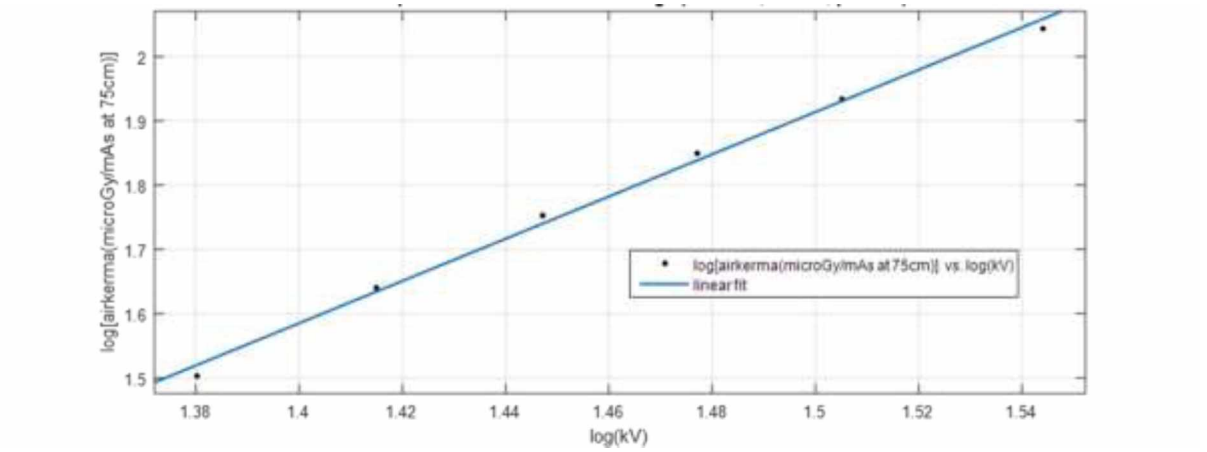

Fig.3.7. Plot of $\log_{10}$(air kerma) against $\log_{10}$(kV) for the Mo/Rh target/filter combination at Siemens Inspiration system.

The solid line is the best linear fit obtained in MATLAB (first order polynomial):

$$f(x) = p_1 * x + p_2 \qquad (3.9)$$

where p_1 is constant n, and p_2 is constant A from equation 3.7.

Coefficients n and A (with 95% confidence bounds) are n=3.286 (2.985, 3.587) and A = -3.015 (-3.455, -2.575) and goodness of fit: Coefficient of Correlation is: R^2= 0.9957, Sum of Squared Errors: SSE= 0.0008427, Root Mean Square Error: RMSE= 0.01451

Figure 3.8 shows HVL plotted against tube voltage for the same conditions we choose to present (Mo/Rh target/filter combination at Siemens Inspiration system, Piranha measuring device). HVLs were calculated by curve fitting in MATLAB with 95% confidence bounds and by Robson's formula, both for a range of kVps from 24kV to 35kV.

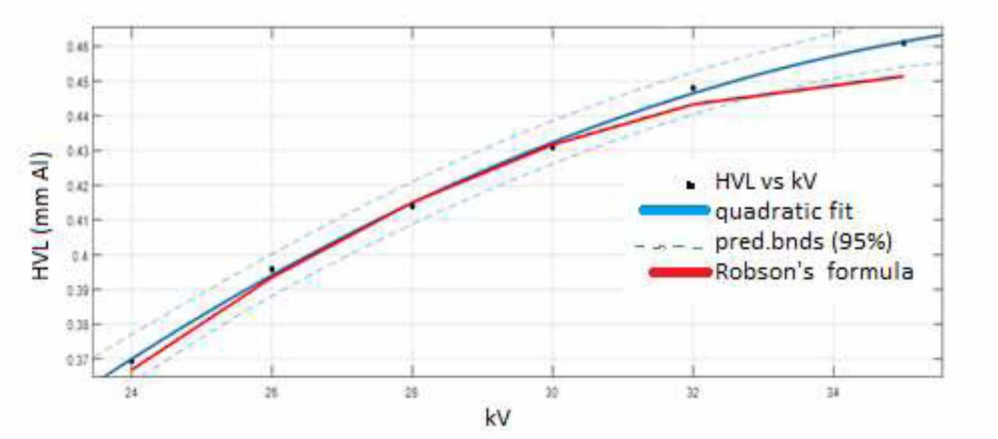

Fig.3.8. Plot of the half value layer (HVL) against tube voltage (kV) for Mo/Rh target/filter combination, on Siemens Inspiration system measured with Piranha measuring device

The blue solid line represent quadratic curve fitting in MATLAB (second order polynomial):

$$f(x) = p_1*x^2 + p_2*x + p_3 \qquad (3.10)$$

where p_1, p_2, and p_3 are constants a, b and c from equation 3.8.respectively.
MATLAB software were calculated the coefficients a, b and c (with 95% confidence bounds) as: a = -0.0004187 (-0.0005937, -0.0002436); b = 0.03301 (0.02267, 0.04334) and c = -0.181 (-0.3318, -0.03026), with goodness of fit: Coefficient of Correlation: R^2= 0.9986, Sum of Squared Errors: SSE=8.326e-06, Root Mean Square Error: RMSE=0.001666

The curves for Robson's formula and quadratic fit were of similar shape. Slight variations occurred above 31 kV.

Figure 3.9. shows results of the experimental verification of Robson's model for measured air kerma versus predicted air kerma, both measured at 50 cm FDD, for the Mo/Rh target/filter combination at the Siemens Inspiration mammography system, using the Piranha measuring device.

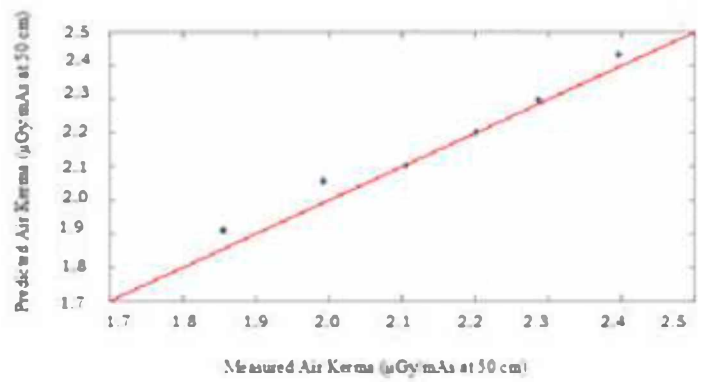

Fig.3.9. Verification of Robson's formula, measured air kerma vs predicted air kerma (Siemens, Mo/Rh, Piranha)

The red solid line is the line of the equality. It shows close agreement between the measured and predicted values of air kerma.
Coefficients n and A from equation 3.7 were calculated by using linear polynomial model (equation 3.9) and MATLAB software were calculated n = 3.286 (2.985, 3.587) and A = -3.015 (-3.455, -2.575) with 95% confidence bounds.

Figure 3.10. shows the verification of Robson's formula for measured and predicted HVL values, both obtained for the Mo/Rh target/filter combination at the Siemens Inspiration mammography system measured by Piranha measuring equipment.

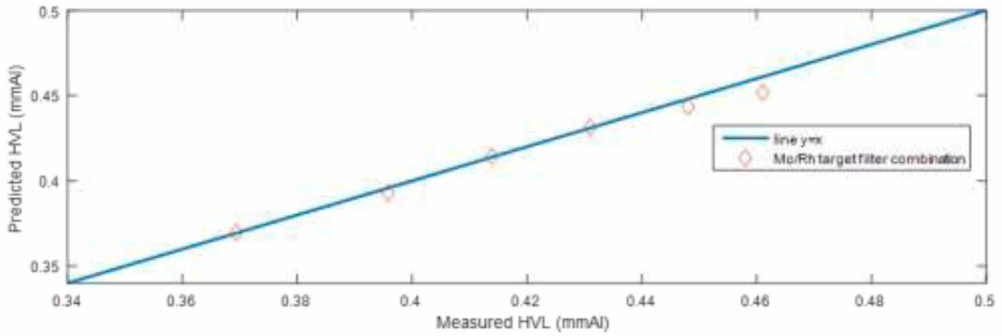

Fig.3.10. Verification of Robson's formula, measured HVL vs predicted HVL (Siemens, Mo/Rh, Piranha)

Blue solid line is line of equality x=y. It shows close agreement between measured and predicted values of HVL, also. The deviations for the HVL are: maximum value: σ_{max} = -2.08% and mean value: σ_{mean} = 0,49%.

3.2.3.3. Conclusion

It were calculated and compered the same measurements for a combinations for Siemens Inspiration and Hologic Selenia Dimensions systems, with Barracuda, Piranha and MagicMax measuring devices, with target/filter combinations of both systems (Mo/Mo, Mo/Rh, W/Rh, W/Ag). In all the cases close agreement between measured and predicted values of air kerma and half value layer confirm the Robson's model.

4. Mammograms Restoration by using Wiener Filter

4.1. Introduction

The goal of x-ray mammography is the identification of small abnormalities. This requires a sophisticated technique of using low-energy photons. To derive useful information from a mammogram, image processing plays an important role. Small details in mammograms, as micro-calcifications, may be the sign of cancer tissues and, need to be clearly distinguished from the very complex background i.e., the image of a woman's breast. To do this successfully, the quality of the imaging system is crucial. The quality of a unit depends on many factors, including the quality of the detectors of X-radiation. The influence of the image system, during image formation, is usually deterioration of the captured image, and needs restoration. The presence of non-avoidable noise makes this procedure complex from a mathematical point of view. The quality of an imaging system is usually characterized by its Point Spread Function (PSF) or its Fourier transformation MTF if the imaging system is linear shift invariant [22,49]. Under this condition, the PSF represents the image of an infinitely small detail in the object. Here we present a study about the effectiveness of restoration of digital mammograms, as a preprocessing tool, by using deconvolution procedures. To do this, the MTF of the mammography unit and mammogram's noise have to be known as the input parameters. The Wiener filter was used for image restoration by deconvolution [50].

4.2. Method

Image restoration is based on the attempt to improve the quality of an image through knowledge of the physical processes which led to its formation. In the same time, any image that is produced with an imperfect imaging system can be considered as a convolution of "true" image we are looking for, with the function which characterizes its imperfectness. To restore the "true" image, through the deconvolution (undo!) process, is quite complex and belongs to so-called ill-posed problems from the mathematical point of view [51]. It means that small fluctuations from the true values can make the solution unstable.
The MATLAB software was used to restore the image by deconvolution procedures, using the Wiener filter in two ways: 1. with a scalar estimate of the noise to signal power ratio (NSR). Only the total amount of power in the noise and in the "true" image is provided and their frequency dependence is not supplied; 2. with a frequency dependent estimate of the noise/power ratio. In both cases the MTF or the Point Spread Function (PSF) has to be known as an input function to the program. In practice, the resolution of an imaging system is determined by the imaging of a lead bar pattern (Fig.4.1). The higher number of line pairs per mm that are displayed separated from each other, the better is the resolution of the whole imaging devices. The MTF is obtained from the image of an edge phantom.

4.3. Results and analysis

The blurred, noisy image is depicted in Fig.4.1a). This is the raw image of the bar-pattern, convolved with Gaussian PSF 1 b) (standard deviation 2), and added white noise (zero mean and standard deviation approx. 10% of mean signal). The bar-pattern was used, instead of a real

breast, due to better visualization of the results. Namely, restoration process should increase spatial resolution and this case can be seen easily.
Restored images are depicted in Fig 4.2. a) using methodology 1, and b) using methodology 2.

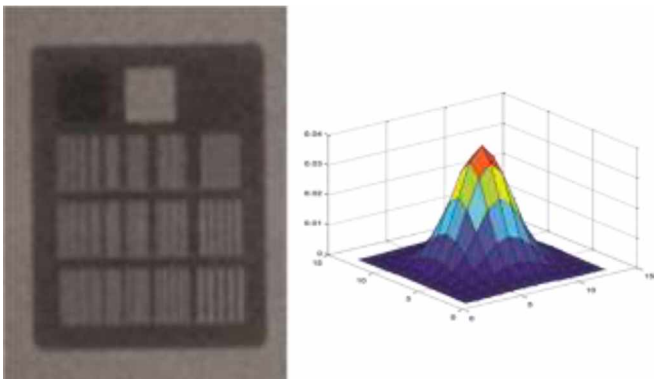

a) *b)*

Fig. 4.1. The blurred and noisy image of: a) the bar pattern; b) the model of the PSF

It is found that in the restored images, the spatial resolution is improved, although the best result is depicted in 2b) where a frequency dependent estimate of the noise/signal power ratio is done via respective autocorrelation functions.
Estimation of PSF and noise are important. The image of the bar pattern, particularly straight lines, can be used for estimation of the PSF. Namely, from one scan perpendicularly to a line edge (1-D profile) in the image of the bar pattern, a Line Spread Function (LSF) can be obtained. The derivative of this profile gives the 1-D PSF in that direction. Repeating the procedure perpendicularly to the previous direction, one can estimate the perpendicular 1-D PSF. Combining these two measurements, the 2-D PSF can be obtained [52].
A way for noise estimation is by using raw images of a homogeneous breast phantom (45mm PMMA). This allows to calculate a 2D noise power spectrum.

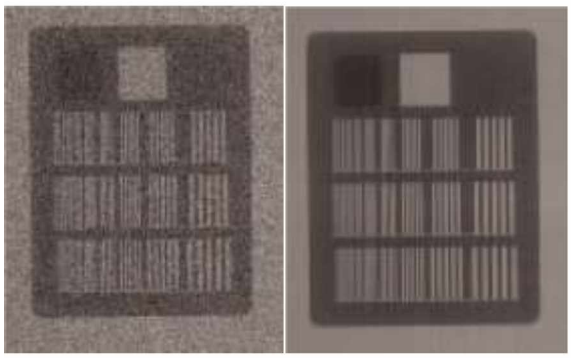

a) *b)*

Fig. 4. 2. The restored images by using: a) methodology 1, and b) methodology 2

4.4. Conclusion

"Cleaning" the image from the imperfectness of the imaging system (x-ray mammography unit), is the main preprocessing task before any further enhancement and processing. We have shown on the test image that the use of the Wiener filter is promising. We did not observe any obvious artefacts created by the procedure.

5. Implementing QC in Screen – Film Mammography in Montenegro: first results

5.1. Introduction

The purpose of this part of the thesis was to show results of the first complete QC on all film-screen mammography units in Montenegro and to establish national dose levels in mammography, considering that QC in mammography did practically not exist. Up to now we were using outdated national requirements which did not specify any dose limit as a function of thickness of the breast and do not consider breast image quality.

In Montenegro, mammography is operational since about fifteen years, with 14 film-screen mammography units and 1 CR system. One digital mammographic unit with tomosynthesis and stereotactic biopsy was donated to the Clinical centre of Montenegro by the IAEA in the beginning of 2015.

5.2. Material and methods

Thanks to our National project with the IAEA (International Atomic Energy Agency), namely "Upgrading the Quality Assurance and Quality Control Programme in Diagnostic Radiology for a National Breast Screening Programme", the Clinical center of Montenegro was provided with quality control equipment. This included a „MagicMax mam multimeter" manufactured by Iba Dosimetry, Germany. The MagicMax multimeter is a PC based, USB powered automatic precision instrument that can display from one single exposure, the following parameters:
- dose, dose rate, and dose per pulse;
- exposure time;
- noninvasively practical peak voltage;
- total filtration;
- first Half Value layer.

The measurements are controlled and displayed by an easy-to-use software (Figure 5.1).
The MagicMax Universal is not intended to be used on patients.

Fig.5.1. Working window of MagicMax software

The study was performed on a total of 15 film-screen mammography units placed in 14 municipalities in Montenegro.

The national project with the IAEA provided a kit of QC tools (Figure 5.2), consisting of a solid state detector with appropriate suitcase (Figure 5.2.a, b), four *Polymethyl Methacrylate* (PMMA) plates (Figure 5.2.c) 18 x 24 cm (three of them are 2 cm thick, one is 1 cm thick) in order to simulate a breast thickness from 2 to 7 cm in accordance with EU standards for AGD calculation [10]), an IBA Anthropomorphic tissue equivalent phantom *Mammo AT* (Figure 5.2.d), a densitometer *Unilight D* (Figure 5.2.e), a set of aluminium filters for mammography 0.1 mm thick (Figure 5.2.f), and bar pattern (Figure 5.2.g).

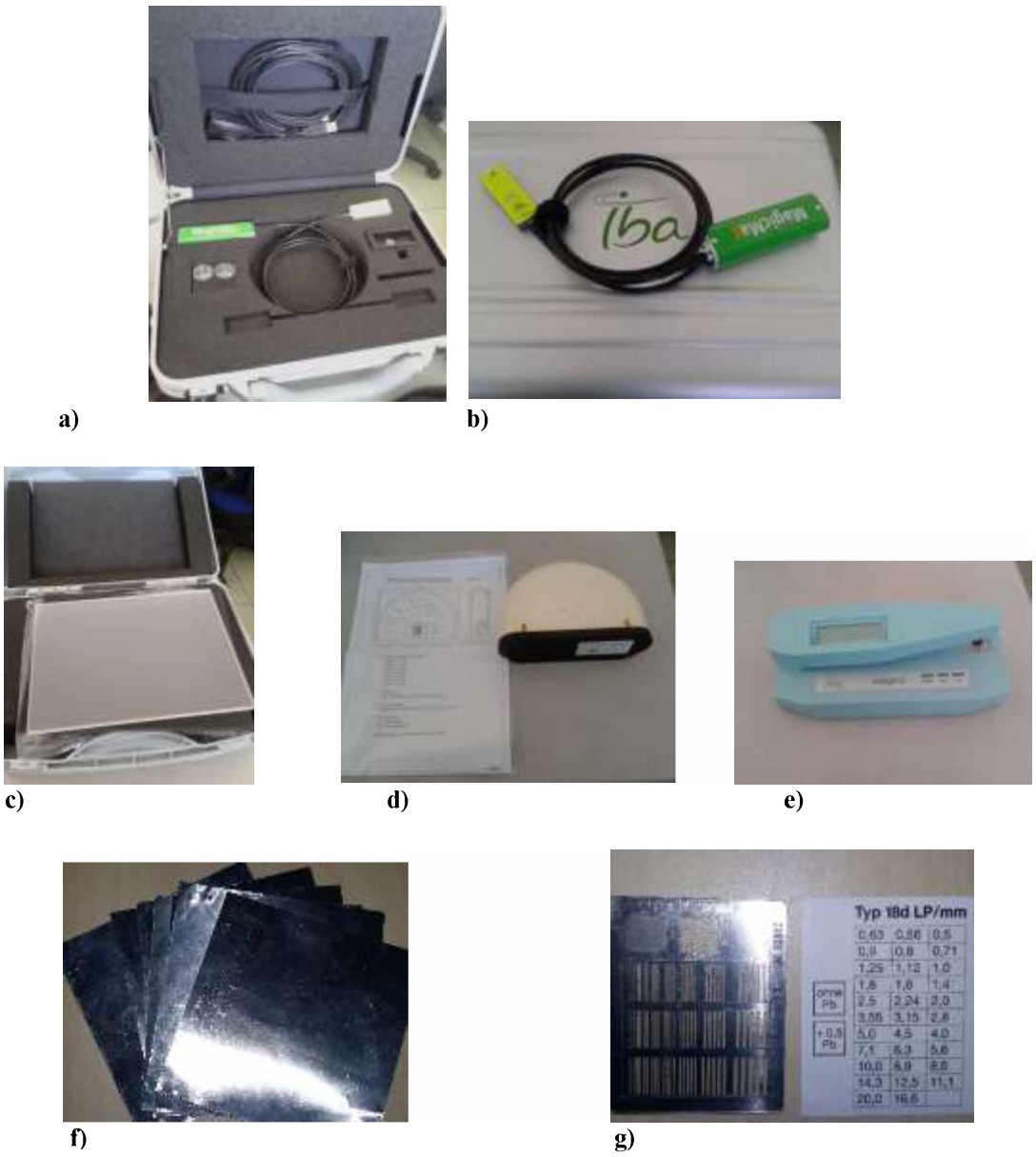

a) b) c) d) e) f) g)

Fig.5.2. Mammography kit

From one exposure the dosimeter calculates six parameters, namely: dose, dose-rate, peak tube voltage (kVp), duration of exposures, filtration, half value layer (HVL) and wave form of tube voltage and dose. For dose calculations we used HVL values obtained by measurements with thin aluminum sheets.

As the glandular tissue is considered to be the tissue at risk in the breast, the radiation risk in mammography is usually evaluated by the mean dose to the glandular tissue for an average breast, also designated as average glandular dose (AGD) [26].
Two approaches are used for patient dose measurement and setting of diagnostic reference levels from radiologic procedures: patient-based dosimetry and phantom-based dosimetry [27, 28, 29]. The use of a phantom has the advantage that only one or two exposures would be needed for each examination type and for each radiologic facility; the disadvantage is that it does not represent a real clinical situation, and the same standard phantom shall be needed for consistency. If patient dose measurements are used, the patient sample should be selected to match the mean body indexes (e.g., patient weight and height or body mass index [weight in kilograms devided by the square of height in meters]) to the predefined „standard-sized" patient. The patient sample should be large enough to ensure that the mean values represent the typical practice in the facility – for example, at least 20 patients within a predefined range of body indexes. In mammography, this BMI based selection is usually not applied. Rather large random (in terms of BMI) population samples are used.
In this study, phantom – based dosimetry has been used.

Estimates of average glandular dose (AGD) were calculated according to the European protocol for the quality control of the physical and technical aspects of screen – film mammography [10].

The dose was determined using the standard clinically selected exposure factors using Automatic Exposure Control (AEC) and the molybdenum/molybdenum (Mo/Mo) anode/filter combination. AGD was calculated [30] using PMMA blocks of 180 x 240 mm with thicknesses of 20, 30, 40, 45, 50, 60 and 70 mm.
The incident air kerma was then measured for each PMMA thickness along with the half-value layer, which can be delivered by the dosimetry system, but in this study it was calculated according the [10].
The mean glandular doses were derived from measurements of the incident air kerma (withoutback scatter) at the surface of the phantom and the HVL, using tabulated conversion coefficients, using equation 5.1.

$$D = K\,gcs \qquad (5.1)$$

where K is the incident air kerma at the upper surface of the breast, measured without backscatter; g is the incident air kerma to mean glandular dose conversion factor, the coefficient g corresponds to a breast with a glandularity of 50 %; the coefficient c corrects for any difference in breast composition from 50 % glandularity and the coefficient s corrects for any difference due to the choice of X-ray spectrum [31].

AEC testing included the assessment of long term variation in mean density due to system variations, the central optical density setting and the difference per step of the selector.

In order to test optical density, the 45 mm polymethylmethacrylate (PMMA) phantom was imaged under clinical conditions and in accordance to the radiographer's input or with the help of the radiographer. Depending on the clinical practice, imaging was performed using an automatic exposure control (AEC) or advanced automatic exposure control (AAEC) system.
OD was measured at the reference point placed at 60 mm from the chest wall edge and laterally centered.

The performance of the film processing greatly affects image quality. The best way to measure this performance is by sensitometry [10].
The films used in mammography should be specially designed for that purpose. Light sensitometry is a suitable method to measure the performance of the processor.
For this purpose we exposed film with light and inserted the exposed side into the processor for every screen-film mammography unit in Montenegro. After developing it was measured optical density of step-wedge using a densitometer. From the graph of values of measured optical density against the logarithm of exposure by light we plot the characteristic curve for all screen-film systems.
The gradient curve in sensitometry determines the film contrast. Important film properties such as optimum film contrast and maximum density can be derived from the characteristic curve and the gradient curve [22]. The gradient γ is:

$$\gamma = \frac{\Delta(OD)}{\Delta(log\frac{\psi}{\psi_0})} \qquad (5.2)$$

where (ψ/ψ_0) is the relative exposure, in this case defined as the quotient of photon energy fluence and Δ(OD) the relevant difference in optical density.

5.3. Results

5.3.1. Dose measurements and Dose Reference Levels

Results are shown in Table 5.1.
Table 5.1. shows calculated AGD (D) for all units compared with limiting values according to [30].

Table 5.1 AGD values for 15 mammo units together with limiting values according

mammo unit	D_{20mm} PMMA (mGy)	D_{30mm} PMMA (mGy)	D_{40mm} PMMA (mGy)	D_{45mm} PMMA (mGy)	D_{50mm} PMMA (mGy)	D_{60mm} PMMA (mGy)	D_{70mm} PMMA (mGy)
1	0.91	2.35	3.84	4.39	5.02	5.47	6.7
2	0.76	1.18	1.83	2.09	2.46	3.62	5.56
3	0.68	1.07	1.63	1.96	2.32	3.51	4.91
4	0.56	0.85	1.32	1.49	1.79	2.66	3.91
5	0.54	0.85	1.36	1.63	1.98	2.86	4.32
6	0.77	1.07	1.49	1.55	1.71	2.21	3.96
7	0.45	0.71	1.16	1.36	1.67	2.48	3.75
8	0.48	0.73	1.15	1.21	1.49	2.11	2.91
9	0.48	0.42	0.51	0.64	0.66	0.64	0.75
10	0.75	1.16	1.81	2.21	2.64	3.81	6.02
11	0.92	1.46	2.33	2.81	3.86	4.27	7.74
12	0.53	0.82	1.41	1.7	2.07	3.5	6.36
13	0.87	1.21	1.78	2.13	2.49	3.64	5.38
14	0.8	1.26	1.97	2.42	2.91	4.21	6.56
15	0.42	0.65	1.02	1.19	1.43	2.07	2.78
acceptable	<1.0	<1,5	<2.0	<2.5	<3.0	<4.5	<6.5
achievable	<0.6	<1.0	<1.6	<2.0	<2.4	<3.6	<5.1

Although we have a small number of units, in order to compute the DRL we presumed a Gaussian distribution and we calculated the covariance of the estimated parameters.
Using MATLAB, we plotted the Probability Density Function (PDF) versus calculated AGD. Figure 5.3. presents the PDF for 40 mm PMMA.

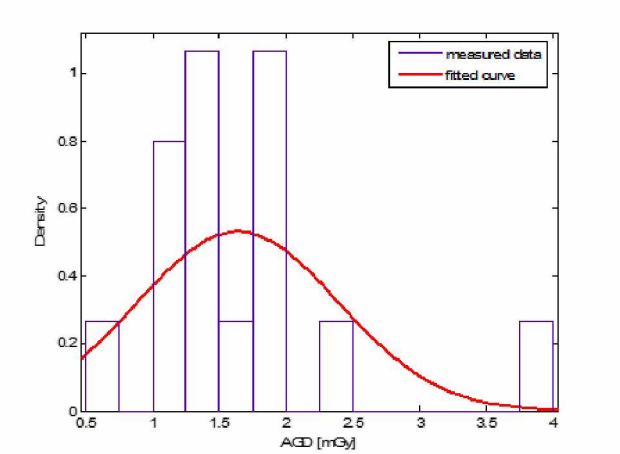

Fig.5.3. Fitted curve of Probability Density Function versus AGDs (mGy) for 40 mm PMMA

Then we plotted the cumulative probability in order to determine the 75% percentile of the distribution of typical doses for the sample (Figure 5.4.).

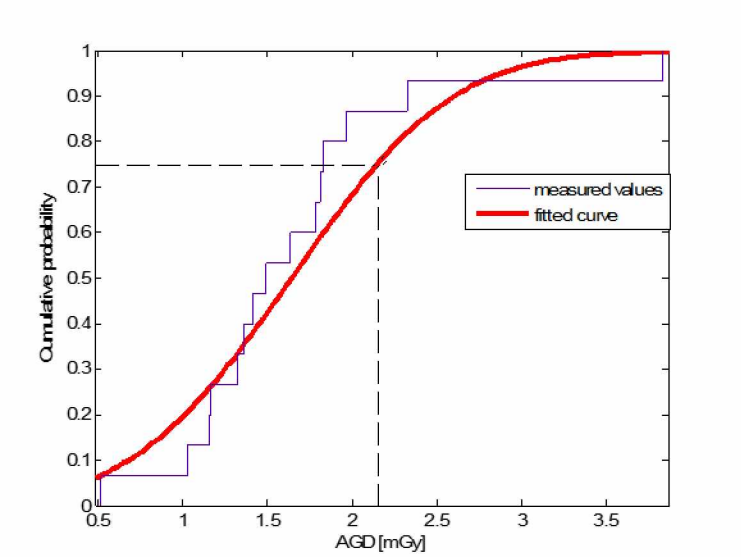

Fig.5.4. Cumulative probability of measured AGDs for 40 mm PMMA

Determination of the DRL value for 60 mm PMMA is shown at Figure 5.5. The experimental data were fitted with a normal (Gaussian) distribution and estimation for mean values and standard deviation was done: In our case Mu=3.137 and Sigma=1.168. Then for probability to be 0.75, the AGD is 3.9248 mGy. The round DRL is 3.9 mGy.

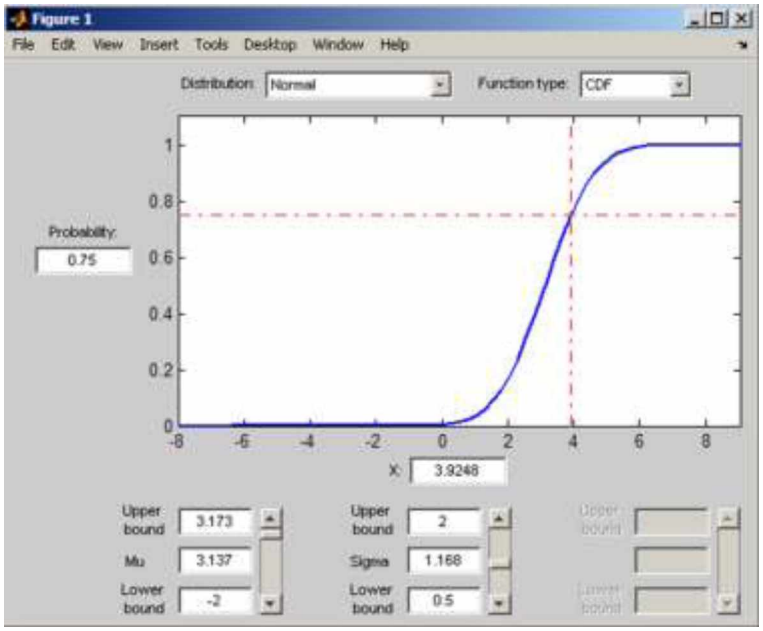

Fig. 5.5. The MATLAB window created for determination of the DRL value for AGDs of 60 mm PMMA

Table 5.2.shows proposed dose reference levels for mammography in Montenegro.

Table 5.2. Proposed DRL

Thickness PMMA (mm)	Equivalent Breast Thickness (mm)	Proposed DRL (mGy)
20	21	0.8
30	32	1.4
40	45	2.1
45	53	2.5
50	60	3.0
60	75	3.9
70	90	6.0

Figure 5.6. shows AGD values from three selected units compared to the acceptable and achievable levels.

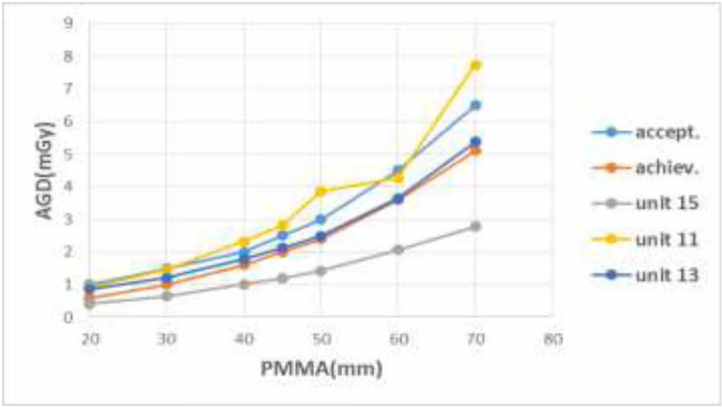

Fig.5.6. AGD values from 3 units compared to acceptable and achievable levels

Those systems are selected as example of system with higher AGD values (unit 11), with lower AGD values (unit 13) and the AGD values between the acceptable and achievable levels. We did not present all units not to make an unclear graph.

5.3.2. Optical density

Figure 5.7.represents OD values of images made at 45 mm PMMA exposed on clinical conditions with AEC or AAEC as it used at facility, Mo/Mo target-filter combination, at a point 6 cm from a chest wall laterally centered.
Two solid lines represents the range of recommended OD values (1.5–1.9)±0.15 OD.

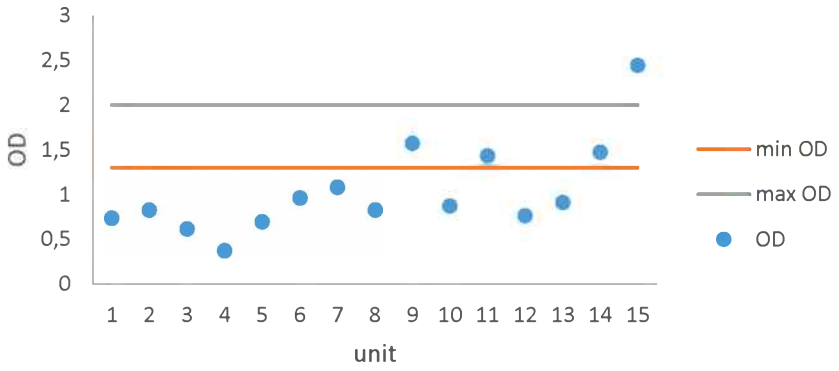

Fig.5.7. Illustration of the OD values for every mammo unit in Montenegro.

5.3.3. Sensitometry

Figure 5.8 shows characteristic curves (the graph of measured optical density against the logarithm of exposure by light) for four selected units.

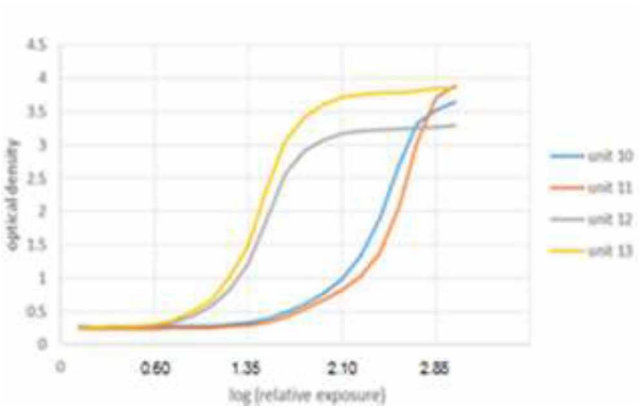

Fig. 5.8. Characteristic sensitometry curves of 4 units

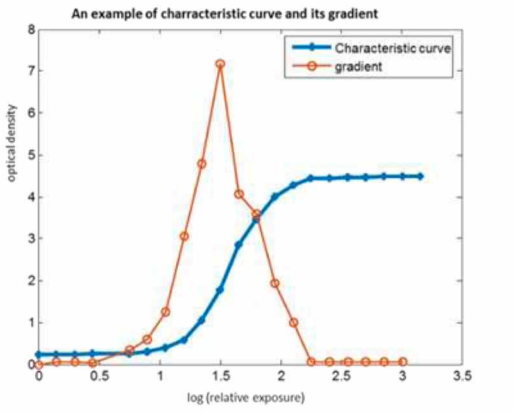

Fig. 5.9.Charcteristic curve and its gradient of 1 unit

Figure 5.9 shows an example of characteristic curve and its gradient for unit 13 from previous graph.

5.4. Discussion

The first AGD assessment in Montenegro shows acceptable level at almost all mammography units.
Unit 9 is excluded from this study, and is today no longer in use because there is no AEC. This is according to [36]. Only two mammography units are over acceptable dose level.
The use of the Gaussian distribution can be criticized due to the limited number of systems.

Considering this was the first dose assessment in mammography in Montenegro the dose findings were satisfying, but we encountered huge image quality problems. Fourteen out of 15 mammography units have acceptable dose levels. However, optimization is certainly recommendable and is an ongoing process now. This study can be used for comparison with regional dose levels that still use film-screen mammography or to show the difference with a new, recently put into operation, digital system.

In general, image quality is not on a good level. Most centers do not use appropriate film processing. Optimization of practice should be organized urgently.

6. CR Mammography - Getting started with protocol for quality assurance of digital mammography in the Clinical centre of Montenegro

6.1. Introduction

The purpose of this work is to work out a test procedure for Quality Assurance (QA) in digital mammography with newly released test equipment, including the MagicMax mam multimeter (IBA, Germany) and the Anthropomorphic tissue equivalent phantom Mammo AT (IBA, Germany), and to determine whether a first digital CR system in Montenegro meets the current European standards. Tested parameters were tube output (μGy/mAs) and output rate (mGy/s), reproducibility and accuracy of tube voltage, half value layer, reproducibility and accuracy of the AEC system, exposure control steps, image receptor's response function, image quality and printer stability test. The evaluated dosimetric quantity is the average glandular dose (AGD) as evaluated from PMMA slabs simulating breast tissue.

Computer radiography (CR) systems are very common in medical applications because of their flexibility to address a variety of clinical applications and a relatively low cost to turn multiple exam rooms into digital units. A cassette with a charge storage phosphor plate is used in place of the conventional x-ray screen-film cassette. It is exposed to radiation using standard techniques and the latent image, stored in the phosphor, is released by a laser scanner as visible light. Finally, the quantity of light emitted at each location is recorded and the scanner forms a digital image [33]. The CR reader in the Clinical Centre of Montenegro is operated with X-ray devices of different manufacturers.

The main disadvantage of CR system is linked with the so-called indirect conversion detector and limited sensitivity of the detector medium. Indirect conversion involves the diffusion of light as part of the x-ray detection process, and this degrades the spatial resolution. Compared to DR systems, CR has the difficulties to achieve good dose efficiency [34, 35]. Yet the European protocol for QA in breast cancer screening and diagnosis [10] as well as the RP162 [36] impose the same minimal image quality criteria for CR and direct radiology (DR) systems. As a consequence, CR systems may have to be set up at higher dose levels to reach a sufficiently high image quality. Some breast cancer screening programs reported on the poorer performance with CR [37], while other programs have found similar performance for CR and DR but at a higher dose level indeed [38]. L. Warren established scientific evidence for these observations using a simulation framework to test the link between the detection of microcalcifications and contrast thresholds [39].

The national Montenegrin law of radiation protection [40] comprises more or less the key principles and concepts important for the effective regulation of radiation protection. Due to a lack of concrete Montenegrin regulations, decisions and guidelines rely on international standards, such as developed by the International Atomic Energy Agency (IAEA) and the EU [41, 42]. The purpose of this work is to work out a test procedure as described in the European protocol with newly released test equipment and an anthropomorphic tissue equivalent phantom and to determine whether a first digital CR system in Montenegro meets the European standards.

6.2. Material and methods for testing CR system

The mammography system used in the Clinical Centre of Montenegro consists of different systems forming all together the complete imaging chain. It consists of a Planmed Sophie mammographic x-ray unit, Konica Minolta CR mammography imaging plate RP-6M, Konica Minolta Regius 190 CR reader, Kodak Dry View 6800 Laser printer, Rogan View Pro-X workstation and viewing boxes.
The testing methods were mainly derived from the European protocol and include: tube output (μGy/mAs), output rate (mGy/s), reproducibility and accuracy of tube voltage, half value layer, reproducibility and accuracy of the AEC system, exposure control steps, image receptor's response function, image quality and printer stability test.
Specific tube output (μGy/mAs) and output rate (mGy/mAs) were measured thoroughly using the Molybdenum-Molybdenum target filter combination and for different tube loads (50, 70,100 mAs).
Average glandular dose (AGD) was used to document the radiation induced risks and image quality was assessed by means of a newly developed phantom 'MammoAT' (IBA DosimetryGmgbH, Germany). Further quality control (QC) test equipment consisted of a newly released multimeter MagicMax-mam multimeter (IBA DosimetryGmgbH), a densitometer Unilight D and PMMA plates. Dosimetric measurements are straightforward: the dosimeter is put in the radiation field and is exposed.

We achieved access to raw data, i.e. images with Dicom tag 'For Processing'. This allowed to measure the response curve and to linearize all the images for subsequent calculations.
The anthropomorphic phantom did not have any limiting values that would guide the decision of acceptability. We applied the phantom on all our current film-screen systems to obtain a first reference level, to which our digital data could be compared. This is in line with the basic approach adopted for the CDMAM phantom, where the readings of film-screen systems were used to set minimal values for digital systems [38].

6.3. Results

6.3.1. Tube output and HVL

Tube output measurements as measured with the newly released dosimeter are assumed to be correct, as the system has a recent dosimeter calibration certificate for kV and dose.
The automated calculation of HVL for a 28kV Mo/Mo spectrum showed a value of (0.33±0.02) mm Al. Explicit measurements with Al sheets led to a value of (0.29±0.01) mm Al (Fig 6.1). This is in line with typical values published in the European Guidelines [10].

Table 6.1. shows typical measurements for tube output, where Us is set voltage, Um is measured voltage, FDD is focus-detector distance, mGy/s is output rate on film, and Y(μGy/mAs)@1m is output rate on 1 m distance.

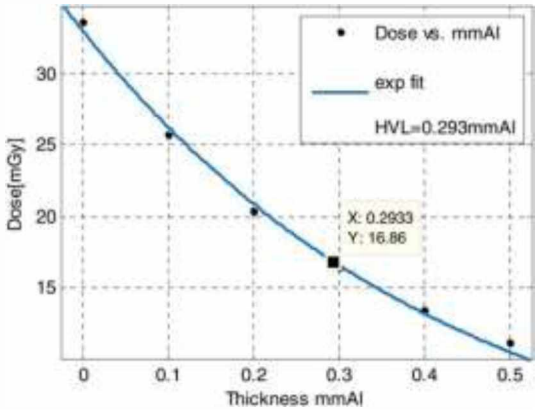

Fig.6.1. Determination of HVL

Table 6.1. Table with OUTPUT measurements

Us (kV)	It (mAs)	FFD (m)	FDD (m)	Um (kV)	t (ms)	D (mGy)	Y (µGy/mAs) @1m	mGy/s
22	50	0,64	0,535	21,6	627,4	4,747	27,17	5,29
	70	0,64	0,535	21,6	866,1	6,6	26,99	5,33
	100	0,64	0,535	21,6	1227,2	9,39	26,88	5,35
23	50	0,64	0,535	22,4	579	5,42	31,03	6,54
	70	0,64	0,535	22,4	817,8	7,83	32,02	6,69
	100	0,64	0,535	22,4	1158,1	11,21	32,09	6,76
24	50	0,64	0,535	23,2	529,8	6,44	36,87	8,49
	70	0,64	0,535	23,2	789,3	9,16	37,46	8,11
	100	0,64	0,535	23,2	1109,2	12,99	37,18	8,18
25	50	0,64	0,535	23,9	505,4	7,26	41,54	10,03
	70	0,64	0,535	23,9	756,7	10,19	41,67	9,41
	100	0,64	0,535	23,9	1062,7	14,62	41,85	9,61
26	50	0,64	0,535	24,7	484,7	8,29	47,48	11,96
	70	0,64	0,535	24,7	725,1	11,60	47,43	11,18
	100	0,64	0,535	24,7	1018	16,56	47,40	11,37
27	50	0,64	0,535	25,5	466,1	9,33	53,43	13,99
	70	0,64	0,535	25,6	652,4	12,81	52,38	13,72
	100	0,64	0,535	25,6	992,4	18,77	53,72	13,22
28	50	0,64	0,535	26,3	453,5	10,26	58,73	15,81
	70	0,64	0,535	26,3	695,8	14,59	59,66	14,65
	100	0,64	0,535	26,3	970,7	20,88	59,76	15,03
29	50	0,64	0,535	27,2	451,8	11,43	65,43	17,68
	70	0,64	0,535	27,2	696,3	16,46	67,30	16,52
	100	0,64	0,535	27,1	972,2	23,27	66,60	16,73
30	50	0,64	0,535	28	472,3	12,66	72,47	18,73
	70	0,64	0,535	28	698,6	17,72	72,46	17,72
	100	0,64	0,535	28	1000,5	25,53	73,07	17,83
31	50	0,64	0,535	28,7	498,6	13,70	78,43	19,20
	70	0,64	0,535	28,7	736,8	19,12	78,18	18,13
	100	0,64	0,535	28,7	1035,7	27,48	78,65	18,54
32	50	0,64	0,535	29,5	502	15,07	86,27	20,98
	70	0,64	0,535	29,5	759,2	21,21	86,73	19,52
	100	0,64	0,535	29,5	1062,1	29,98	85,81	19,72
33	50	0,64	0,535	30,4	526,1	16,61	95,08	22,06
	70	0,64	0,535	30,4	787,3	22,63	92,53	20,09
	100	0,64	0,535	30,4	1121,3	32,96	94,34	20,54

6.3.2. Tube voltage

A number of clinically used tube voltages was checked for accuracy and reproducibility. In all the cases the reproducibility was within range ≤±0.5kV or even less, but the accuracy was out of range i.e. ≥± 1 kV but within the range of ±2 kV in line with the calibration certificate.

6.3.3. AEC- system

The Planmed Sophie mammographic x-ray unit has two modes: Automatic Exposure Control (AEC) and Advanced Automatic Exposure Control (AAEC). The first requires a manual setting of the tube voltage. With advanced AEC, the kV value is selected after the patient's breast has been compressed and this value is then automatically corrected during the exposure [26]. The kV value is based on the tissue density of the patient's breast [42].
The measurements were performed for anode/filter Mo/Mo in two working condition: with fixed kV value (AEC), and "all automatic" working condition (AAEC). First values (for AEC) (Table 6.2.a) showed deviations for the measured tube voltage.
Most current protocols impose a tube voltage measurement at one beam quality only, if available Mo/Mo. Specific correction factors may be required for other beam qualities.
According to EC limiting values [10], AGD obtained by AEC (Table 6.2.a) are on achievable level, while AGD obtained by AAEC (Table 6.2.b) are on acceptable level.

Table 6.2. Deviations for the measured tube voltages a) when AEC mode and b) when AAEC mode is used

a)

PMMA(mm	U (kV) set	U(kV) MM	t (ms)	D (mGy)	It (mAs)	AGD
20	26	24,6	142,70	1,81	15	0,66
30	27	25,5	250,00	3,91	27	1,07
40	28	26,2	435,56	8,00	47,9	1,62
45	29	27,1	491,00	10,22	54,1	1,88
50	30	28,1	689,10	14,10	65,8	2,37
60	31	28,7	1,09	24,85	103	3,52
70	32	28	2,53	56,98	246	6,79

b)

PMMA(mm)	U(kV) 1	U (kV) 2	U(kV) MM	t (ms)	D (mGy)	It (mAs)	AGD
20	24	22	22,1	385,80	2,64	34	0,89
30	24	24	23,1	660,00	5,77	57	1,58
40	26	25	23,9	1,04	11,71	98	2,39
45	26	25	23,9	1,61	18,03	149	3,31
50	26	26	24,7	1,76	23,49	168	3,94
60	28	28	26,3	2,03	37,73	208	5,35
70	30	30	28	2,52	58,88	246	7,02

6.3.4. The short term reproducibility

The short term reproducibility of time readings was calculated from the deviation of the incident air kerma of ten routine exposures (26 kV, 45mm PMMA). The mean duration of exposures was 1.097 s, with a deviation less than ±0.3%

6.3.5. Exposure control steps

Exposure control steps were measured using standard test block for steps from -7 to +7. Calculated differences per step Diff % = (10.7- 14.8) % are in line with prescribed increases of (5-15)% per exposure step [10]. Measurements (Table 6.3) were performed at reference conditions with 4 cm PMMA, compression 15 kg, equivalent breast 4,5cm, AEC, 28 kV

Table 6.3. Exposure control steps (central value and difference per steps)

step	D(mGy)	t (ms)	It (mAs)	Dif (%)
7	13,95	827,6	83,3	11,78
6	12,48	747,5	74,9	11,73
5	11,17	673,7	66,8	14,10
4	9,79	540,1	59,1	11,76
3	8,76	485,1	53,1	11,45
2	7,86	433,1	47,4	13,09
1	6,95	386,1	42,3	13,01
0	6,15	341	37,4	12,02
-1	5,49	303,2	33,3	10,91
-2	4,95	273,2	30	14,85
-3	4,31	240,2	26,4	10,80
-4	3,89	217,2	23,9	12,10
-5	3,47	193,3	21,3	13,03
-6	3,07	171,3	18,9	12,04
-7	2,74	153,3	16,9	

6.3.6. Image receptor response

The response function of the detector was assessed by imaging the standard test block (45mm PMMA), with different entrance doses (tube loading) at the clinically used beam quality (Figure 6.2); (26kV).

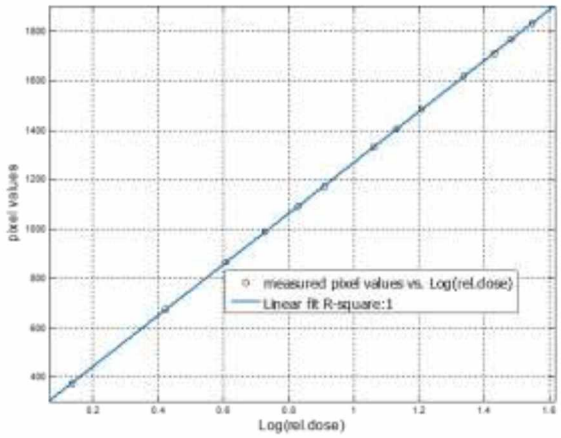

Fig. 6.2. The Response function of the image plate detector

6.3.7. Noise evaluation

The squared standard deviation against entrance surface air kerma is plotted to estimate noise (Figure 6.3).

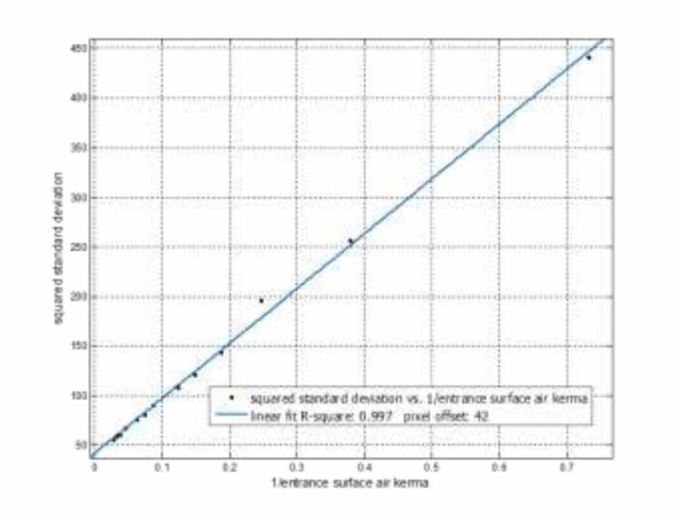

Fig. 6.3. Noise evaluation graph

6.3.8. Image receptor homogeneity

A typical unprocessed image of the standard test block (45mm PMMA) is shown in Figure. 6.4, together with its histogram. The MATLAB program is used to calculate the mean pixel value (1310) and standard deviation over the whole image (96).

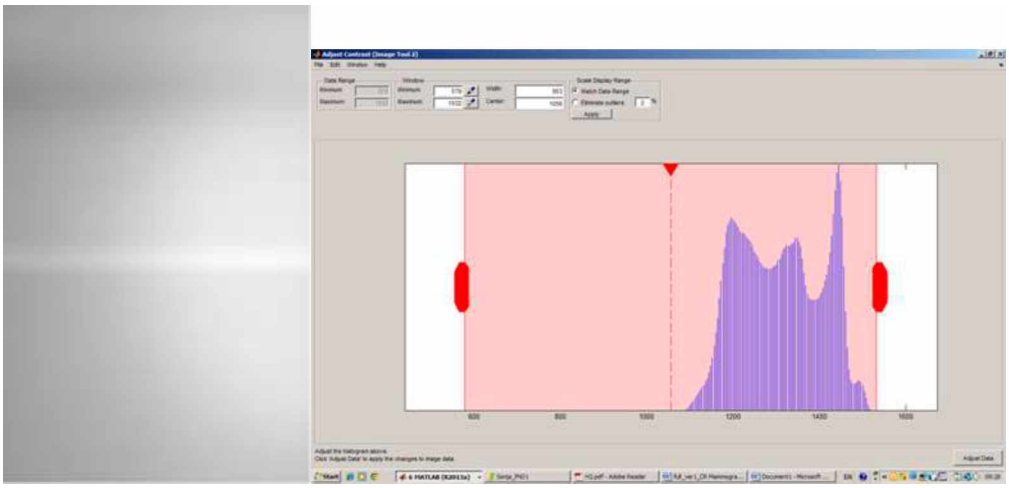

Fig. 6.4. The image of the standard block for homogeneity test and its histogram

The white band in the center of the left image is an artefact of the laser printing system.

6.3.9. Image quality

Image quality is assessed in two ways: with a standard test block (45mm PMMA) together with 2mm of added Al and with the anthropomorphic phantom *Mammo AT*.
In order to obtain reference values from film-screen systems, the phantom was taken to 11 conventional sites, tested by the Authorized Technical Services of Montenegro according [30] (Table 6.4**,** Figure 6.5). On the three Siemens units, the phantom was exposed manually, until proper optical density was obtained. On the other conventional units (Planmed Sophie Classic – Finland), the AEC mode were used. The conventional systems show between 7 and 14

objects. We consider the values of 7 and 9 as outliers, or at least suspicious for poorer performance and propose as a minimal criterium '11 objects detectable'.
The phantom was then exposed by the CR unit using the steps from -5 to +5 with AEC (fixed kV and Mo-Mo). We have then used the AAEC exposure, where only the step can be selected, and the beam quality is chosen by the system (Table 6.5, Fig.6.5) In clinical practice, step 0 is in use; the corresponding mAs values and kV values are shaded in the Table 6.5. It can be seen that at AEC step 0 for all tube voltages below 30kV, the minimal criterium of 11 objects is met. This is not the case for the 30kV setting, an issue worth exploring.

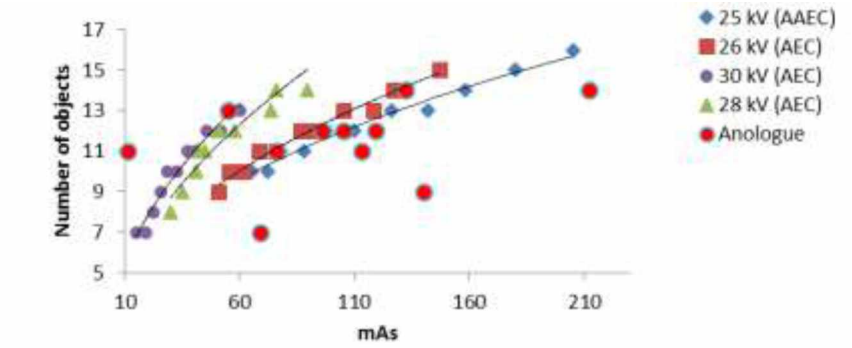

Fig.6.5 Curves shows CR values NO/mAs, and circles shows values NO/mAs of analog units (considered the reference), NO – number of objects

Table 6.5. Objects scores for all tested units (screen-film and CR)

	Clinical centre - CR unit (1)								Analogue (11 units)		
	30 kV, AEC		28 kV, AEC		26 kV, AEC		AAEC (25 kV)			AEC	
step	mAs	No object	mAs	No object	mAs	No object	mAs	No object	kV	mAs	No object
-5	18	7	30	8	51	9	65,2	10	25	119	12
-4	19	7	35	9	55,5	10	72,3	10	26	75,8	11
-3	22,5	8	41	10	61,7	10	78	11	24	212	14
-2	25,7	9	42	11	68,4	11	88,2	11	27	69	7
-1	28,6	10	44,6	11	75,8	11	97,7	12	25	105	12
0	32,5	10	50,7	12	86,8	12	110	12	25	132	14
1	37,2	11	57,9	12	93,3	12	126	13	25	113	11
2	40,6	11	54,5	13	105	13	142	13	25	140	9
3	45,9	12	73,5	13	118	13	158	14	28	55	13
4	51,9	12	76	14	127	14	180	15	25	96	12
5	60,2	13	89,6	14	147	15	205	16	35	11,2	11

6.4. Discussion

The basic characterization of the x-ray source is done through the measurements of the tube output. The results satisfy the requirements for the specific tube output (μGy/mAs), i.e., it is far greater than 30μGy/mAs at all clinically used voltage settings.

The beam quality is determined by measuring reproducibility and accuracy of the tube voltage and HVL. An interesting fact was found: the accuracy of the tube voltage was out of range i.e. $\geq \pm$ 1kv (required by European protocol [10]), but within the range of ±2 kv as specified in [43]. Moreover, the measured values of the tube voltage are always lower than given voltages at the console of the mammographic unit, with a consequence that HVL values were decreased as well. Namely, the values of HVL were under or at the low limit of recommended values.
AEC-system works properly with expected performances as reproducibility and accuracy. The mammography unit comprises fifteen exposure control steps and the exposures per step (11-15%), are in accordance with the requirements (5-15%).
The response function, as a dependence of the mean pixel value in the ROI of unprocessed data versus log relative entrance surface air kerma, shows almost perfect linearity with presence of pixel value offset about 300.
The homogeneity test is fulfilled i.e., the maximum deviation in mean pixel values is about 7% and is far less than allowed-15%. Visual checking of homogeneity shows a strong intensity line at half of the test block and could be due to Heel effect.
On this mammography unit the AGD values were below the reference of the EU protocol.
Image quality-contrast visibility tests done by imaging standard test block (45mm PMMA) together with added 2mm *Al,* is used for stability checking of the system by calculating the ratio *mean pixel (signal)/mean pixel(background).* The average ratio in the case of unprocessed image is about 0.93. *Mammo AT* phantom comprises standard sizes microcalcifications and tumors, located in known positions within the phantom and provided qualitative evaluation of the quality of the imaging system.
Spatial resolution test shows distinguishable 5 line pairs/mm, and 6 line pairs/mm for unprocessed and processed images respectively.
The overall quality of the imaging system is acceptable.

This was the first complete QC test on this unit performed thanks to equipment obtained through a national project with the IAEA, RER 6004, „*Upgrading the Quality Assurance and Quality Control Programme in Diagnostic Radiology for National Breast Screening Programme*". The equipment allows the set-up of a test procedure in line with other European protocols.
The main findings are that QA can be organized in Montenegro.

(1) All measured parameters are within the range described in European protocols except the tube voltage which deviated more than ±1kV. The automatic determination of the HVL was satisfactorily. Average glandular dose ranged from 0.66 to 7.02mGy for PMMA thicknesses from 20 to 70mm, and is in accordance with literature data.

(2) The image quality score as obtained with the Anthropomorphic tissue equivalent phantom Mammo AT for the CR system was similar to findings on our conventional screen-film mammography

(3) In clinical practice the mammograms are printed. The CR reader produces images with a pixel size of 43.75μm, which is compatible with the laser printer (39μm laser spot spacing). The image processing algorithm embedded in the reader successfully processes mammograms with desirable image brightness and contrast in the printed image.

7. Initial QC on the Digital Breast Tomosynthesis (DBT) system

7.1. Introduction

Podgorica's Clinical center has got Hologic Selenia Dimensions DBT mammography system with a Prone Biopsy Stereotactic System through the National project with the IAEA „Upgrading the quality Assurance and Quality Control Programme in Diagnostic Radiology for National Breast Screening Programme" in 2015. Thanks to this project CcoM is also equipped with QC equipment for digital mammography. In addition, the visit of prof. Nicholas Marshall, with whose help we have launched QC in tomosynthesis, was also possible within the same IAEA framework. The results presented here are the first QC results of the new DBT system.

7.2. Materials and methods

The draft EUREF Digital Breast Tomosynthesis (DBT) protocol v 1.0 was applied. The system acquires 15 projections over 15° in 3.7 seconds using a moving focus during acquisition. Pulse length for a projection image is as short as ~20 ms. A different target/filter combination is used, for DBT mode (W/Al). No antiscater grid is used for DBT.
We do not have an accepted measurement of image quality in DBT, still. Other measures of system performance were done for purpose of acceptance test.

In tomosynthesis, the beam quality of the emitted X- ray beam is determined by tube voltage, anode material and filtration, as in 2D mammography and therefore some of the parameters can be measured in 2D [10].

Both the accuracy and reproducibility of the tube voltage are measured. The method and the limiting values are the same as for the screen-film mammography.
To test kV accuracy, the static projection acquisition mode (0° tomo) was used, along with the multimeter CB2-14020679 and the dose probe 1310211.
For each selected kVp, the percentage deviation between the nominal value and the measured kVp was calculated in accordance with equation (7.1) taken from the [44]:

$$\text{Deviation (\%)} = 100*(kVp_{nom} - kVp_{meas}) / kVp_{meas} \qquad (7.1)$$

where kVp nom is the value indicated on the equipment and kVp meas is the measured value. This percentage deviation may be taken as a measure of the accuracy.

The Half Value Layer was assessed (same as for the screen-film mammography) by adding thin aluminium (Al) filters to the X-ray beam and measuring the attenuation.
For the HVL calculation, we used the following equation (7.2) taken from [1]:

$$HVL = [t_2 \ln(2M_1/M_0) - t_1 \ln(2M_2/M_0)] / \ln(M_2/M_1) \quad (7.2)$$

where:
t_1 and t_2 are the thicknesses (in mm) of the filters used;
M_0 is the average value of readings measured without any added filter;
M_1 and M_2 are the readings that are respectively just above and just below 50% of M_0

For patient dose calculation in Dance et al (2011) [45] the formalism of equation (5.1) has been extended to digital breast tomosynthesis (DBT) using

$$D = KgcsT \quad (7.3)$$

where the factor T for the a series of full field projections counts as:

$$T = \sum_i \alpha_i t_i \quad (7.4)$$

where t_i are the tomosynhesis factors for the individual tomosynthesis projections and the α_i are the weights of the individual projections.
Values of t are provided below as a function of projection angle (Table 7.4) and values of T as a function of angular range. Values of T are also provided for selected commercially available (at the time of writing) DBT systems [45].

Image detector performance could be fully characterized by applying the linear shift-invariant (LSI) system theory [46]. This theory describes how an image detector acts on the input signal to produce the image, using the concept of "transfer function".
The response function is the curve which relates the output signal (typically the mean pixel value measured in a region of the image) with the input signal (radiation dose) [47]. This is a linear function for DR systems, mostly.

Another quantification on the performance of the imaging system is noise analysis. This test expresses contribution of three different components: electronic, quantum and structural noise. Bouwman 2009 and Monnin 2014 presented equation:

$$SD^2 = k_e^2 + k_q^2 * p + k_s^2 * p^2 \quad (7.5)$$

SD - standard deviation in reference ROI
k_e – electronic noise coefficient
k_q – quantum noise coefficient
k_s – structural noise coefficient
p – average pixel value in reference ROI

Electronic noise is assumed to be independent of the exposure level and arises from the number of sources: dark noise, readout noise, amplifier noise.
Structural noise is present due to spatially fixed variations of the gain of an imaging system. The flatfielding performed in DR systems will largely remove the effect of the structural noise. Due to the limited number of images used for the flatfield mask and the associated noise in the mask, some structural noise remains. Furthermore, flatfielding might not be performed for projection images individually, leading to some additional structural noise.
Quantum noise arises due to the variations in the X-ray flux.

In digital mammography the major system related physical factor affecting spatial resolution is the signal blurring within the detector and the integration of the signal over the area of the del to form a single reading [1]. This is described with the Modulation Transfer Function (MTF). The MTF calculates from the spread of the signal in the image of a square object with the sharp, high contrast, edges. The edges of both directions (horizontal and the vertical) can be measured, and an equation can be performed for both signal rising and signal falling conditions. Slanting the edge slightly allows determination of "pre-sampled" MTF, that is, the MTF that would exist before sampling to form the digital image.

To evaluate image quality in mammography, phantoms with similar to anatomical details are used. Here is presented CD MAM phantom and its analysis Figure 7.1.

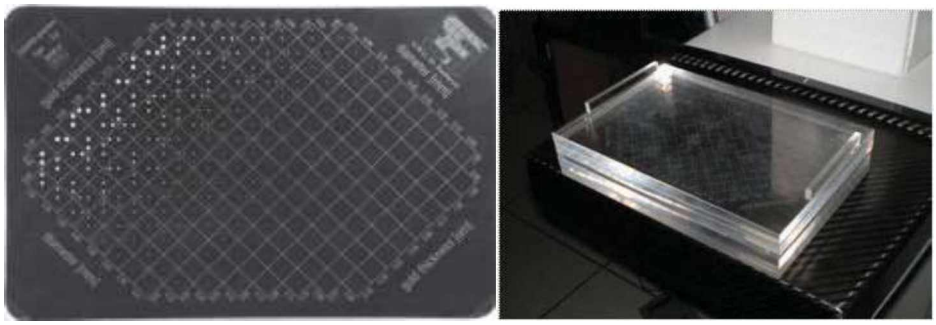

a) b)

Fig. 7.1. CD MAM phantom: a) aluminum base with golden discs and b) position of exposition- between PMMA plates of 20 mm

CD MAM phantom is consists of aluminum base with 16 rows and 16 columns which forming squares. Each square has a golden disc in the middle and in the one of the randomly selected four corners. The discs are with different thickness and different diameters. Software packages for automatic analysis of CDMAM images and calculation of threshold contrast for different disk diameters while removing inter-observer variability have been developed.

To assess the degree and source of artefacts that is visualized in full field digital mammograms or phantom images it should be checked detector uniformity, ie. uniformity in terms of signal level and noise.

To make sure a mammogram will appear similarly on different viewing stations and on printed film, the mapping of grayscale values to display luminance or optical density should be consistent [14]. In this measurement it is determined whether a display conforms to the DICOM Grayscale Standard Display Function (GDSF).

7.3. Results

Some DBT systems can perform both DBT and FFDM imaging. In this case some of the measurements have only to be performed in FFDM mode, but it must be verified first that all relevant (exposure) conditions are similar in FFDM and tomosynthesis (e.g. target and filter) and the working of the detector is identical (e.g. binning of detector elements and detector corrections).

7.3.1. Quality control – X ray source

QC measurements for FFDM was performed according [10].

7.3.1.1. kVp accuracy and reproducibility

kVp accuracy and reproducibility were checked according [10]. Acceptable accuracy is within ±5%. and reproducibility <1% what is in line with [10]. (Table 7.1 and Table 7.2. respectively)

Table 7.1. kVp accuracy

set values	measured val	R	deviation	
kV	*kV*	*mes/set*	*%*	*anode/filter*
24	**24.0**	1.00	**0.1%**	*W/Rh*
25	**24.9**	1.00	**-0.5%**	*W/Rh*
26	**25.6**	0.99	**-1.4%**	*W/Rh*
28	**27.6**	0.99	**-1.4%**	*W/Rh*
29	**28.7**	0.99	**-1.0%**	*W/Rh*
31	**30.9**	1.00	**-0.3%**	*W/Rh*
34	**34.2**	1.01	**0.5%**	*W/Rh*
36	**36.6**	1.02	**1.7%**	*W/Al*
42	**42.4**	1.01	**1.0%**	*W/Al*

Deviation between measured and set kV is shown on Figure 7.2.

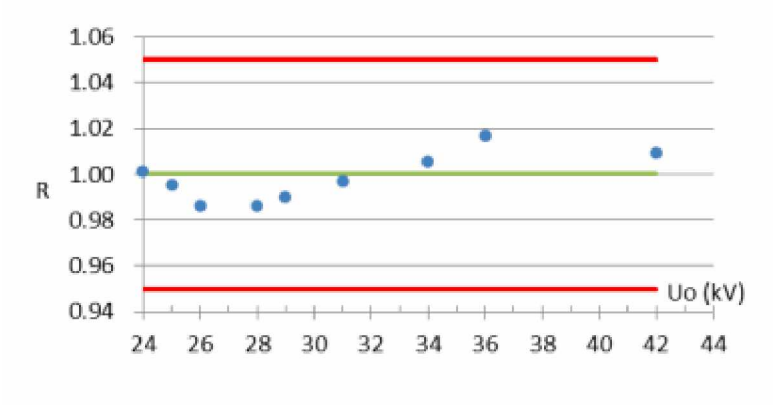

Fig.7.2. Shows deviation between measured and set values of kV

Table 7.2. kVp reproducibility

Uo	t	K	
kV	*ms*	*mGy*	
27.6	498.3	1.719	
27.5	498.3	1.719	
27.6	498.3	1.717	
27.8	498.8	1.716	
27.5	498.3	1.719	
27.6	**498.4**	**1.718**	***average value***
0.4%	**0.0%**	**0.1%**	***standard deviation SD***

7.3.1.2. Tube output

Kerma in air K(mGy) was measured with ionization chamber considering correction factors for preasure and temperature. Value Y(μGy/mAs) – tube output is specific kerma calculated at 1m distance from the source of X ray. With 95% confidence level, standard deviation of measurements was <10%. Results are shown at Table 7.3.

Table 7.3. Measurements for tube output

Anoda	Filter	FDD (m)	Uo (kV)	It (mAs)	K (mGy)	Y = K/It (μGy/mAs)
W	Rh	0.655	24	50	1.08	9.3
W	Rh	0.655	25	50	1.26	10.8
W	Rh	0.655	26	50	1.42	12.2
W	Rh	0.655	28	50	1.72	14.7
W	Rh	0.655	29	50	1.87	16.1
W	Rh	0.655	31	50	2.17	18.6
W	Rh	0.655	34	50	2.62	22.5
W	Ag	0.655	28	50	2.26	19.4
W	Ag	0.655	31	50	2.92	25.1
W	Ag	0.655	34	50	3.58	30.7
W	Al	0.655	26	50	2.73	23.4
W	Al	0.655	28	50	3.43	29.4
W	Al	0.655	30	50	4.15	35.6
W	Al	0.655	31	50	4.50	38.6
W	Al	0.655	33	50	5.26	45.1
W	Al	0.655	36	50	6.39	54.8
W	Al	0.655	42	50	8.89	76.3

7.3.2.3. HVL

Results on measurement of the tube output (Y) and half value layer (HVL) are shown at a Table 7.4. Meaurements are performed for all given anode/filter combinations.

Table 7.4. HVL measurements for all anode/filter combinations

Uo	It	Ka	Y = Ka/It	HVL
kV	mAs	mGy	µGy/mAs	mm Al
		(anode/filter):W/Rh		
24	50	1.08	**21.7**	0.51
25	50	1.26	**25.2**	0.52
26	50	1.42	**28.4**	0.53
28	50	1.72	**34.4**	0.55
29	50	1.87	**37.4**	0.55
31	50	2.17	**43.4**	0.57
34	50	2.62	**52.4**	0.59
		(anode/filter): W/Ag		
28	50	2.26	**45.2**	0.58
31	50	2.92	**58.4**	0.61
34	50	3.58	**71.7**	0.64
		(anode/filter):W/Al		
26	50	2.73	**54.6**	0.46
28	50	3.43	**68.6**	0.50
30	50	4.15	**83.0**	0.53
31	50	4.50	**90.1**	0.55
33	50	5.26	**105.2**	0.59
36	50	6.39	**127.8**	0.64
42	50	8.89	**177.8**	0.72

Figure 7.3. shows dependence of tube output Y(K_a/It) from tube voltage (U_0) for different anoda/filter combinations

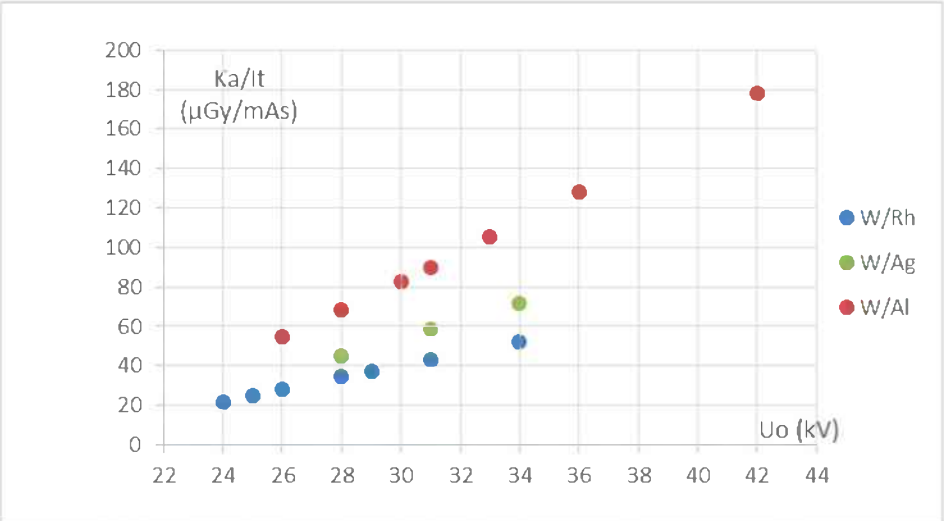

Fig.7.3. Tube output (µGy/mAs) versus tube voltage (kV) for W/Rh, W/Ag and W/Al anoda/filter combinations

7.3.2. Quality control – AEC and MGD

7.3.2.1. SDNR – Signal difference to noice ratio is shown here in order of AEC evaluation.

This is use to establish the baseline factors to be used for weekly check. Results are shown in Table 7.5.

Table 7.5. Results for calculation of SDNR

PMMA (cm)	Exposure values			PMMA		+ 0,2 mm Al		SDNR
	A / F	Uo (kV)	It (mAs)	PV	± SD	PV	± SD	
2	W/Rh	25	60	352	4.9	300	4.5	**11.0**
3	W/Rh	26	88.4	350	5.0	302	4.7	**10.0**
4	W/Rh	28	113.5	353	5.0	309	4.7	**9.1**
4.5	W/Rh	29	134.4	361	5.1	318	4.6	**8.9**
5	W/Rh	31	168.7	465	6.1	413	5.7	**8.8**
6	W/Ag	31	177.5	607	7.3	546	7.0	**8.5**
7	W/Ag	34	179.6	650	8.1	596	7.6	**6.8**

PV-pixel value, SD-standard deviation

In a Table 7.6. is shown comparison of SDNR with limits given at [1].

Table 7.6. Comparison of SDNR (CNR-contrast to noise ratio) with given limits

PMMA (mm)	C	N	CNR	limit values	
				acceptable	achievable
20	52	4.7	**11.0**	4.4	6.7
30	48	4.8	**10.0**	4.2	6.4
40	44	4.9	**9.1**	4.0	6.1
45	43	4.9	**8.9**	3.9	6.0
50	52	5.9	**8.8**	3.8	5.8
60	61	7.1	**8.5**	3.6	5.5
70	54	7.9	**6.8**	3.4	5.2

Figure 7.4 shows graphical comparison of measured SDNR (CNR) and given limits.

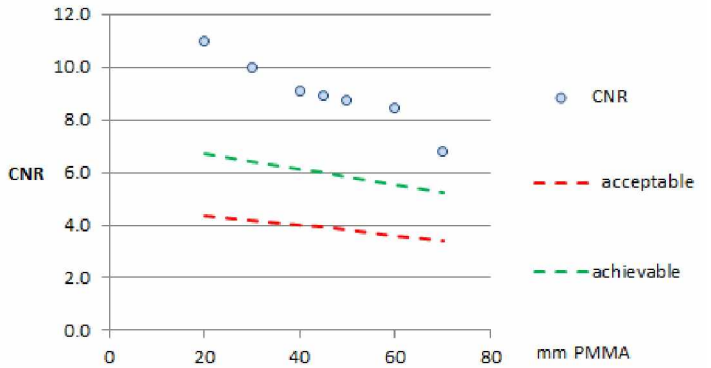

Fig. 7.4. Comparison of CNR measured values with limits

7.3.2.2. Average Glandular Dose (AGD) or Mean Glandular Dose (MGD)

Table 7.7. shows MGD (or AGD – Average Glandular Dose) values for 2D FFDM and DBT mode.

Table 7.7. Measurements for MGD (AGD)

PMMA (mm)	indicated thickness (mm)	anode/ thickness (mm)	kVp	mAs	incident dose (mGy)	AGD for 2D FFD mode (mGy)	tomo f. for -7.5to+7.5 scan range	AGD for tomo mode (mGy)	reference value (mGy)
20	22	W/Al (0.7 mm)	26	34	1.8	0.65	0.997	0.89	1.00
30	32	W/Al (0.7 mm)	28	38	2.5	0.8	0.996	1.06	1.50
40	45	W/Al (0.7 mm)	30	46	3.7	1.1	0.996	1.37	2.00
45	53	W/Al (0.7 mm)	31	58	5.2	1.4	0.995	1.79	2.50
50	60	W/Al (0.7 mm)	33	59	6.2	1.9	0.994	2.12	3.00
60	75	W/Al (0.7 mm)	36	74	10.0	2.7	0.994	3.14	4.50
70	90	W/Al (0.7 mm)	42	69	14.0	3.5	0.992	4.04	6.50

Mean Glandular Dose (MGD) for DBT is slightly higher than for 2D mode (Figure 7.5); there are no limiting values for DBT MGD currently but the MGD values are within Reference values given in the EUREF protocol for 2D FFDM.

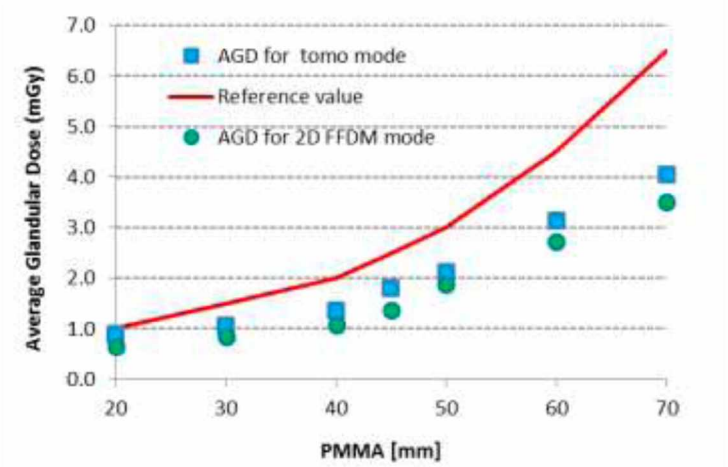

Fig. 7.5. Compares reference AGD values with AGD for 2D FFDM mode and AGD for tomo mode

7.3.3. Quality control – Detector performance

7.3.3.1. Noise analysis

Noise analysis is performed in projection images acquired in zero degree angle stationary mode. In Table 7.8, are presented the results for noise analysis. Measurement are conducted with 2 mm Al added on X ray tube, with W/Rh anode/filter combination, at 28 kV.

Table 7.8.

It (mAs)	PV	± SD	Noise(N) SD^2	SNR
4	22.8	1.57	2.5	15
9	59.1	2.24	5.0	26
20	122	3.11	9.7	39
30	182	3.76	14.1	48
39	241	4.32	18.7	56
50	305	4.91	24.1	62
60	346	5.29	28.0	65
75	455	5.95	35.4	77
100	606	6.78	46.0	89
140	848	8.1	65.6	105
200	1231	9.8	96.8	125

Table 7.9.

structural	quantum	electronic	S	Q	E
3.00E-06	**0.0742**	**0.7836**		shares of	
1.56E-03	1.69	0.78	0%	68%	32%
1.05E-02	4.39	0.78	0%	85%	15%
4.49E-02	9.08	0.78	0%	92%	8%
9.97E-02	13.53	0.78	1%	94%	5%
1.74E-01	17.88	0.78	1%	95%	4%
2.79E-01	22.64	0.78	1%	96%	3%
3.60E-01	25.69	0.78	1%	96%	3%
6.22E-01	33.78	0.78	2%	96%	2%
1.10E+00	44.97	0.78	2%	96%	2%
2.16E+00	62.91	0.78	3%	96%	1%
4.55E+00	91.34	0.78	5%	94%	1%

Figure 7.6. shows that mean pixel values measured at the region of interest related with the radiation dose is a linear function, as it is mostly in DR.
Graph at a Figure 7.7. is used to take coefficients for structural, quantum and electronic noise respectively from the equation for second order polynomial derived through excel. All results are given at Table 7.9.

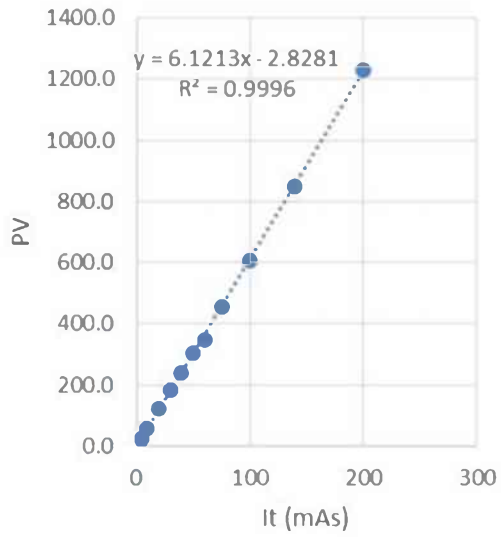

Fig. 7.6. The response function relation between output signal (mean PV) with the input signal (radiation dose)

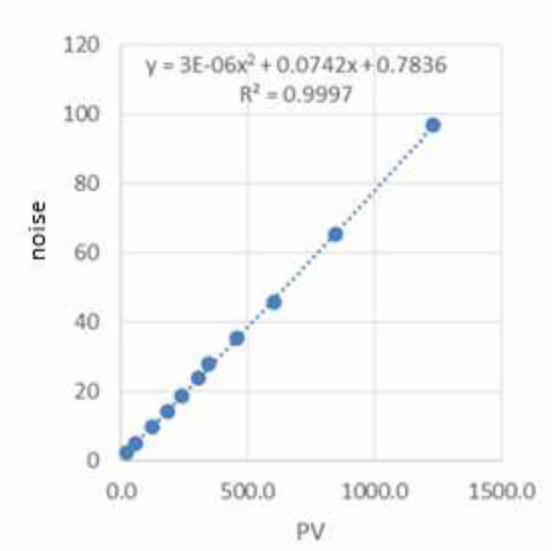

Fig. 7.7. Shows noise as a function of pixel value: noise=f(PV)

Figure 7.8. shows standard deviation against radiation dose with coefficient of correlation R^2=0.9979.

Figure 7.9. shows contribution of electronic, quantum and structural noise. The biggest contribution is given by quantum noise which is variations in the X-ray flux. For detector performance this combination is as it should be.

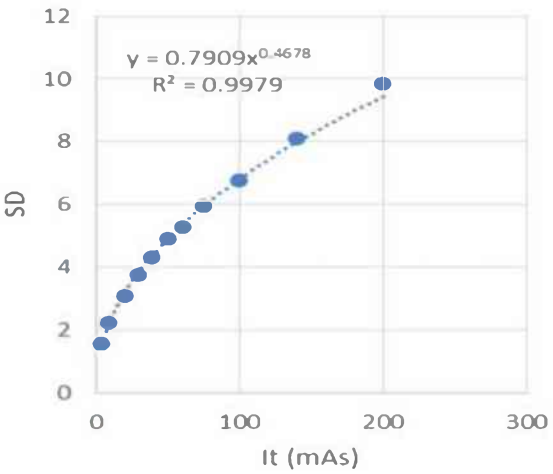

Fig. 7.8. Standard deviation versus radiation dose with coeff.of correlation R^2=0,9979

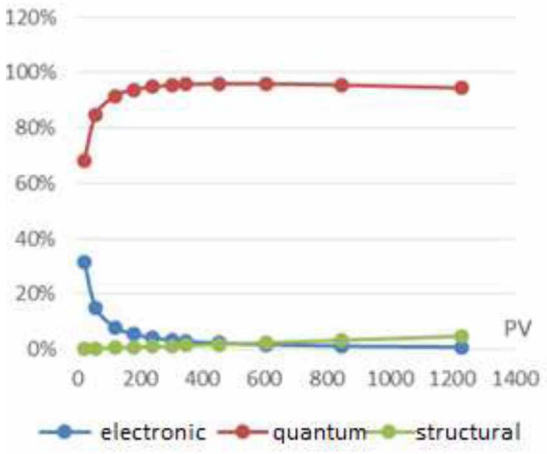

Fig. 7.9. Contributions of different parts to noise

7.3.4. Quality control – Image Quality

7.3.4.1. CD MAM analysis

Analysis of obtained 'for processing' images was conducted with CDCOM (V.1.6.) in CD MAM Analyser (V.1.5.3). CD MAM phantom was exposed with parameters: auto filter mode, 28 kV, W/Rh anode/filter combination. Results are shown in the Table 7.10.

Table 7.10. Results of measured thickness with analyser

diameter	thickness of gold (um)				measured thickness	
(mm)	automatically	human provided	Fit	2 SD	acceptable	achievable
0.08	0.779	1.129	0.889	0.111		
0.10	0.426	**0.647**	0.657	0.078	**1.68**	**1.10**
0.13	0.283	0.456	0.461	0.049		
0.16	0.220	0.372	0.354	0.038		
0.20	0.159	0.280	0.267	0.032		
0.25	0.106	**0.195**	0.206	0.024	**0.35**	**0.24**
0.31	0.077	0.149	0.161	0.019		
0.40	0.063	0.127	0.123	0.014		
0.50	0.049	**0.103**	0.098	0.013	**0.15**	**0.10**
0.63	0.036	0.079	0.079	0.012		
0.80	0.026	0.062	0.064	0.010		
1.00	0.022	**0.055**	0.054	0.010	**0.09**	**0.06**

At Figure 7.10. it is shown that measured results for CD MAM phantom of golden thicknesses are on achievable level, sometimes even under.

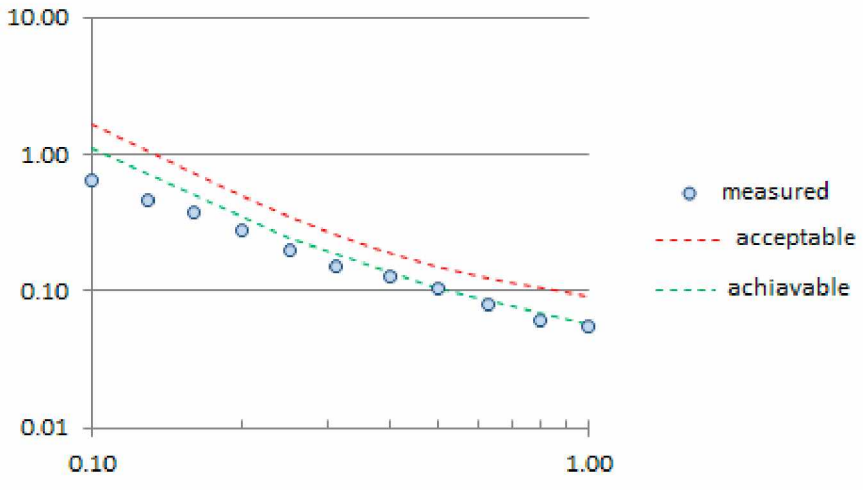

Fig.7.10. showing measured results of golden thickness compared with acceptable and achievable results

7.3.4.2. MTF (Modulation Transfer Function)

The modulation transfer function of the image signal on detector describes the spatial resolution of the images. It defined as Fourier transform image edge in both directions of detector.
Figure 7.11. shows result of MTF analysed in ImageJ plugins COQ for mammography.

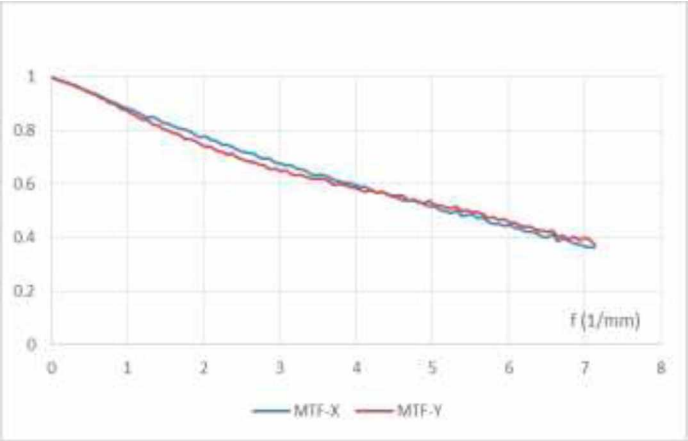

Fig.7.11. shows MTF in both direction, x and y

Figure 7.12. shows results for MTF measurements conducted during acceptance test for DBT and analysed by professor Nicholas Marshall at the himself developed software, where frequencies could go under Nyquist frequeny.
Measurements were performed for the W/Al anode/filter combination, 31 kVp, 100 mAs and with 2 mm Al added filter. Spatial frequency was recorded for the 50% and 10% points for the MTF (Table 7.

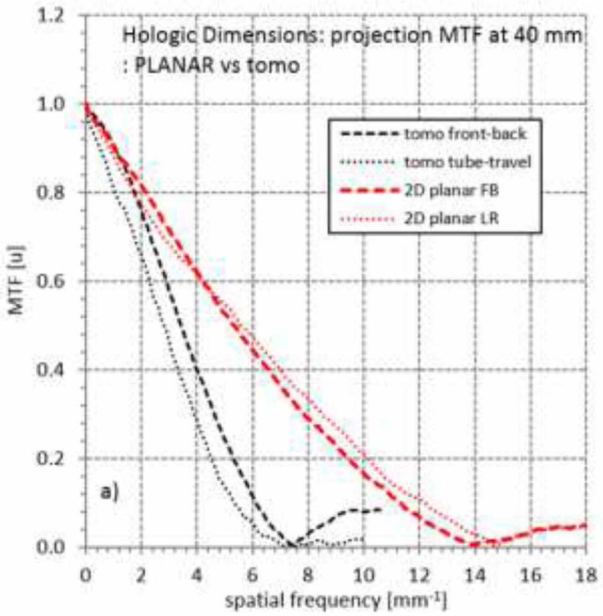

Fig. 7.12 Hologic Dimensions: projection MTF at 40 mm:PLANAR vs Tomo

Table. 7.11. Spatial frequency recorded for 50% and 10% points for the MTF

	front-back direction	tube-travel direction
point for 50% MTF mm	2.25	2.05
point for 10% MTF mm	4.45	3.85

7.3.4.3. Quality control – Image display quality

Luminance range

For the luminance range, we measured the maximum and minimum luminance of the display device using test pattern TG18-LN12-01. Results are presented in Table 7.12.

The ratio of maximum and minimum display luminance, in the presence of ambient light, is an indicator of luminance contrast response capabilities of the monitor (under the current environmental condition) [10].

Table 7.12. The ratio of max and min display luminance

Lmax and Lmin:	use measurement of 4.1.6.2 DICOM Greyscale Standard Display Function		
	Left monitor:	Right monitor:	
Lmax	522.90	538.30	Cd/m2
Lmin	0.98	0.97	Cd/m2
Luminance ratio	535.76	552.67	-

This result showing that maximum luminance exceed 500 cd/m^2, as it should be according [1].

The grayscale display function (GDF) is determined by measuring the luminance of the 18 AAPM luminance test pattern (TG18-LN12-01 through TD18-LN12-18). Luminance is measured at the center of the screen, with test pattern displayed full screen.
The measured values are inserted into a EUREF spreadsheet and GDSF is automatically determined.
The calculated contrast response was within ±10% of the GDSF contrast response for primary class displays. Measured values are shown in Table 7.13.

Table 7.13. Measured luminance values (left monitor)

Left Monitor:

Measured luminance values:

testpattern TG18-LN12-#	p-value	Luminance L	JND j(L)	dL/L	deviation compared to DICOM (%)
1	0	0,976	70,505		
2	240	2,099	106,631	0,730	3,4
3	480	3,831	142,834	0,584	2,7
4	720	6,344	179,156	0,494	2,2
5	960	9,755	214,693	0,424	4,0
6	1200	14,68	252,393	0,403	1,6
7	1440	21,26	289,826	0,366	0,7
8	1680	30,19	328,034	0,347	2,4
9	1920	41,9	366,040	0,325	1,6
10	2160	57,77	405,276	0,318	4,6
11	2400	77,62	442,950	0,293	0,3
12	2640	104,3	482,008	0,293	3,7
13	2880	137,6	519,747	0,275	0,2
14	3120	182,2	558,947	0,279	3,9
15	3360	238,1	597,088	0,266	1,1
16	3600	309,7	635,196	0,261	1,0
17	3840	404,1	674,304	0,264	3,6
18	4080	522,9	712,626	0,256	1,5

Figure 7.13.shows the graph results of the contrast response of the left monitor.

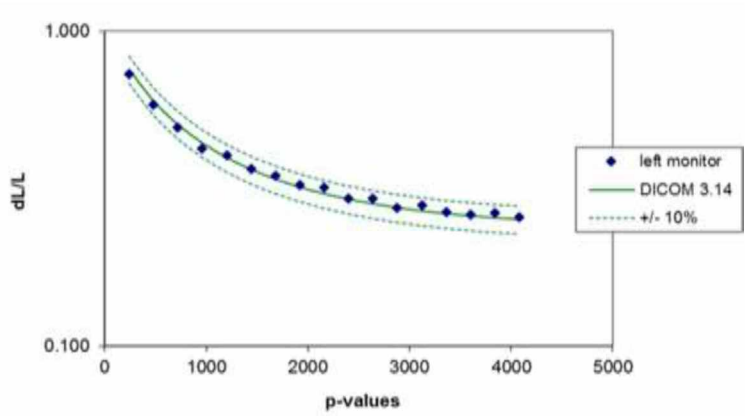

Fig. 7.13.Contrast response for left monitor

Results for both monitor (left and right) were similar, as it should be.

In the Figure 7.14 are shown result relation between p value and JND-index.

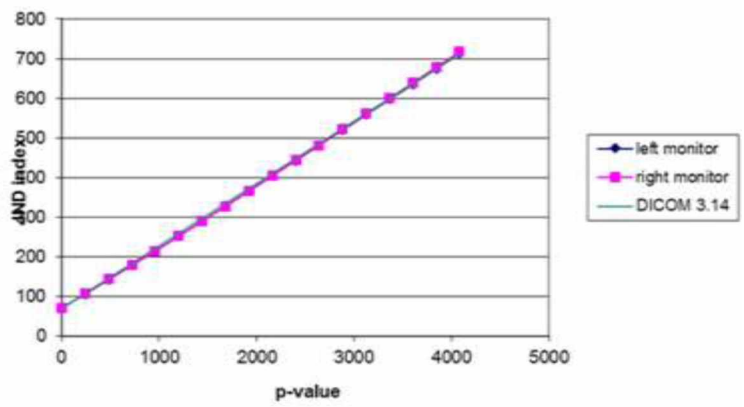

Fig.7.14. Relation between p value and JND-index

In a order to check display uniformity it were performed following measurements:
For the measurements of display luminance it were used the test patterns TG18-UNL10 and TG18-UNL80 and measured display luminance at five locations for each monitor (Fig.7.15)

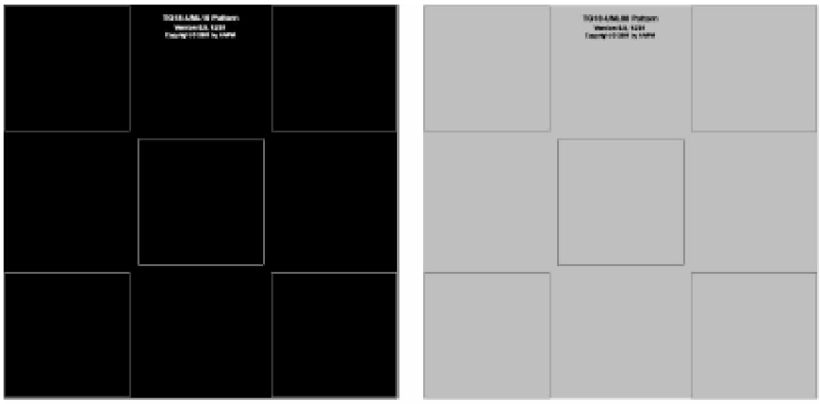

Fig.7.15. TG18-UNL10 and TG18-UNL80 test pattern

Table 7.14. shows results on luminance uniformity measurements.

Table 7.14 Luminance uniformity measurements

testpattern TG18_UNL10:	monitor					
	left	right			left	right
upper left	2.866	3.283	Cd/m2	max. luminance deviation:	6.2	9.2 %
upper right	2.826	2.998	Cd/m2			
centre	2.929	3.097	Cd/m2			
bottom left	3.007	3.249	Cd/m2			
bottom right	2.868	3.144	Cd/m2			
testpattern TG18_UNL80:	monitor					
	left	right			left	right
upper left	202.3	214.2	Cd/m2	max. luminance deviation:	9.1	8.5 %
upper right	195.6	204.8	Cd/m2			
centre	215.2	223.9	Cd/m2			
bottom left	212.9	220.1	Cd/m2			
bottom right	203.8	218	Cd/m2			

Maximum optical density deviation was less than 10% according formula taken from [10]: (Dmax-Dmin)/Dcentre < 0.1.

7.4. Conclusion

This Hologic Selenia Dimensions system is the first DBT mammography system in the region. Since QC of TOMO systems is being developed in the EU, Montenegro is able to follow established rules according EU protocols. Starting with QC in tomosynthesis in Montenegro is a huge step.

8. Overall conclusion

High quality of QA and QC in mammography is of utmost importance for early detection of breast cancer. At the start of this thesis, QC of mammography systems was on a poor level in Montenegro. With the measurements conducted in this thesis, the level of QC has significantly increased. We started to implement EU and IAEA guidelines for QC in mammography and got the first results.
First, we measured all parameters on all systems we have in the country needed for assessment of beam quality. Then we calculated the AGD for all these systems and we determined the national Dose Reference Levels. For the thickness of 2, 3, 4, 4.5, 5, 6 and 7 cm, the DRLs are 0.8, 1.4, 2.1, 2.5, 3.0, 3.9 and 6.0 mGy respectively. These values were then included in a new regulation, as there was no existing national regulation. All AGDs were lower than the acceptable levels according to the EU protocol.
Then we conducted an assessment of image quality. For this purpose we tested optical density, sensitometry and densitometry for all screen-film systems, and we evaluated the image receptor response, noise and homogeneity of our CR system. Image quality was assessed with the anthropomorphic phantom *Mammo AT*. The phantom was applied on film-screen systems to find reference levels. Some systems showed very poor image quality and urgent action was needed! At the present, a few of the lowest image quality systems are excluded from use.
We investigated QC for DBT systems according the EU protocol, that we could now apply on other systems, with some minor limitations due to a lack of equipment or software for analysis.

The main scientific contributions of this thesis are assessment of uncertainties in half value layer determination in mammography; the impact of using different aluminum measurements, validation of automated filter measurements on the new MagicMax instrumentation; validation of Robson's formula and mammographic quality restoration by using Wiener filter.
In order to verify the validity of the new measuring equipment which gives a direct value of HVL from a single measurement, we performed a large set of measurements at different mammography systems. It was shown that the difference between the direct HVL measurements of the Magic Max and the HVL calculated through the EUREF formula does not exceed 0.02 mm Al. Estimates of the standard deviation were approximately 0.1 mm Al; we concluded that direct HVL measurements of the Magic Max were in the range of the errors of HVL determination.
We validated also Robson's method that gives a procedure to calculate the air kerma and HVL for any value of tube voltage (in the range 25-32 kV) from a measurement of the tube output and HVL for each target/filter combination made at a single tube voltage. We simulated many cases and close agreement between measured and predicted values of air kerma and half value layer confirm Robson's model.
To enable good visibility of small details in mammograms, such as micro-calcifications, and to be able to clearly distinguished it from the very complex background, the quality of the imaging system is crucial. Images may benefit from restoration. We have shown on the test image that "cleaning" the image from the imperfectness of the imaging system (x-ray mammography unit), by using the Wiener filter is promising.
Another achievement of the PhD project is the optimization of image quality of the screen-film systems throughout Montenegro. Thanks the IAEA support we got new, calibrated test equipment for assessment of image quality. We are well prepared for a global roll out of the QC practice for all modalities, film-screen, digital mammography and tomosynthesis.

Literature

[1] Quality Assurance programme for digital mammography, IAEA Human Health Series No. 17, International Atomic Energy Agency Vienna, 2011

[2] McGuire, A; Brown, JA; Malone, C; McLaughlin, R; Kerin, MJ (22 May 2015). "Effects of age on the detection and management of breast cancer.". Cancers 7 (2): 908–29. doi:10.3390/cancers7020815. PMID 26010605

[3] "World Cancer Report". *International Agency for Research on Cancer*. 2008.

[4] *"Breast cancer: prevention and control"* World Health Organization.

[5] Stewart B. W. and Kleihues P. (Eds): World Cancer Report. IARCPress. Lyon 2003

[6] Laurance, Jeremy (29 September 2006). *"Breast cancer cases rise 80% since Seventies"*. *The Independent* (London). Retrieved 9 October 2006

[7] *"Breast Cancer: Statistics on Incidence, Survival, and Screening"*. Imaginis Corporation. 2006. Retrieved 9 October 2006.

[8] Breast Cancer: Breast Cancer in Young Women WebMD. Retrieved 9 September 2009

[9] 142 Nearly 85% of women diagnosed with breast cancer now survive for 5 year or more Office for National Statistics, 2013

[10] Engen R, Woundeberg S.,Young KC, Bosmans H, Thijssen M. The European protocol for the quality control of the physical and technical aspects of mammography screening. In: European Guidelines for Breast Cancer Screening, 4th edn. Luxembourg: European Commission, 2006

[11] CRAWFORD, M.K., BRIXNER, L.H., Photostimulable phosphors for X-ray imaging: Applications and mechanism, J. Luminescence **48, 49** (1991) 37–42.

[12] TAKAHASHI, K., MIYAHARA, J., SHIBAHARA, Y., Photostimulated luminescence (PSL) and color centers in BaFX:Eu2 + (X=Cl), J. Electrochem. Soc **132** (1985) 1492–1494.

[13] SAMEI, E., RANGER, N.T., DELONG, D.M., A comparative contrast-detail study of five medical displays, Med. Phys. **35** (2008) 1358–1364.

[14] Protocol for the Quality Control of the Physical and Technical Aspects of Digital Breast Tomosynthesis Systems http://www.euref.org/european-guidelines/physico-technical-protocol#breasttomo, on the 11.03.2016.

[15] Diagnostic Radiology Physics: A Handbook for Teachers and Students, International atomic energy agency,Vienna, 2014

[16] ICRP. The 2007 Recommendations of the International Commission on Radiological Protection. ICRP publication 103. *Ann ICRP* 2007; 37:1-332

[17] European Commission. The Health Protection of Individuals Against the Dangers of Ionizing Radiation in Relation to Medical Exposure. Council Directive 97/43/Euratom,OJ L180 p22 . Luxemburg, 1997

[18] Jenia Vassileva, Madan Rehani, Diagnostic Reference Levels WEB This is a web exclusive article. *AJR* 2015; 204:W1–W3 0361–803X/15/2041–W1 © American Roentgen Ray Society

[19] L. F. Brateman and Ph. H. Heintz, Medical Physics 42, 542 (2015).

[20] J. Diffey, L. Carwright, J. Crocker, J. Heggie, Combined Scientific Meeting CSM/R-0127, EPOS TM, (2014) DOI: 10.1594/ranzcr2014/R-0127 http://dx.doi.org/10.1594/ranzcr2014/R-0127

[21] J. Zoetelief,M. Fitzgerald, W. Leitz, M. Säbel, EUROPEAN PROTOCOL ON DOSIMETRY IN MAMMOGRAPHY EUR 16263 EN 1996
[22] Horst Aichinger Joachim Dierker Sigrid Joite-BarfuB Manfred Sabel, Radiation Exposure and Image Quality in X-Ray Diagnostic Radiology Physical Principles and Clinical Applications© Springer-Verlag Berlin Heidelberg 2004 Originally published by Springer-V erIag Berlin Heide1berg New Y 0I:k in 2004 Softcover reprint of the hardcover lst edition 2004,
[23] M. Worrall, D. G. Sutton J. Radiol. Prot. 35, 209-222 (2015).
[24] M. A. S. Lacerda, T. A. Silva, A. H. Oliveira, Radiol. Bras. 40, No 5. (2007)
http://dx.doi.org/10.1590/S0100-39842007000500010
[25] A parametric method for determining mammographic X-ray tube output and half value layer, K.J.Robson, BSC, *The British Jounal of Radiology, 74 (2001), 335-340 2001 The British Institute of Radiology*
[26] Evaluation of exposure in mammography: limitations of average glandular dose and proposal of a new quantity, N. Geeraert, R. Klausz, S. Muller, I. Bloch and H. Bosmans, Radiation Protection Dosimetry (2015), Vol. 165, No. 1–4, pp. 342–345
[27] Directorate-General, Environment, Nuclear Safety and Civil Protection, European Commission. Radiation protection 109: guidance on diagnostic reference levels (DRLs) for medical exposures (radiation protection). ec.europa.eu/energy/nuclear/ radiation_protection/doc/publication/109_ en.pdf. Published 1999. Accessed September 16, 2014
[28] National Radiological Protection Board and The Royal College of Radiologists. Patient dose reduction in diagnostic radiology. London 1990; 1–46
[29] National Council on Radiation Protection and Measurements (NCRP). Reference levels and achievable doses in medical and dental imaging: recommendations for the United States. Bethesda, MD: NRCP, 2012:report 172
[30] International Atomic Energy Agency. Dosimetry in diagnostic radiology: an international code of practice. In: Technical Reports Series No. 457 (2007). ISBN 92-0-115406-2
[31] Dance, D. R., Skinner, C. L., Young, K. C., Beckett, J.R. and Kotre, C. J. Additional factors for the estimation of mean glandular breast dose using the UK mammography dosimetry protocol. Phys. Med. Biol. 45, 3225–3240 (2000).
[32] ROWLANDS, J.A., The physics of computed radiography, Phys. Med. Biol. **47** (2002) R123 –R 165.]
[33] Y. Tateno, T. Iinuma and M. Takano (Eds); *Computed Radiography* Springer-Verlag Tokyo 1987
[34] A. P. Smith, *Fundamentals of Digital Mammography: Physics, Technology and Practical Considerations*HologicIncwww. hologic.com R-B1-016 March 05
[35] A. Smith, *Image Quality of CR Mammography* HologicInc, www. Hologic.com W-B1-CR (11/06) US/International
[36] *Criteria for Acceptability of Medical Radiological Equipment used in Diagnostic Radiology, Nuclear Medicine and Radiotherapy*, Directorate-General for Energy Directorate D — Nuclear Safety & Fuel Cycle Unit D4 — Radiation Protection, 2012
[37] Séradour B, Heid P, Estève J. *Comparison of direct digital mammography, computed radiography, and film-screen in the French national breast cancer screening program.* AJR Am J Roentgenol. 2014 Jan;202(1):229-36. doi: 10.2214/AJR.12.10419. Erratum in: AJR Am J Roentgenol. 2014 Feb; 202(2):459.
[38] Bosmans H, De Hauwere A, Lemmens K, Zanca F, Thierens H, Van Ongeval C, Van Herck K, Van Steen A, Martens P, Bleyen L, Vande Putte G, Kellen E, Mortier G, Van

Limbergen E. *Technical and clinical breast cancer screening performance indicators for computed radiography versus direct digital radiography*. EurRadiol. Oct; 23(10):2891-8, 2013
[39] Warren LM, Mackenzie A, Cooke J, Given-Wilson RM, Wallis MG, Chakraborty DP, Dance DR, Bosmans H, Young KC. *Effect of image quality on calcification detection in digital mammography*. MedPhys. 2012 Jun; 39(6):3202-13
[40] *The Law on Radiation Protection and Radiation Safety*; Official Document of Montenegro No 56/09 (2009)
[41] Food And Agriculture Organization Of The United Nations, International Atomic Energy Agency, International Labour Organisation, Oecd Nuclear Energy Agency, Pan American Health Organization, World Health Organization, International Basic Safety Standards for Protection against Ionizing Radiation and for the Safety of Radiation Sources, Safety Series No. 115, IAEA, Vienna (1996)
[42] EUROPEAN GUIDELINES ON QUALITY CRITERIA FOR DIAGNOSTIC RADIOGRAPHIC IMAGES 16260 EN Luxembourg: Office for Official Publications of the European Communities, 1996
[43] Planmed Sophie mammographic x-ray unit, User's Manual 7888000/20 1996
[44] Quality Assurance Programme for Screen Film Mammography IAEA Human Health Series No. 2, International Atomic Energy Agency Vienna, 2009
[45] Dance et al, 2011, EUREF 2014 MGD Conversion Factors, https://medphys.royalsurrey.nhs.uk/nccpm/?s=mgd
[46] C Pater (2004) Equivalence and non-inferiority trials – are they viable alternatives for registration of new drigs ? (III),Curr Control Trial Cardiovasc Med 5:6-14.
[47] Quality Controls In Digital Mammography Protocol Of The Efomp Mammo Working Group, April 2014
[48] Experimental investigation on the choice of the tungsten/rhodium anode/filter combination for an amorphous selenium-based digital mammography system. Toroi P, Zanca F, Young KC, van Ongeval C, Marchal G, Bosmans H. Eur Radiol. 2007 Sep;17(9):2368-75. PMID: 17268798
[49] A. M. Gurevich, Fizicheskie osnovi Radiacionogo kontrola i diagnostiki, (energoatomizdat, Moskva 1989). (in Russian)
[50] A. Jannetta, J. C. Jackson, C. J. Kotre, I. P. Birch, K. J. Robson, R. Padgett Phys. Med. Biol. 49, 21 (2015).
[51] A. N. Tikhonov and A. V. Goncharski , Ill posed Problems, (Moscow, University Press, 1987).
[52] C. Solomon and T. Breckon, Fundamentals of Digital Image Processing, (Wiley-Blackwell 2011), pp.141-165.

Biography of the author

Sonja Ivanovic was born on July 17th 1972 in Belgrade, Serbia.
She completed the elementary and high school in Podgorica as an excellent student.
She got the University degree for physics at the Faculty of Natural Sciences, Department for Physics, University of Serbia, Prishtina in 1999.
She obtained the Master's Degree at ACIMSI (Association of Centres for Interdisciplinary and Multidisciplinary Studies and Research), University of Serbia, Novi Sad in 2009-, with a Master's thesis entitled *Defining the physical parameters of the X ray beam generated by the CT unit and QA at diagnostic radiology department*
She started the doctoral school at the Faculty of Natural Sciences and Mathematics, Department for Physics, University of Montenegro, Podgorica in 2013. This PhD study was performed under the umbrella of the International Atomic Energy Agency (IAEA) Coordinated Research Project (CRP) E24019 Doctoral CRP in "Advances in Medical Imaging Techniques".

Sonja started to work in the Radiotherapy Department at Clinical centre of Montenegro as physicist in January 2000. Her duties were: treatment planning for radiotherapy patients and dosimetry on the LINAC - radiotherapy machine.
In 2006, she started to work as Head of the Department for Safety at Work with a special duty as Radiation Protection Officer (RPO). On December 2007 she was awarded for her achievements in the field of Safety at Work by the Government of Montenegro, Chamber of Commerce MNE, Trade Union Federation and Employer's Union of MNE.

During her years of work, she was involved as a Counter Part in many IAEA projects. Most important are „*Strengthening Radiological Protection of Patients and Medical Exposure Control"* where she was in charge for collecting patient doses data for Interventional Radiology and CT (Computed Tomography) and „*Upgrading the qualtiy Assurance and Quality Control Programme in Diagnostic Radiology for National Breast Screening Programme*" where she is a medical physicist in charge for patient doses and Quality Control of the DBT mammography system. With the results from these projects she published several scientific papers in scientific journals in area of medical physics in diagnostic radiology.

In 2008 she was a member of the working group for drafting the Montenegrian Law Against Ionizing Radiation.
In 2009, she was a member of the working group for drafting the National Action Plan in case of chemical, biological and radiological accidents.
She was a participant in working groups for nuclear safety and radiation protection within the framework of the negotiation of Chapter 15 – Energy, within the process of integration of Montenegro into the European Union.
In 2015, she worked part time for a group Establishing Quality Assurance/Quality Control in X-Ray Diagnostics by developing guidelines and criteria for Regional Centers of Competence concerning QA/QC in diagnostic radiology.
In 2016, she was a participant in a working group for drafting a Handbook of Basic Quality Control tests for Diagnostic Radiology - Draft document RER6032 Strengthening Quality Assurance and Quality Control in Diagnostic X rays
From 2010, she is a member for RASIMS (Radiation Safety Information Management System) for Montenegro, her area is TSA3 - Radiological Protection in Medical Exposure.
From 2016, she is a National Focal Point for ionized radiation for the Montenegrian Ministry of Health.

Izjava o autorstvu

Potpisana Sonja Ivanović
Broj indeksa

Izjavljujem

Da je doktorska disertacija pod naslovom **„Unapređenje kontrole kvaliteta i osiguranja kvaliteta (QA i QC) u skriningu i dijagnostičkoj mamografiji u Crnoj Gori"**

- rezultat sopstvenog istraživačkog rada,
- da predložena disertacija ni u cjelini ni u djelovima nije bila predložena za dibijanje bilo koje diplome prema studijskim programima drugih ustanova visokog obrazovanja,
- da su rezultati korektno navedeni, i
- da nijesam povrijedila autorska i druga prava intelektualne svojine koja pripadaju trećim licima

Potpis doktoranta

U Podgorici,

Izjava o istovjetnosti štampane i elektronske verzije doktorskog rada

Ime i prezime autora: Sonja Ivanović

Broj indeksa:

Studijski program: Fizika

Naslov rada: „Unapređenje kontrole kvaliteta i osiguranja kvaliteta (QA i QC) u skriningu i dijagnostičkoj mamografiji u Crnoj Gori"

Mentor: Prof. dr Slavoljub Mijović

Potpisana: Sonja Ivanović

Izjavljujem da je štampana verzija mog doktorskog rada istovjetna elektronskoj verziji koju sam predala za objavljivanje u Digitalni arhiv Univerziteta Crne Gore.

Istovremeno izjavljujem da dozvoljavam objavljivanje mojih ličnih podataka u vezi sa dobijanjem akademskog naziva doktora nauka, odnosno zvanja doktora umjetnosti, kao što sui me i prezime, godina i mjesto rođenja, naziv disertacije i datum objave rada.

Potpis doktoranta

U Podgorici,

Izjava o korišćenju

Ovlašćujem Univerzitetsku biblioteku da u Digitalni arhiv Univerziteta Crne Gore pohrani moju doktorsku disertaciju pod naslovom: **„Unapređenje kontrole kvaliteta i osiguranja kvaliteta (QA i QC) u skriningu i dijagnostičkoj mamografiji u Crnoj Gori"**, koja je moje autorsko djelo.

Disertaciju sa svim prilozima predala sam u elektronskom format pogodnom za trajno arhiviranje.

Moju doktorsku disertaciju pohranjenu u Digitalni arhiv Univerziteta Crne Gore mogu da koriste svi koji poštuju odredbe sadržane u odabranom tipu licence Kreativne Zajednice (Creative Commons) za koju sam se odlučila.

1. Autorstvo
2. Autorstvo – nekomercijalno
3. Autorstvo – nekmercijalno – bez prerade
4. Autorstvo – nekomercijalno – dijeliti pod istim uslovima
5. Autorstvo – bez prerade
6. Autorstvo – dijeliti pod istim uslovima

Potpis doktoranta

U Podgorici,

Izjava o autorstvu

Potpisana Sonja Ivanović
Broj indeksa

Izjavljujem

Da je doktorska disertacija pod naslovom **„Unapređenje kontrole kvaliteta i osiguranja kvaliteta (QA i QC) u skriningu i dijagnostičkoj mamografiji u Crnoj Gori"**

- rezultat sopstvenog istraživačkog rada,
- da predložena disertacija ni u cjelini ni u djelovima nije bila predložena za dibijanje bilo koje diplome prema studijskim programima drugih ustanova visokog obrazovanja,
- da su rezultati korektno navedeni, i
- da nijesam povrijedila autorska i druga prava intelektualne svojine koja pripadaju trećim licima

Potpis doktoranta

U Podgorici,

Izjava o istovjetnosti štampane i elektronske verzije doktorskog rada

Ime i prezime autora: Sonja Ivanović

Broj indeksa:

Studijski program: Fizika

Naslov rada: „Unapređenje kontrole kvaliteta i osiguranja kvaliteta (QA i QC) u skriningu i dijagnostičkoj mamografiji u Crnoj Gori"

Mentor: Prof. dr Slavoljub Mijović

Potpisana: Sonja Ivanović

Izjavljujem da je štampana verzija mog doktorskog rada istovjetna elektronskoj verziji koju sam predala za objavljivanje u Digitalni arhiv Univerziteta Crne Gore.

Istovremeno izjavljujem da dozvoljavam objavljivanje mojih ličnih podataka u vezi sa dobijanjem akademskog naziva doktora nauka, odnosno zvanja doktora umjetnosti, kao što sui me i prezime, godina i mjesto rođenja, naziv disertacije i datum objave rada.

Potpis doktoranta

S. Ivanović

U Podgorici,

Izjava o korišćenju

Ovlašćujem Univerzitetsku biblioteku da u Digitalni arhiv Univerziteta Crne Gore pohrani moju doktorsku disertaciju pod naslovom: **„Unapređenje kontrole kvaliteta i osiguranja kvaliteta (QA i QC) u skriningu i dijagnostičkoj mamografiji u Crnoj Gori"**, koja je moje autorsko djelo.

Disertaciju sa svim prilozima predala sam u elektronskom format pogodnom za trajno arhiviranje.

Moju doktorsku disertaciju pohranjenu u Digitalni arhiv Univerziteta Crne Gore mogu da koriste svi koji poštuju odredbe sadržane u odabranom tipu licence Kreativne Zajednice (Creative Commons) za koju sam se odlučila.

1. Autorstvo
2. Autorstvo – nekomercijalno
3. Autorstvo – nekmercijalno – bez prerade
4. Autorstvo – nekomercijalno – dijeliti pod istim uslovima
5. Autorstvo – bez prerade
6. Autorstvo – dijeliti pod istim uslovima

Potpis doktoranta

U Podgorici,